THE CHINESE UNIVERSITY OF HONG KONG

SOLAR RADIATION IN URBAN HONG KONG

A THESIS SUBMITTED TO FULFILL THE PARTIAL REQUIREMENT FOR THE DEGREE

OF

MASTER OF PHILOSOPHY

DIVISION OF GEOGRAPHY

GRADUATE SCHOOL

LAU YUN NGAU, PATRICK

JUNE 1985

ACKNOWLEDGEMENTS

I wish to dedicate my sincere gratitude to my supervisor, Dr. Hsu Sheng-I, for his constructive criticisms, suggestions, painstaking perusal of the manuscripts and participation in the design and development of the data logger. Thanks are also given to Dr. Bruce Taylor, the co-supervisor for contributing advice and valuable comment from time to time.

Special thanks are given to Mr. Fong Chi-kong, Francis for his enthusiastic participation in the design and development of applicable hardware for data acquisition and associated software for data management.

I also wish to acknowledge the Institute of Social Studies of the Chinese University of Hong Kong for providing research grants. The assistance of the Environmental Protection Agency of Hong Kong in providing data for pollution level is also appreciated.

Thanks are also directed to the assistance of my classmates and colleagues. Among these I would especially mention Miss Fan Chi-fun, Cindy and Lo Ho-kwan. Moreover, thanks are conveyed to Mr. Yeung Kam-wing, Philip and Mr. Lee Kwong-chi, Kelvin for developing the data loggers and drawing diagrams and maps.

Finally, thanks must be given to my friend, Marianna for her many encouraging words and unfailing help.

ABSTRACT

This thesis evaluates the urban-suburban variation in the reception of solar radiation in Hong Kong and examines the effect of building morphological structures on the reception of solar radiation.

Based on thirty-two sampling hours, the reception of horizontal solar radiation at the suburban reference site is 2.9mW/cm^2(5.12%) higher comparison with the upper level urban site and 3.4mW/cm^2(6.29%) higher when compared with the lower level urban site. However, the reception of diffuse radiation at the suburban reference site is 0.4 mW/cm^2(5.02%) lower than at the lower level urban site.

Four types of building structures varying in orientation, configuration, cladding material and height are selected for study. The reflectance index, defined as the ratio of the solar radiation intensity received in front of a wall surface to that at a control site where the reflecting effect is minimized, is found to be negatively correlated with the solar altitude. The maximum reflectance index of the selected building morphological structures ranges from 1.06 at the Postgraduate Hall Complex which is rather roughly configured to 1.24 at the Tsim Sha Tsui Centre which is clad with highly reflective material (curtain wall).

Incoming solar radiation on a normal day is compared with radiation received on a day where mixing height is lowered. The study observes that when a very stable atmospheric condition is established (such as a temperature inversion), unfavourable dispersion conditions may result. Consequently, a marked increase in the pollutant concentration and a significant decrease in solar reception are experienced on the day of a pollution episode.

TABLE OF CONTENTS

LIST OF TABLES page

LIST OF MAPS

LIST OF PLATES

LIST OF FIGURES

LIST OF APPENDICES

CHAPTER I

INTRODUCTION

1.1 Introduction

Throughout history, man has always modified his climatic environment. Industrialization and urbanization have brought about the most radical changes. Hong Kong is also experiencing climatic modification.

Due to its rapid industrialization and modernization in the past decades, the Colony is now suffering from an atmospheric environmental problem. Pollution sources, such as electric power plants and incinerators, are sited nearby or inside the urban area. Many industrial areas are developed adjacent to residential area without enough open space or a green belt as barriers between them. Roads are also jammed with motor vehicles, which also severely pollute the urban atmosphere. The increase of atmospheric aerosols, dust, gaseous pollutants and airborne particulates in the urban atmosphere of the Colony will inevitably attenuate the incoming solar radiation, but increase the diffuse radiation because of the scattering created by atmospheric pollutants.

Also, due to the limited available flat land, the Colony is characterized by a large number of high-rise buildings with different heights, configurations and cladding material that may cause the modification of incoming solar radiation through shading and multi-reflection from the city blocks.

Like most large cities in the world, it is believed that Hong Kong may also experience a decrease of global solar radiation due to atmospheric contamination.

1.2 Hypotheses

Hong Kong is characterized by a dense population and by various economic activities in the urban area which may result in higher pollution level. The reception of horizontal and diffuse solar radiation between the suburban area and the urban area is expected to be vary.

Owing to the existence of vertical variation in the mass concentration of total suspended particulates (Yau, 1982), more horizontal solar radiation is expected to be attenuated at the lower elevation of the urban area.

Congested high-rise buildings in the urban area reflect incoming solar radiation and create a shading effect. Variations in height, orientation, configuration and cladding material may also greatly influence the reception of solar radiation at the ground level.

In addition, it is expected that the higher the concentration of atmospheric aerosols, the more the incoming solar radiation will be attenuated.

For an understanding of differences in the incoming solar radiation in urban and suburban areas, four tentative hypotheses are suggested and will be thoroughly evaluated in the study. They are as follows:

(a) The suburban area may receive more solar radiation but less diffuse radiation than the urban area due to its less polluted atmosphere.

(b) The upper level of the urban area may receive more solar radiation than the lower level due to the vertical difference in the concentration of atmospheric pollutants.

(c) The amount of solar radiation reflected by building block varies with the height, orientation, configuration and cladding material.

(d) Although the concentration of atmospheric pollutants and aerosols is expected to be higher in urban area, the pollution level may vary from time to time. The attenuation of solar radiation is expected to be stronger when there is an increase in the concentration of pollutants and aerosols.

1.3 Objectives of the Study

In order to evaluate the above hypotheses, the objectives of the study basically are:

(a) Assessing the suburban-urban variation in the reception of solar radiation

- to compare and contrast the amount of horizontal solar radiation received in the suburban and urban areas
- to compare and contrast the amount of diffuse radiation received in the suburban and urban areas

(b) Assessing the vertical variation in the reception of solar radiation in the urban area

- to compare and contrast the amount of horizontal solar radiation received at a higher site and a lower site in the urban area.

(c) Evaluating the effect of various building structures on the reception of solar radiation

- to quantify the amount of solar radiation being reflected by buildings of different types.

(d) Assessing the effect of atmospheric pollutants and aerosols on the attenuation of the incoming solar radiation.

1.4 Limitations of the Study

In this study, field measurement is conducted only when the sky condition is clear. By doing so, the effect of clouds can be ignored.

When quantifying the amount of solar radiation due to the reflection from a building block, sites selected for study and days of measurements are limited due to the lack of manpower and the availability of instruments.

When assessing the implication of atmospheric pollutants and aerosols on the attenuation of incoming solar radiation, the local measurement of the atmospheric pollutants concentration at the monitoring site should be used. However, due to the limited manpower and the

availability of instruments, the records of the concentration of atmospheric pollutants kept by the Environmental Protection Agency of Hong Kong are employed. In addition, though the effect of the meteorological parameters will also be evaluated, as they are considered as the important factors for the dilution of atmospheric pollutants, the meteorological data used in the analysis are records from the Royal Hong Kong Observatory.

1.5 The Significance of the Study

It is hoped that this study on the effect of atmospheric pollutants on the attenuation of incoming solar radiation can provide valuable information about the variation of daylight illumination in urban Hong Kong, in addition to its effects on the city micro climate. Besides, some ideas on the modification of the daytime energy budget in the urban area, which is basic to an understanding of the thermodynamic behaviour of urban air temperature and the dynamic of urban air flow, can also be given.

Moreover, by studying the effect of building on the reception of solar radiation, more information about the micro climate modified by the building can be offered, which may in turn serve as a reference for the planning of new towns or urban renewal projects.

CHAPTER II

LITERATURE REVIEW

2.1 The Nature of Solar Radiation

The sun continuously sheds part of its mass by radiating waves of electromagnetic energy and high speed particulates into the space. This constant emission is termed solar radiation.

The electromagnetic spectrum of the sun ranges from 0.15 microns to 4 microns (Seller, 1965). Of this, 9 percent is in the ultraviolet spectrum (wavelength less than 0.4 microns), 45 percent in the visible light spectrum (wavelength between 0.4 microns and 0.74 microns), and 46 percent in the infrared spectrum (wavelength greater than 0.74 microns).

The solar radiation density normally incident on a flat surface at the mean earth-sun distance without the presence of the atmosphere is termed the "solar constant". This "constant", in fact, undergoes periodical variations.

Fluctuations of this constant may come from the variation in the earth-sun distance due to the elliptical orbit of the earth. Solar activity variations may also contribute up to ±1.5% of the variation in the solar constant. Consequently, the solar constant is not a "true" constant but fluctuates by as much as ±3% (Barry and Chorley, 1968).

A number of determinations of the solar constant have been made. Some of them are based on data taken by the Smithsonian Institution while others conducted independent measurements from mountain tops, balloons,

aircraft or spacecraft. The estimated values for the solar constant varied between 1.92 and 2.02 cal $cm^{-1} min^{-1}$. The most accepted value currently is 1.940 ±0.03 cal $cm^{-1} min^{-1}$., or 135.3 ±2.1 mW/cm^2 (Coulson, 1975).

In fact, the solar radiation received at the earth surface is much smaller than the solar constant since a considerable portion of the solar radiation is absorbed and attenuated by the atmosphere during its downward traverse to the ground. About 30 percent of the solar radiation is directly reflected and scattered back to the space by clouds (24 percent) and atmospheric constituents (6 percent). About 18 percent is absorbed by water vapour and ozone. The former absorbs an appreciate quantity of infra-red radiation (between 0.8 microns and 2.4 microns) while the latter absorbs all the ultra violet radiation below 0.29 micron. Thus, more than half of the solar radiation is intercepted by the atmosphere before it eventually arrives at the earth surface.

Solar radiation received at the earth surface can basically be divided into two components: direct radiation and diffuse radiation. The latter is caused by the scattering effect of air molecules, water vapour and aerosols that exist in the atmosphere. Parts of the diffuse radiation may also come from the reflection from clouds and large airborne particulates. In a city canyon, multi-reflections by the urban blocks have been found to significantly increase the amount of solar radiation received at the city street levels (Tsjung and Louie, 1973).

2.1.1 Solar Attenuation in the Atmosphere

Passing through the atmosphere, solar radiation is attenuated by atmospheric constituents (air molecules, water vapour, aerosols and

airborne particulates) and clouds.

The amount of solar radiation attenuated by atmospheric constituents under clear sky conditions is an exponential function of the optical thickness, which is measured at the zenith direction. Efficiency of attenuation depends on the wavelength of the incoming solar radiation. The shorter the wavelength, the stronger the attenuation is (Coulson, 1975). Forbes and Hamilton (1979) analyzed the attenuation of solar radiation attributed to atmospheric aerosols in Lerwick, Stockholm. They concluded that the amount of solar radiation being attenuated decreased as the optical thickness decreased.

Clouds are the other strong attenuators of solar radiation. The amount of solar radiation being attenuated basically depends on the amount of cloud cover and thickness. The proportion of incident radiation reflected back to the space is termed as albedo, or reflection coefficient. Cloud type affects the albedo. Aircraft measurements show that the albedo of complete overcast ranges from 44% to 55% for cirrostratus and to 90% for cumulonimbus. In other words, only a small portion of incoming solar radiation will be transmitted when the sky is covered with cumulonimbus clouds.

2.1.2 Solar Diffusion in the Atmosphere

On arriving at the atmosphere, the solar radiation is not only depleted and attenuated by the atmosphere, but also scattered by atmospheric aerosols and airborne pollutants. The total extra scatter of the aerosol layer slightly exceeds its total absorption (Paltridge, 1972). The essence of the scattering process is that under the influence of the

oscillating electric vector of the incident electromagnetic wave, the electrons in the scattering particles begin to "describe" forced oscillations and emit waves. Consequently, the scattering particles themselves become a source of electromagnetic wave emitters (Tverskoi, 1962). The scattering of electromagnetic radiation in the atmosphere involves molecules and particles both larger and smaller than the wavelength of the incoming solar radiation. Those with physical dimensions which are smaller than the wavelength of the radiation are termed as Rayleigh scatters, while those with comparable size to or larger than the wavelength are known as Mie scatters (Twomey, 1977).

The scattering intensity depends on the wavelength of the incident radiation and on the number and size of the scattering particles. The scattering intensity increases with decreasing wavelength. As the size of the scatters increases, the wavelength of maximum scattering intensity shifts towards longer wavelengths. Besides, spectral components of scattering radiation change markedly with respect to the zenith angle of the sun and the azimuth angle of the observing direction to the sun. The spectrum of diffuse radiation is expected to have a maximum intensity in the blue light region when the zenith angle of the sun is low and the azimuth angle of the observing direction and the sun is large (Kondrat'er, 1969).

2.1.3 Solar Reflection in the City Canyon

Reflected radiation in a city is mainly caused by reflections or multi-reflections from the wall surfaces of urban blocks. It involves a complex web of multiple reflections mathematically and geometrically. The

amount of reflected radiation mainly depends on the relative orientation, configuration, geometry and especially on the construction materials of the urban blocks (Anderson, 1977).

This factor has not been taken into consideration in the estimation of the incoming solar radiation received at the urban ground surface made during the past few decades. In predicting the amount of solar radiation received at horizontal urban surface, Robinson (1971), Nunez (1975) and Awater (1976) all generally adopted the model suggested by Houghton (1954); that is, the incoming solar radiation comprises of two components: direct and diffuse radiation. The model is less appropriate in analyzing the receipt of the solar radiation in an urban morphological system since it does not incorporate the reflection and shading effects of urban blocks.

Terjung and Louie (1973, 1974) and Nunez and Oke (1980) extended the model to incorporate the effect of canyon geometry for a three-dimensional urban morphological system. The components of solar radiation not only include direct and diffuse radiation but also reflected radiation. In addition, Terjung and Louie showed that the ratio of the amount of solar radiation being received in the urban morphological system to a horizontal urban surface forms an inverse relationship with the solar altitude, that is, the higher the solar altitude, the smaller the ratio is.

2.2 Solar Radiation Measuring Apparatus

A wide variety of analytical instruments are available for measuring the intensity of different components of solar radiation. A pyrheliometer is used to measure the solar radiation at normal incidence.

A pyranometer is used to measure the horizontal solar radiation. A pyrgeometer is used to measure the infra-red radiation while a pyrradiometer and a net radiometer are used to measure the net radiation.

2.2.1 Pyrheliometer

Pyrheliometers are designed to measure direct-beam solar radiation at normal incidence tracking the path of the sun. During the past century, a large number of pyrheliometers have been developed. Some of them, such as Herschel's pyrheliometer, Hodgkinson's pyrheliometer, Crova pyrheliometer, Pouilett's pyrheliometer and Abbot's Balloon pyrheliometer, are no longer in use and have been superseded by other types of pyrheliometers which include more superior features. The Abbot silver disk pyrheliometer, Angstrom compensation pyrheliometer and Smithsonian water-flow pyrheliometer are now considered to be more accurate and maintain an accuracy on the order of ±0.5%. These pyrheliometers are commonly used as calibration standards. A number of operational pyrheliometers are also available for routine observations. However, they are not as accurate as the Abbot, Angstrom and Smithsonian instruments, and must be recalibrated periodically (Budgen and Price, 1981).

Pyrheliometers are classified according to their sensitivity, stability, temperature compensation, selectivity, linearity and time constant. The classification by the World Meteorological Organization (WMO) in 1965 was as follows (Coulson 1975):

a. Standard pyrheliometer
   - Angstrom electrical compensation pyrheliometer
   - Abbot silver-disk pyrheliometer

b. First class pyrheliometer

- Michelson bimetallic pyrheliometer
- Linke-Feussner iron-clad pyrheliometer
- New Eppley pyrheliometer (temperature compensated)
- Yanishersky thermoelectric pyrheliometer

c. Second class pyrheliometer

- Moll-Gorczynski pyrheliometer
- Old Eppley pyrheliometer (not temperature compensated)

The detailed criteria for classification are shown in Table 2.1.

2.2.2 Pyranometer

Pyranometers are designed to measure global and diffuse radiation. They can be exposed continuously in all kinds of weather. Consequently, they are sturdy and should be mounted securely.

On the basis of their accuracy and overall system performance, pyranometers were also classified by the WMO (World Meteorological Organization) in 1965 into three categories (Coulson, 1975):

a. First class pyranometer

- Selected thermopile pyranometer

b. Second class pyranometer

- Moll-gorczynski pyranometer
- Volacine thermopile pyranometer
- Yanishersky thermoelectric pyranometer
- Spherical Bellani pyranometer

Table 2.1 Detailed criteria for the classification of pyrheliometers

	Standard	1st class	2nd class
Sensitity ($mWcm^{-2}$)	± 0.2	± 0.4	± 0.5
Stability (% change per year)	± 0.2	± 1.0	± 2.0
Temperature (*)	± 0.2	± 1.0	± 2.0
Selectivity (**)	± 1.0	± 1.0	± 2.0
Linearity (***)	± 0.5	± 1.0	± 2.0
Time constant (maximum)	25 sec.	25 sec.	1 min.

Source: Coulson, 1975.

* maximum error due to changes of ambient temperature, in %.

** maximum error due to departure from assumed spectral response, in %.

*** maximum error due to nonlinearity not accounted for, in %.

c. Third class pyranometer

- Robitzsch bimetallic pyranometer

The detailed criteria for classification are shown in Table 2.2.

Several new types of pyranometers have been developed since 1965; for instance, the Eppley thermopiles pyranometer and the silicon photovoltaic pyranometer. The latter is adopted by the author in this research on the study of solar radiation in urban Hong Kong. Pyrheliometers and pyranometers are seldom self-contained. Accessory units are needed for recording the signals detected by the devices. Automatic recording features are particularly desirable for remote operation.

For the study of solar radiation in urban Hong Kong, pyrheliometers are inapplicable since they only measure direct-beam solar radiation at normal incidence and are difficult to operate. However, pyranometers and their accessory units (such as data recorders) are rather expensive. Consequently, applicable hardware, including solar sensors and data loggers for data acquisition and associated software for data management (refer to chapter IV) have been designed and developed to cope with the needs of this research.

2.3 Urban Solar Radiation

2.3.1 The Impacts of Atmospheric Pollutants

Many studies concerning the effect of atmospheric pollutants on the incoming solar radiation received at the city have been done in many

Table 2.2 Detailed criteria for the classification of pyranometers

	1st class	2nd class	3rd class
Sensitivity ($mWcm^{-2}$)	± 0.1	± 0.5	± 1.0
Stability (% change per year)	± 1.0	± 2.0	± 5.0
Temperature (*)	± 1.0	± 2.0	± 5.0
Selectivity (**)	± 1.0	± 2.0	± 5.0
Linearity (***)	± 1.0	± 2.0	± 3.0
Time constant (maximum)	25 sec.	1 min.	4 min.
Cosine response (#)	± 3.0	± 5-7	± 10.0
Azimuth response (##)	± 3.0	± 5-7	± 10.0

Source: Coulson, 1975.

* maximum error due to the change of ambient temperature, in %.

** maximum error due to departure from assumed spectral response, in %.

*** maximum error due to nonlinearity not accounted for, in %.

\# deviation from that assumed, taken at sun elevation 10 degree on clear day, in %.

deviation from that assumed, taken on clear day, in %.

developed countries, for instance: Mateer (1961) in Toronto, Ontario; Rouse and Mead (1972) in Hamilton, Ontario; Glazier (1975) in Sutton Bonington, England; Wesley and Lipschutz in Chicago, Illinois (1976); Ackerman (1977) and Peterson (1978) in Los Angeles, California. These researchers concluded consistently that atmospheric pollutants played an important role in the attenuation of the incoming solar radiation which reduced significantly the amount of solar radiation received at the urban lower boundary layer.

White (1977) examined the net radiation over various types of land use within the St. Louis metropolitan area and the surrounding rural area. He concluded that the incoming solar radiation did not show any appreciable difference between urban and rural environments in St. Louis. However, variations in the amount of terrestrial radiation emitted were found to be related to mesoscale changes in land use types. Peterson and Stoffel (1980) also analyzed the urban-rural variation on the reception of solar radiation over St. Louis under cloudless conditions and reported that the urban-rural differences were about 4.5% in winter and 2% in summer.

Lyon and Forgan (1975) concluded that the role of the pollutant layer appeared to be not only in the absorption of direct radiation but also in the increase of diffuse radiation. The result was empirically supported by the increased diffuse radiation observed at an urban site in comparison with a rural site in Adelaide, South Australia.

Estournel (1982) indicated that attenuation of incident solar radiation over the Toulouse urban area, a middle-sized city (400,000 inhabitant) in France, was mainly caused by traffic and urban emission

sources. It was about 30 Wm^{-2} (3.5%) when compared with a rural reference site. However, significant differences in the diffuse radiation between rural and urban sites were not found.

Li (1978) used a mathematical approach to evaluate the impacts of airborne particulates on the receipt of solar radiation at Lanzhou, China. He concluded that 30% of direct solar radiation was depleted in winter due to aerosol contamination in the atmosphere, but the effect was not significant in summer. Moreover, Shao (1981) investigated the changes in the intensity of direct, diffuse and global solar radiation received in Shanghai, China under clear sky conditions in the past two decades. He discovered that the amount of direct radiation decreased by 10% and diffuse radiation increased by 14%. Overall, about 6% of global solar radiation had been depleted since 1973. Wong (1984) compared the direct solar radiation being received at Guangzhou Shi (city) and Zhongshan Xian (county) in Guangdong Province under clear sky conditions, and concluded that about 13% of direct solar radiation flux was attenuated due to the more severe atmospheric pollution in Guangzhou Shi.

2.3.2 The Impacts of Building Structure

Although studies on the effects of atmospheric pollutants on incoming solar radiation are common, research concerning the implications of building blocks on the reception of solar radiation in an urban morphological system is very limited. Nevertheless, some of them are discussed below.

Bach and Peterson (1969) studied the heat budget in Greater

Cincinnati, Ohio, and discovered that the city received 6% less incoming solar radiation, when compared with a rural reference site, because the solar beam had to travel through a more polluted air mass. Though less incoming short-wave radiation was received, the city showed a net short-wave radiation gain of 8.2% higher than that of a rural site. They attributed their finding to the great variety of tall building structures in the city which trapped and multi-reflected the short-wave radiation especially when the altitude of the sun was low.

Terjung and Louie (1973, 1974) analyzed the influences of city structure on the potantal absorption of solar radiation. They concluded that tall building skylines absorbed more than six times the radiation of non-urban plains while shading effects could create absorption less than that of a plain surface. The height and the relative orientation of the building were also found to have significant effects on the reception of solar radiation. However, the roof structure and the construction materials of the buildings were not taken into consideration in this study.

Oke and Nunez (1980) modelled the energy balance for an urban morphological system and mathematically derived procedures for the calculation of different radiation fluxes, for instance, mean incoming solar radiation, reflected short-wave radiation and net all-wave radiation in a canyon system. The results were verified by experimental field data. Field measurements were conducted at a city canyon located approximately 6 km south-east of the downtown core of Vancouver, B.C. under cloudless conditions. The measured and the calculated values of the amount of radiation were compared and found to have close agreement (± 5%). Unfortunately, comparisons of the reception of radiation at various parts

of the canyon were neglected.

CHAPTER III

METHODOLOGY

3.1 Introduction

This study basically has three main objectives: (1) to evaluate the effect of urban morphological structures with different construction materials, configurations and orientations on the reception of solar radiation; (2) to determine the variation in the horizontal and diffuse radiation intensity between urban and suburban areas, and to assess the vertical variation in the horizontal solar radiation intensity in an urban area; (3) to evaluate the implication of high pollution episodes on the attenuation of incoming solar radiation in Hong Kong.

In the first part of the study, the effect of some selected building structures on the reception of solar radiation is evaluated. The study attempts to determine the reflectance index of the wall surfaces of these building structures at various solar altitudes. The reflectance index of a wall surface is defined as the ratio of the solar radiation intensity received in front of a wall surface to that at a control site where the reflecting effect is minimized.

In the second part of the study, an attempt is made to assess the variation in horizontal and diffuse radiation intensity between urban and suburban areas, and the vertical variation of horizontal solar radiation in an urban area. The temporal variation in the vertical difference in the solar radiation intensity will also be investigated. This part of the study includes the measurement of:

(a) The difference in the horizontal solar radiation intensity between a suburban reference site and an upper level monitoring site in the urban area.

(b) The difference in the horizontal solar radiation intensity between a suburban reference site and a lower level monitoring site in the urban area.

(c) The difference in the diffuse radiation intensity between the suburban reference site and the urban site.

(d) The difference in the horizontal solar radiation intensity between the upper level and the lower level monitoring sites in the urban area.

(e) The relationship between the vertical difference in the horizontal solar radiation intensity (the upper level and lower level monitoring sites in the urban area) and the change in the solar altitude.

The third part of the study attempts to evaluate the implications of high pollution episodes on the attenuation of incoming solar radiation in Hong Kong. It is expected that the unusually elevated concentration of atmospheric pollutants may lead to a stronger attenuation of incoming solar radiation. The effect of the meteorological parameters will be assessed as well since they are considered as important factors in the dilution and dispersion of atmospheric pollutants.

Field measurements were conducted from mid-July 1984 to early February 1985 since clear sky conditions are much more frequent at these times of year due to the influence of anticyclones covering mainland China.

3.2 Measurement of Solar Radiation

Applicable hardware for measuring the solar radiation and associated software for subsequent data measurement have been designed and developed by the author as described in Chapter IV (Instrumentation).

Data collected by the data logger are analyzed with an Apple II+ micro-computer and associated software. All radiation data are expressed in mW/cm^2 (milliwatts per square centimeter).

3.3 The Effect of Urban Morphological Structures

There are many types of buildings to be found in Hong Kong. However, due to limited manpower and resources, only some of them are selected for study. Detailed description of these morphological structures are found in section 3.3.1.

When assessing the amount by which solar radiation is increased due to the effect of building structures, inferential statistical techniques are employed. The paired t-test is used to evaluate if there is a significant difference in the intensity of solar radiation received in front of the wall surface and that received at the control site where the multi-reflective and shading effects of building blocks are minimized. Bivariate regression analysis is adopted to investigate the intricate relationships between the reflectance index of the wall surface and the solar altitude.

3.3.1 Site Selection

Altogether, four morphological structures varying in construction material, orientation, height, colour and configuration are selected. Three of them are located on the campus of the Chinese University of Hong Kong while the other is located in Tsim Sha Tsui East, which is a newly developed commercial and hotel district. The details of these sites are as follows:

3.3.1.1 The Postgraduate Hall Complex

This is a nine storey building with a height of approximately 30 meters. The wall being investigated faces east, is balconied and roughly surfaced. The configuration of the wall and the site of the building are depicted in Plate 3.1 and Map 3.1 respectively.

3.3.1.2 The Basic Medical Science Building

This is a building of six storeys with a height of approximately 20 meters. The wall facing east with less than 10% glass coverage is selected for study. The surface of the wall is smooth. The appearance of the wall and the location of the building are illustrated in Plate 3.2 and Map 3.1 respectively.

3.3.1.3 The Madam Ho Hall

This is a six storeyed building with a height of about 20 meters. The wall facing south is selected for study. More than 30% of the wall is covered with glass and it is smooth. The configuration of the wall and the site of the building are shown in Plate 3.3 and Map 3.1 respectively.

3.3.1.4 The Tsim Sha Tsui Centre

The south facing wall of the Tsim Sha Tsui Centre is selected for

Plate 3.1 The outlook of the Postgraduate Hall Complex (east wall)

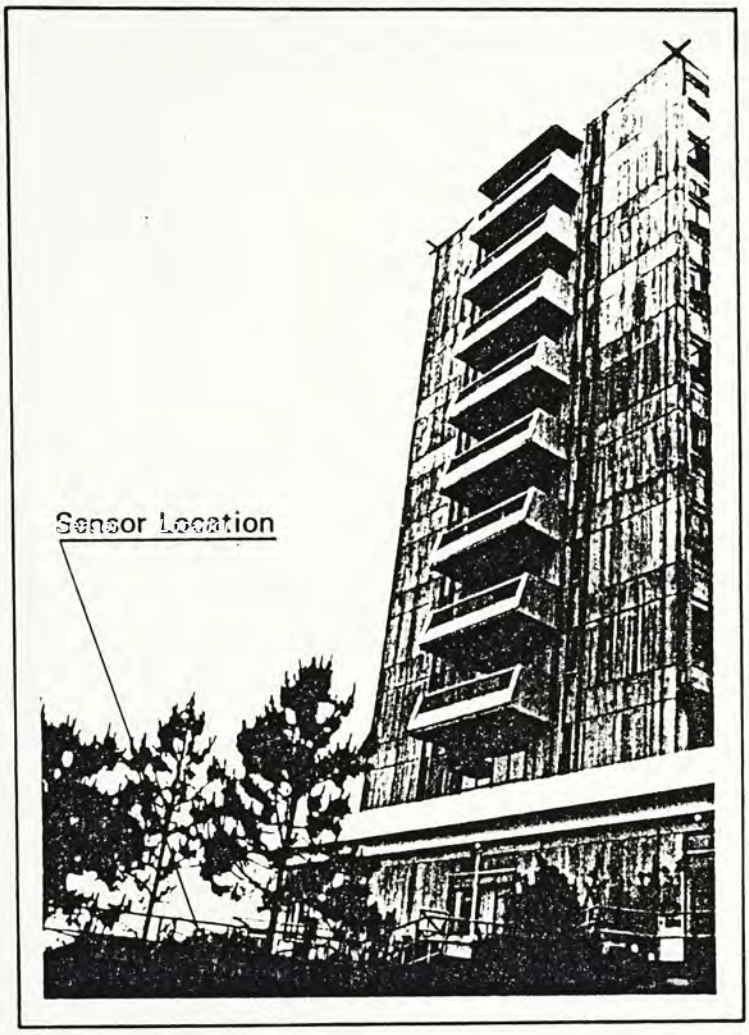

Plate 3.2 The outlook of the Basic Medical Sicence Building (east wall)

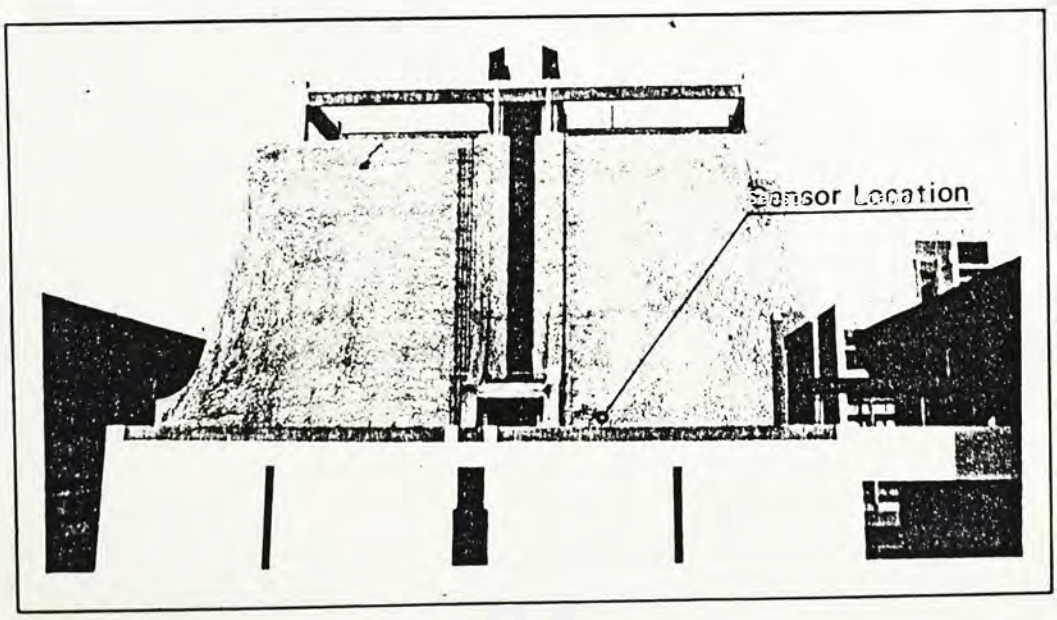

Map 3.1 The site of the experimental buildings

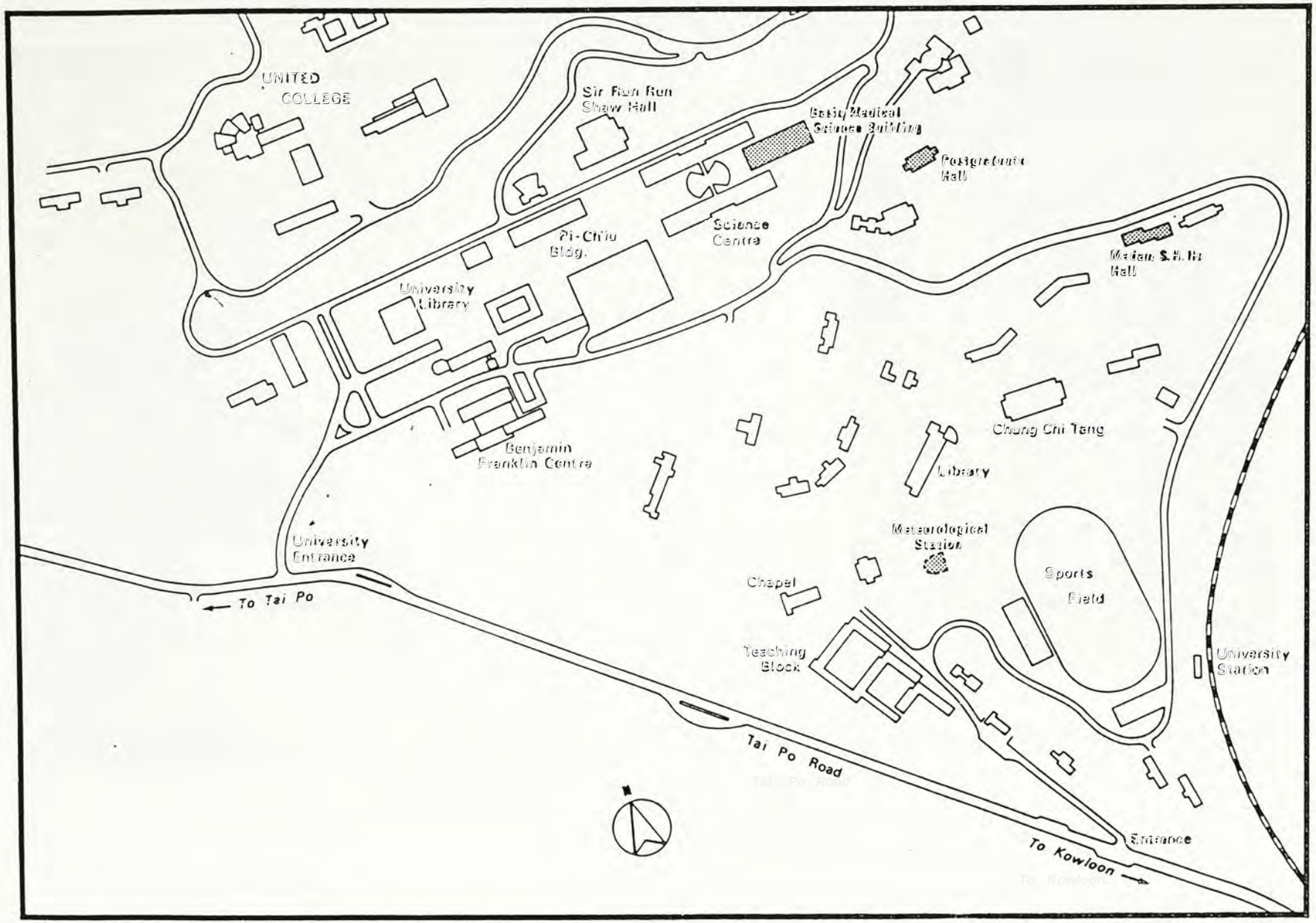

Plate 3.3 The outlook of the Madam Ho Hall (south wall)

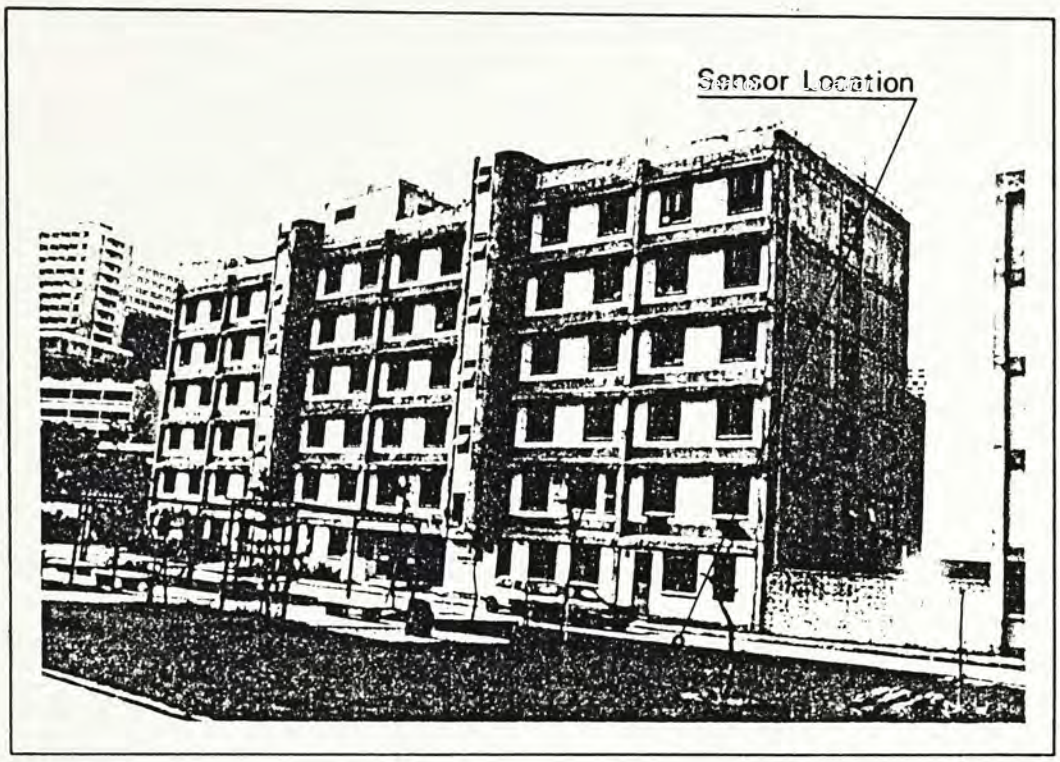

Plate 3.4 The outlook of the Tsim Sha Tsui Centre (south wall)

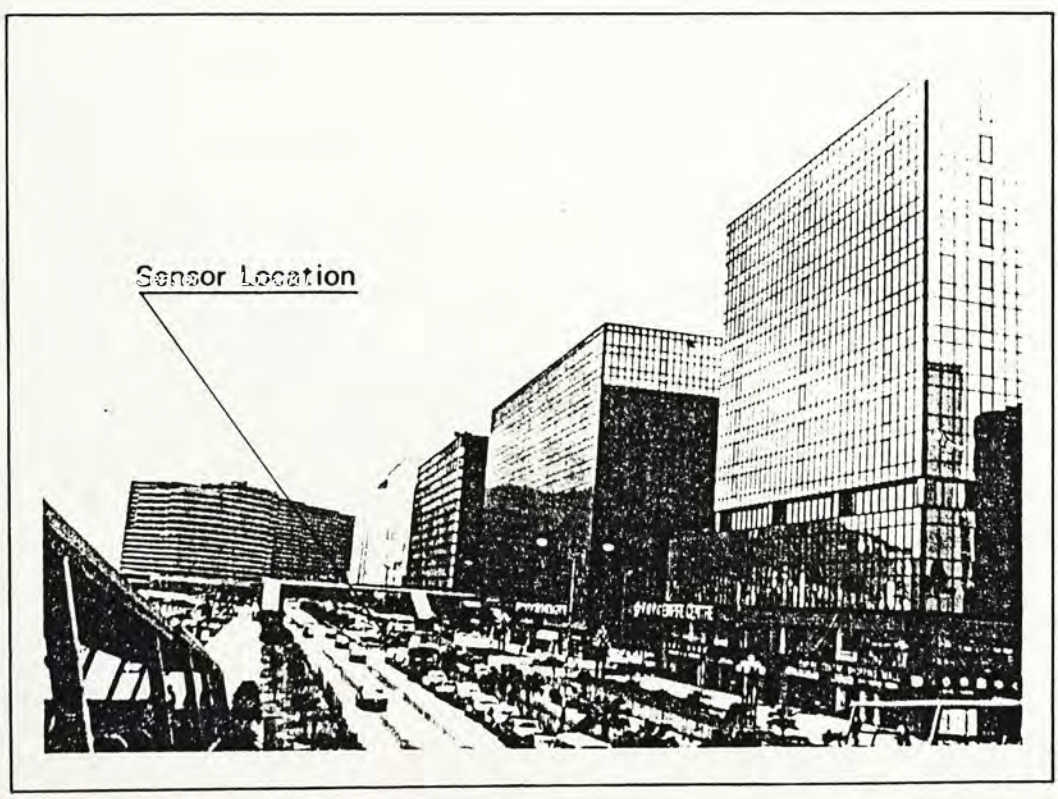

study. It is a building block of fifteen storeys located in Tsim Sha Tsui East, which is a newly developed commercial and hotel district in downtown Kowloon. The height of the building is approximately 45 meters. It is fully clad with highly reflective glass and is smooth. Its configuration and location are shown in Plate 3.4 and Map 3.2 respectively.

3.3.2 Data Sampling

To assess the effect of the building blocks located on the campus of the Chinese University of Hong Kong on the reception of solar radiation, three days with clear sky conditions were chosen for field measurements at each experimental site. A radiation sensor was placed one meter above the ground level and five meters in front of the wall surface while another sensor serving as a control reference was placed at the roof of the selected building.

However, due to limitations of time and available man power, only two cloudless days were chosen to evaluate the reception of solar radiation at the building block located downtown. As the space available for erecting a sensor was restricted, the radiation sensor was placed one meter above the ground level and fifteen meters in front of the wall surface, while the control reference site measurements were carried out at the roof of the Ocean Terminal located about one kilometer from the building.

The data loggers located in front of the wall surface and at the control reference site were operated simultaneously to collect samples for comparisons. The sensor at the control reference site was placed in a way so that the multi-reflective and shading effects of the building blocks

Map 3.2 The location of the Tsim Sha Tsui centre

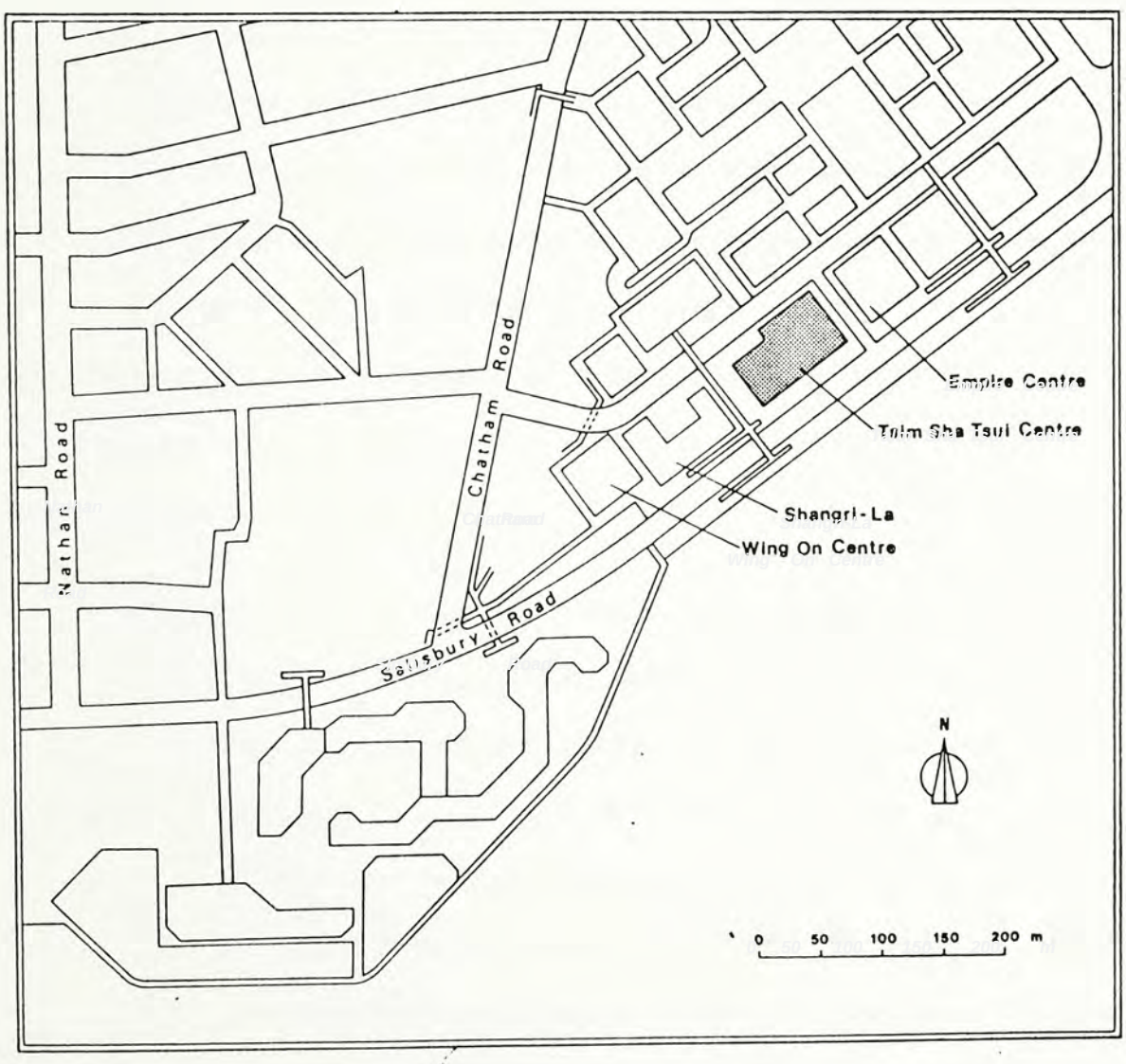

were minimized. The sampling rate of the data loggers was set to 2 minutes. Field measurements were conducted when the selected wall surface of the building was sunlit.

3.3.3 Method of Analysis

3.3.3.1 Paired t-test Analysis

For comparing the intensity of solar radiation received in front of the wall surfaces and that received at the control reference sites, the paired t-test analysis is adopted. As the data loggers were operated simultaneously, the samples collected are paired samples. For this reason, time-to-time variability has little effect on the comparisons. The linear correlation between the intensity of solar radiation received in the front of the wall surface and that of the control reference site can be calculated from the paired values.

The null hypothesis is that there is no difference in the mean intensity of the solar radiation being received in front of the wall surface and that of the control reference site under clear sky conditions. The level of significance is set at 0.05. The observed significance level can be calculated from the values of Student's t-distribution with N-1 degree of freedom, where N is the number of pairs. To compute the testing statistics for paired samples, the paired difference variable (D), defined as the difference between the two investigating samples, is formed. The variable (D) is normally distributed with mean v. If the sample mean and variance of the difference are symbolised as d and S_d, then

$$t = \frac{(d - v)}{S_d}$$

$$\text{and } S_d = \left(S_1^2 + S_2^2 - 2\frac{X_1 * X_2}{N - 1}\right)^{1/2}$$

where X_1, X_2 are the two investigating variables,

S_1, S_2 are the standard deviation of X_1, X_2 respectively

and N is the sample size.

Under the null hypothesis, v is equal to zero. If the level of significance is less than 0.05, the null hypothesis is rejected.

3.3.2.2 Bivariate Regression Analysis

To investigate the relationships between the reflectance index of the wall surface and the solar altitude, bivariate regression analysis is employed. The reflectance index of the wall surface is defined as the ratio of solar radiation intensity received in front of the wall surface to that received at a control site where the reflecting effect is minimized. The solar altitude is defined as the complement angle of the solar zenith angle and taken as independent variable while the reflectance index is regarded as dependent variable.

There are two basic parameters, the regression coefficient and the intercept, derived from the computation. The former illustrates the slope of the regression equation and indicates the expected change in the dependent variable with a change of one unit in the independent variable. The intercept shows the point at which the regression line crossing the Y axis and represents the predicted value when the independent variable is equal to zero.

The null hypothesis is that there is no significant linear correlation between the reflectance index of the wall surface and the solar altitude. The testing statistic employed is:

$$F = \frac{\text{variance due to regression (explained variance)}}{\text{variance due to residuals (unexplained variance)}}$$

which is a F-distribution with degrees of freedom (1, N-1). The higher the F value, the more significant the model is. The observed level of significance can be obtained from a table of F-distribution values with the appropriate degrees of freedom.

3.4 Spatial Variation in Solar Radiation Intensity

The second part of the study attempts to assess the suburban-urban variations in the intensity of horizontal and diffuse radiation, and the vertical variation of the horizontal solar radiation in the urban area. Also, the temporal variation of the vertical difference in horizontal solar radiation intensity is investigated. One-way analysis of variance is employed for preliminary comparison while a paired t-test is used to further evaluate the difference in the solar radiation intensity among the monitoring sites. When investigating the temporal variation of the vertical difference in horizontal solar radiation intensity, bivariate regression analysis is applied.

3.4.1 Site Selection

The radiation sensors are placed at three locations which represent

the suburban area and the lower and upper elevations in the urban area. The locations for these sampling sites are as follows (Map 3.3):

3.4.1.1 The Suburban Area

The Meteorological Station of the Chinese University of Hong Kong was chosen as suburban reference site because the campus is sparsely populated and is rather remote from the industrial and densely populated areas in urban Hong Kong.

3.4.1.2 The Lower Level Urban Site

The sensor was placed at the roof of Block C of the Shaung Li Uk Estate in Sham Shui Po District. The district is one of the most densely populated area in Hong Kong and is characterized by a commercial and residential land use pattern (Liang, 1972). Research by Yau (1982) indicated that it was lightly polluted by airborne suspended particulates and that vertical variation in the concentration of total suspended particulates (TSP) did exist between ground-level and roof-level.

3.4.1.3 The Upper Level Urban Site

A knoll located in Sham Shui Po to the north-west of the lower level urban monitoring site was chosen. The sensor was placed at the top of this low hill. The horizontal distance between the two monitoring sites is approximately 100 meters and the height of the knoll is approximately 120 meters. The difference in elevation between the sensors is about 100 meters.

When evaluating the suburban-urban variation in diffuse radiation intensity, only the suburban site and the lower level urban site were selected for study, in view of the limited resources and available

Map 3.3 The locations of urban (Sham Shui Po) and suburban (CUHK) site

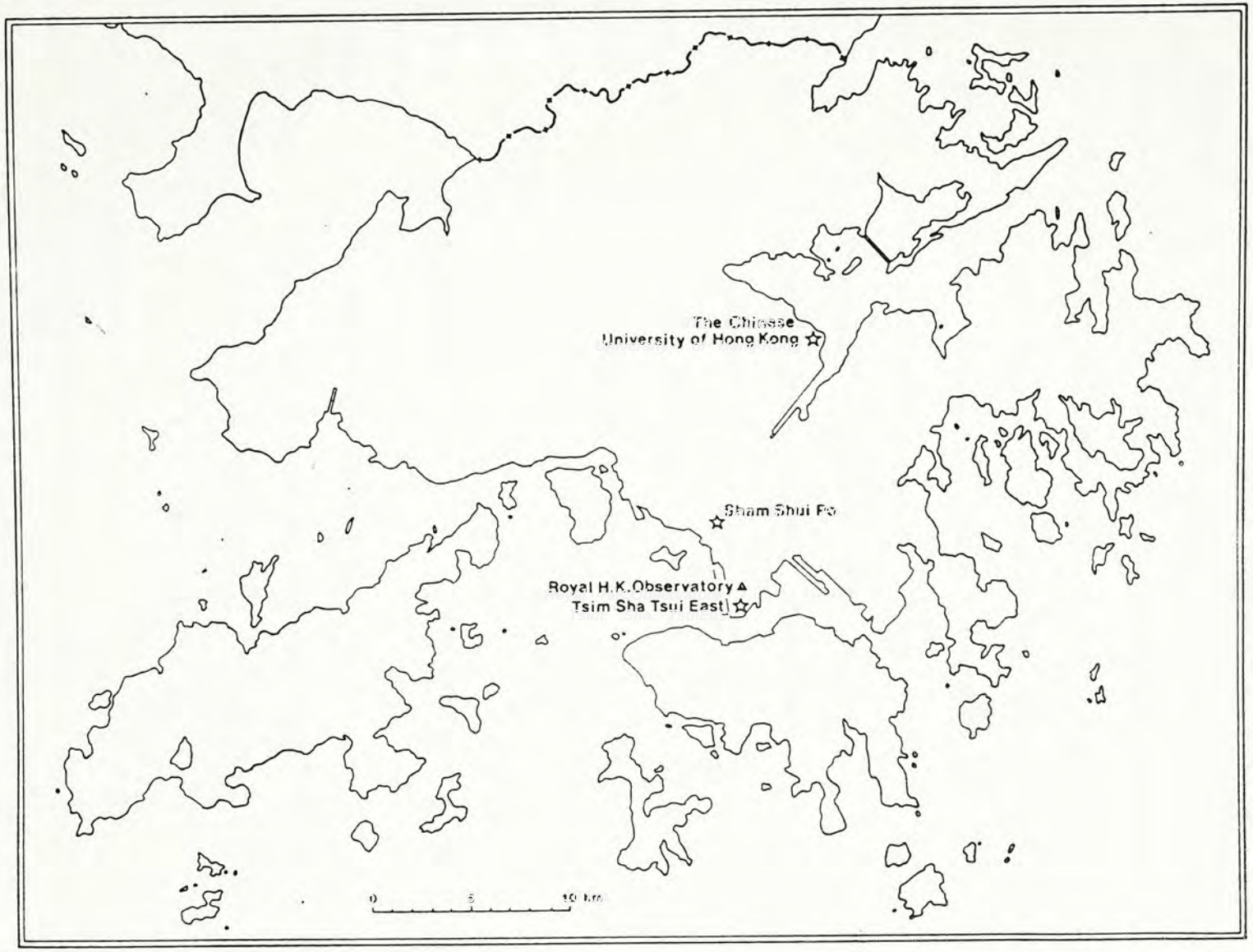

manpower.

3.4.2 Data Sampling

All the field measurement was conducted under clear sky conditions. Eight days were chosen to assess the spatial variation in horizontal radiation intensity while four days were selected for the evaluation of the spatial variation in diffuse radiation. In order to eliminate temporal variability among the collected samples, the data loggers were simultaneously operated. The sensors were placed and mounted securely in a way so that the multi-reflective and shading effects of city canyons were minimized. When evaluating the suburban-urban variation in the intensity of diffuse radiation, the sensors were covered with non-reflective semi-circular cardboard so that they were protected from the reception of direct solar radiation. The sampling rate of the data loggers was set to 2 minutes.

3.4.3 Method of Analysis

3.4.3.1 One-way Analysis of Variance

In order to evaluate the spatial variability of horizontal solar radiation intensity, one-way analysis of variance is employed. Here, the observed variation in the collected samples is subdivided into the variability between areas and the variability within areas. The null hypothesis is that there is no difference in the intensity of horizontal solar radiation among the experimental sites. To test the hypothesis, the following statistic is calculated.

$$F = \frac{\text{variance among areas}}{\text{variance within areas}}$$

The larger the F statistic, the greater the difference in the mean horizontal solar radiation intensity among the monitoring sites is. In this study, the level of significance is set at 0.05. Thus, if the observed level of significance is less than 0.05, the null hypothesis is rejected.

3.4.3.2 Paired t-test

Although the result of one-way analysis of variance can indicate whether there is a significant difference in the horizontal solar radiation intensity among the monitoring sites, it fails to give any idea of the magnitude of the intensity difference. In order to complement the analysis, paired t-test (refer to section 3.3.3.1) is again employed. The null hypotheses are set as follows:

(1) there is no difference in the mean horizontal solar radiation intensity between the suburban reference site and the lower level monitoring site of the urban area.

(2) there is no difference in the mean horizontal solar radiation intensity between the suburban reference site and the upper level monitoring site of the urban area.

(3) there is no difference in the mean diffuse radiation intensity between the suburban reference site and the lower level monitoring site of the urban area.

(4) there is no difference in the mean horizontal solar radiation

intensity between the lower level and the upper level site of the urban area.

If the observed level of significance is greater than 0.05, the null hypothesis will be accepted.

3.4.3.3 Bivariate Regression Analysis

Bivariate regression analysis is employed for the investigation of the correlation between the vertical difference in the horizontal solar radiation intensity and the solar altitude. In this study, the solar altitude is taken as the independent variable while the the vertical difference in horizontal solar radiation is regarded as the dependent variable. For the details of bivariate regression analysis, please refer to section 3.3.2.2.

The null hypothesis is that there is no significant linear correlation between the vertical difference of the intensity solar radiation and the solar altitude. The test statistic employed is:

$$F = \frac{\text{variance due to regression (explained variance)}}{\text{variance due to residuals (unexplained variance)}}$$

The larger the F value, the more significant the explanatory power the model is. The observed significance level can be obtained from an F-distribution table.

3.5 The Pollution Episode

The third part of the study attempts to assess the implications of

high pollution episodes on the attenuation of incoming solar radiation. Also, the effect of meteorological parameters is taken into consideration because they are regarded as important factors in the dilution and dispersion of atmospheric pollutants and aerosols.

In the study of the implications of atmospheric pollutants and aerosols on the attenuation of incoming solar radiation, the local records of the atmospheric pollutant concentration and the meteorological condition at the monitoring site should be used. However, due to limited manpower and the availability of instruments, the daily average levels of the atmospheric pollutants (basically sulphur dioxide and total suspended particulates) measured by the Environmental Protection Agency of Hong Kong at Sham Shui Po District, and the surface and upper air meteorological conditions (basically wind speed, wind direction, temperature and atmospheric pressure) recorded by the Royal Hong Kong Observatory are used. Since only the atmospheric pollutant concentration in the urban area is available, the study will focus on the daily variation in the incoming solar radiation intensity in the urban area in relation to the concentration of atmospheric pollutants.

3.6 Data Manipulation

All the raw data were analyzed first with an Apple II+ micro-computer and stored on mini floppy magnetic diskettes. The processed data were transferred to files at the Computer Services Centre of the Chinese University of Hong Kong. Programs for the detailed analyses mentioned in the previous sections are selected from the Statistical

Package for the Social Sciences (SPSS).

CHAPTER IV

INSTRUMENTATION

4.1. Introduction

A wide variety of analytical instruments are available for measuring the intensity of different components of solar radiation. These instruments include; the pyrheliometer - measuring direct radiation at normal incidence, the pyranometer - measuring direct radiation at horizontal incidence, the pyrgeometer - measuring infra-red radiation, and the pyrradiometer - measuring net radiation.

Pyrheliometers are instruments designed to measure the direct beam solar radiation at normal incidence tracking the path of the sun. The Abbot silver disk pyrheliometer and the Angstrom compensation pyrheliometer are considered to be more accurate and maintained an accuracy of the order of ±0.5 percent. Other models are also available for routine observation. However, they are not as accurate as the Abbot and Angstrom instruments, and must be recalibrated periodically. Examples include the Eppley pyrheliometer, Michelson bimetallic pyrheliometer and Linke-Feussner pyrheliometer (actinometer). These apparatus usually have an accuracy of the order of ±3-5 percent (Griffins, 1976).

Apart from the pyrheliometer, a number of instruments which are known as pyranometers have also been developed. Unlike the pyrheliometer, the pyranometer detects global incident short wave solar radiation. Also, pyranometers are sturdy and mounted securely and can be exposed continuously under all kinds of weather conditions. The sensor or receiver

is inclosed in a dome which is made of glass or quartz. The dome not only protect the sensor or receiver from wind and rain but also transmits only short wave radiation between 0.35um and 2.8um for glass and 0.25um and 4um for quartz. The common models are Moll-Gorcznski pyranometer (solarimeter), Robitzsch bimetallic pyranography (actinography) and Balliani spherical pyranometer (Sellers, 1965).

The most common instrument used in the solar radiation study is the pyranometer, although the pyrheliometer may be used when more accurate measurement of direct radiation is required (White et al., 1977; Peterson et al., 1981; Reed, 1981). Due to the expensive cost of these apparatus, other models of radiation instruments such as "Economical Radiometer", "CSIRO Radiometer" and "Dial Silicon-cell Radiometer" are also frequently used (Bach et al., 1969; Rouse et al., 1973; Wesley, 1981). Radiometers are sensitive to the change of ambient air temperature instead of a specific solar spectrum. The radiation intensity can be calculated from the temperature as obtained from the apparatus (Swan et al., 1969).

4.2 Economical Solar Radiation Detector

In addition to the high cost of the pyranometer and radiometer, the data recorders for the subsequent analysis are expensive. Thus, without a large research grant, it seems rather difficult to carry out field studies on the spatial variation of solar radiation. Because of this, the author has designed and developed applicable hardware for data acquisition and associated software for data management this particular purpose.

4.2.1 Hardware Configuration

The instrument basically consists of three main parts: (a) a solar sensor, (b) a data logger and (c) an accessory unit - namely, an Apple II+ micro-computer. The block diagram of the instrument is shown in Figure 4.1 while the detailed circuit diagram of the data logger is portrayed in Appendix 4.1.

4.2.1.1 The Solar Sensor

A solar panel, which is built with silicon photovoltaic cells and manufactured by Solarex Electric Limited, is used as a solar sensor. The built-in photovoltaic cells are serially connected and mounted securely by ecosil (a chemical substance specially developed by the manufacturer for the construction of solar panel). The size of the panel is 18cm by 24cm and its edge is framed with aluminium. An integrated circuit temperature sensor (section 4.2.4) is also built in the panel to meet the special need of other field studies. The configuration of the solar panel is shown in Figure 4.2.

It has a relatively high response to a broad range of wavelengths ranging from ultra-violet, through the visible portion of the spectrum, into infra-red. Its spectral response ranges from 350-1100 nanometers.

The sensor responds well in both clear and cloudy conditions. The output signal of the sensor is a voltage which varies linearly according to the intensity of solar radiation received. A maximum output of 4.5 volts is equivalent to the condition of "full-sun" intensity (1 kw/m^2) which is the maximum possible solar radiation received with reference to Air Mass One (AM1) standard. The solar panels are calibrated individually against a

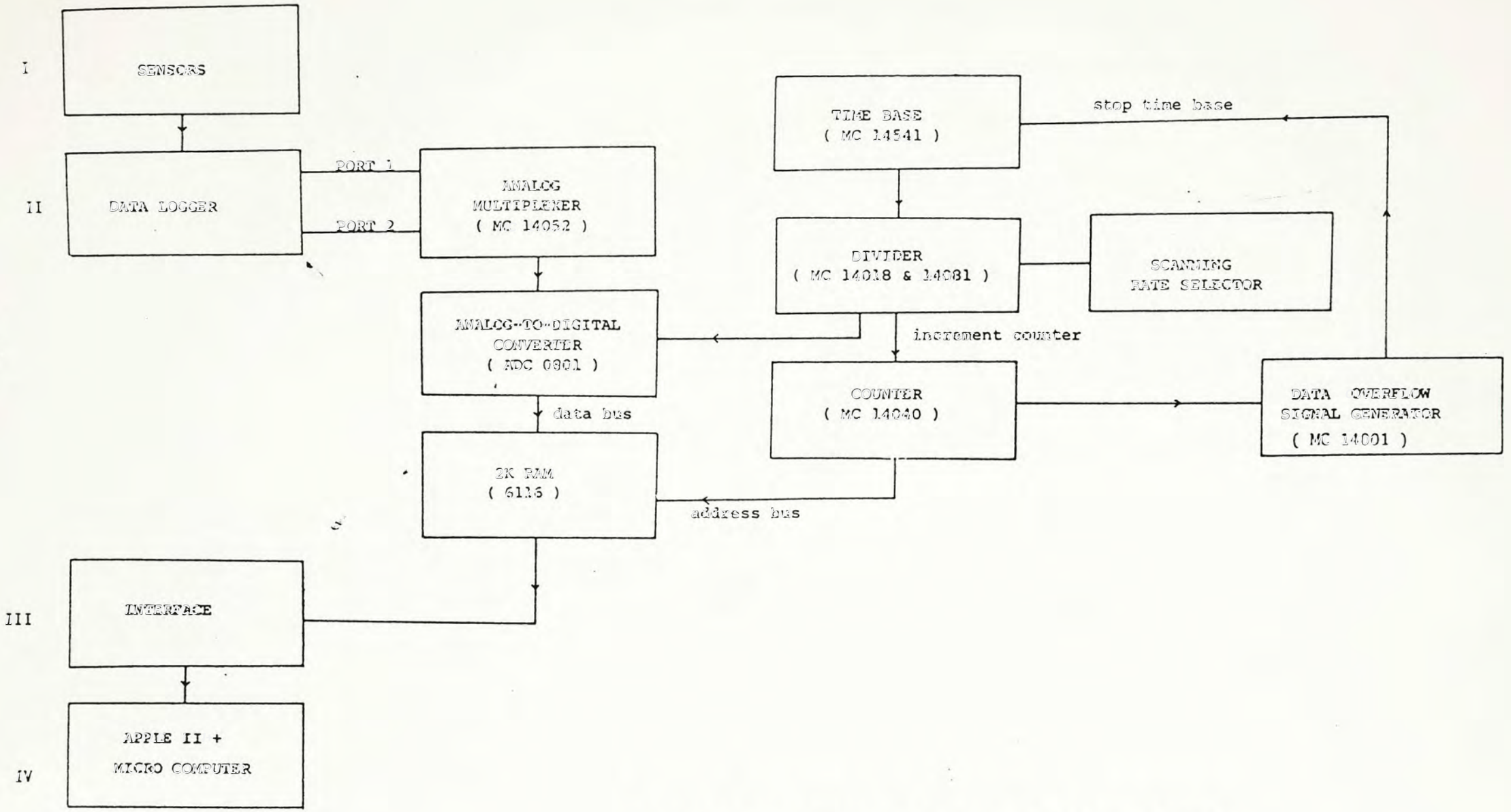

Figure 4.1 The block diagram of the data logger

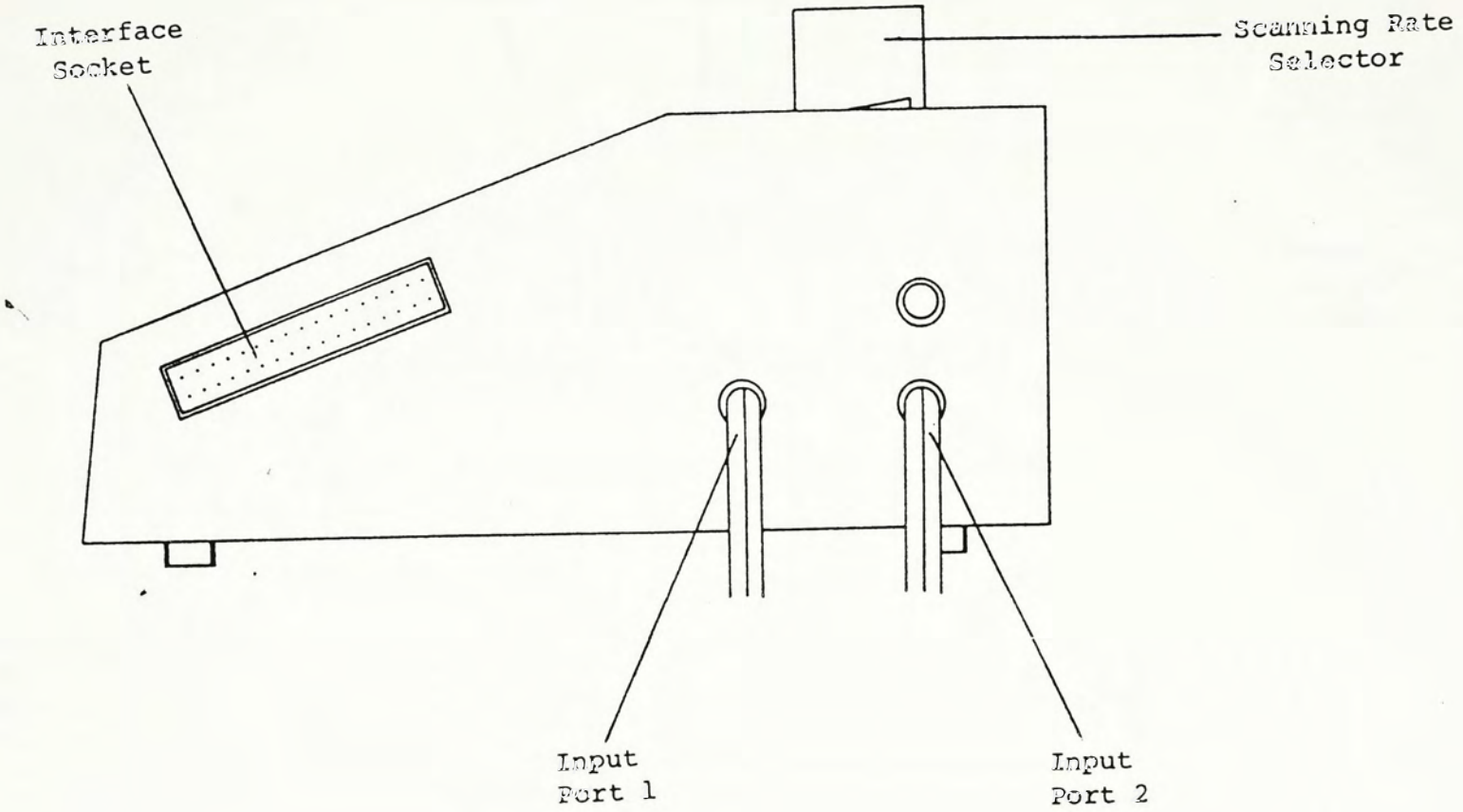

Figure 4.1 The block diagram of the data logger (con't)

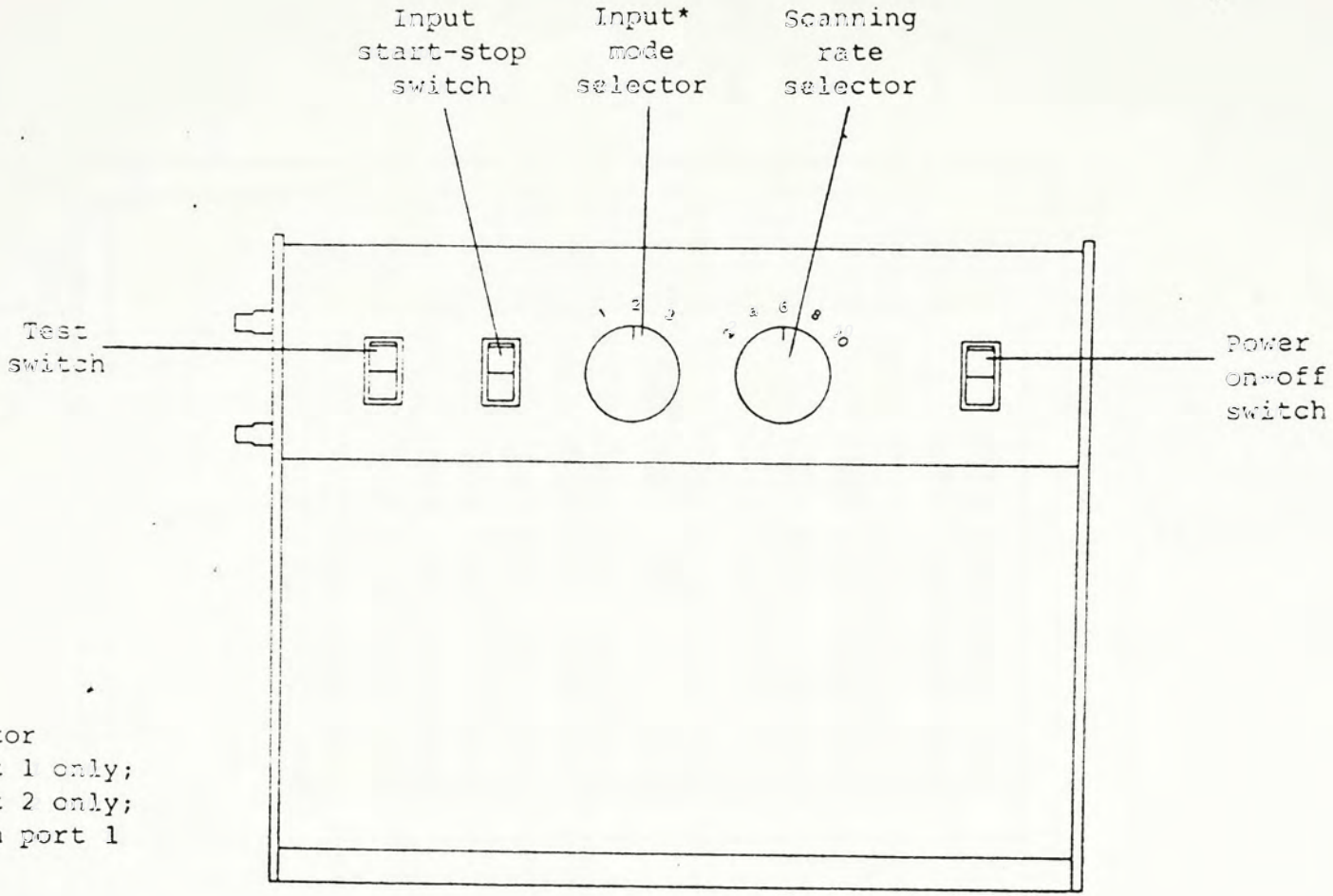

Figure 4.1 The block diagram of the data logger (con't)

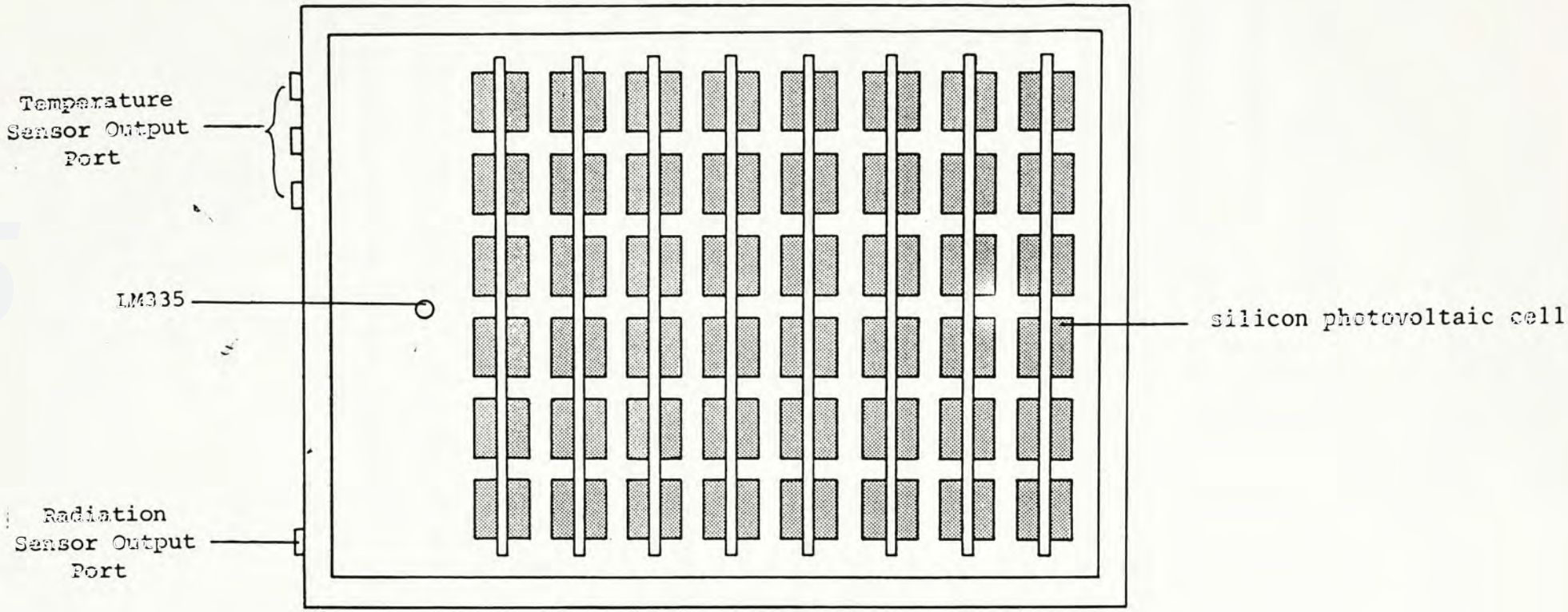

Figure 4.2 The configuration of the solar panel

Solarex Standard Cell which is standardized using an Eppley pyranometer (Model 8-48).

4.2.1.2 The CU Data Logger

The CU data logger is a general measuring and recording instrument. It records the instantaneous output voltages from transducers (i.e. the solar sensor and the temperature sensor in this particular research), sequentially over a designated period of time. All data taken are stored in a built-in IC memory until the final measurement. Later, the data can be accessed and transferred by an interface to a micro-computer for further manipulation and analysis. The data logger has two input ports. Both of them can detect voltages from 0 to 5 volts. The data logger can take data from input port 1 or input port 2 or both alternately. The output voltages from the input ports are scanned at selected times. The period can be selected to be 2 min., 3 min., ... or 10 min. The sampled analog voltages will then be proportionally converted to a digital scale of 0 - 255 with the help of an 8 bit analog-to-digital converter. The digital data are then stored in a 6116 RAM chip with a capacity of 2K.

The hardware can be divided into six major parts: time base, input stage, analog to digital converter, memory, interface and power supply.

(a) Time Base

A time base chip MC14541 is used to generate a clock signal every minute. This signal is then passed into 2 to 10 dividers MC14018 and MC14081. Thus, a clock signal of period 2 min. to 10 min. can be generated. This clock signal is used to control the scanning rate of data measurement.

(b) Input Stage

The input signal with voltage ranging from 0 to 5 volts can be directly fed into the analog multiplexer MC14052.

(c) Analog-to-digital Converter

The signal selected by the analog multiplexer MC14052 is then input to an analog-to-digital converter ADC0801, which converts the analog signal to 8 bit parallel digital data. The digital data are then sent on to the system data bus.

(d) Memory

The digital data are stored into a CMOS (Complementary Metal-oxide-Silicon) 6116 RAM chip. As the 6116 has 2K bytes RAM, a maximum of 2048 observations can be stored. When the memory is full, an overflow signal is generated by a R-S (reset and set) flip flop through MC14001 that controls the time base. When the RAM is full, no more data will be taken. Thus, the previous sampled data will not be overwritten.

The address of the RAM is controlled by the counter MC14040. It increases the memory address value by 1 each time when a clock signal is detected.

(e) Power Supply

Since CMOS chips consume a small amount of DC current, a pack of six 1.5 volts dry batteries is used as power supply. The voltage is kept at 5 volts by a 5V voltage regulator (7805).

(f) The Interface

The interface is built on a standard Apple expansion card which can be plugged into a slot of the Apple II+ micro-computer. On the card,

there is a PIA 8255A through which the Apple II+ can read the data stored in the 2K RAM chip through the system data bus.

4.2.1.3 Apple II+ Micro Computer

A 48K Apple II+ micro-computer with at least one disk driver serves as an accessory unit.

4.2.1.4 The Temperature Sensor

An integrated circuit temperature sensor LM335, produced by the National Semiconductor Corporation, is used. The temperature sensor can detect temperatures from -40^{o}C to 100^{o}C.

With the accessory 2.7V zener, the output voltage of the temperature sensor at 25^{o}C can be adjusted for 2.73V and is linearly proportional to the change of temperature at 10mV/^{o}C. It possesses an accuracy of an order of $\pm 1^{o}$C.

4.2.2 Software Configuration

The software is written in Applesoft BASIC and 6502 assembly language. The programs are listed in Appendix 4.2 and Appendix 4.3. The hierarchical structure of the software is shown in Figure 4.3. Details are as follows:

4.2.2.1 Configuration Subsystem

This subsystem allows the users to specify the input and output facilities such as the slot number of the interface card (section 2.1.2.5), the slot number of the printer interface card and the type of printer interface card used. Four types of printer interface card are taken into consideration. They are the Apple II parallel interface card, parallel

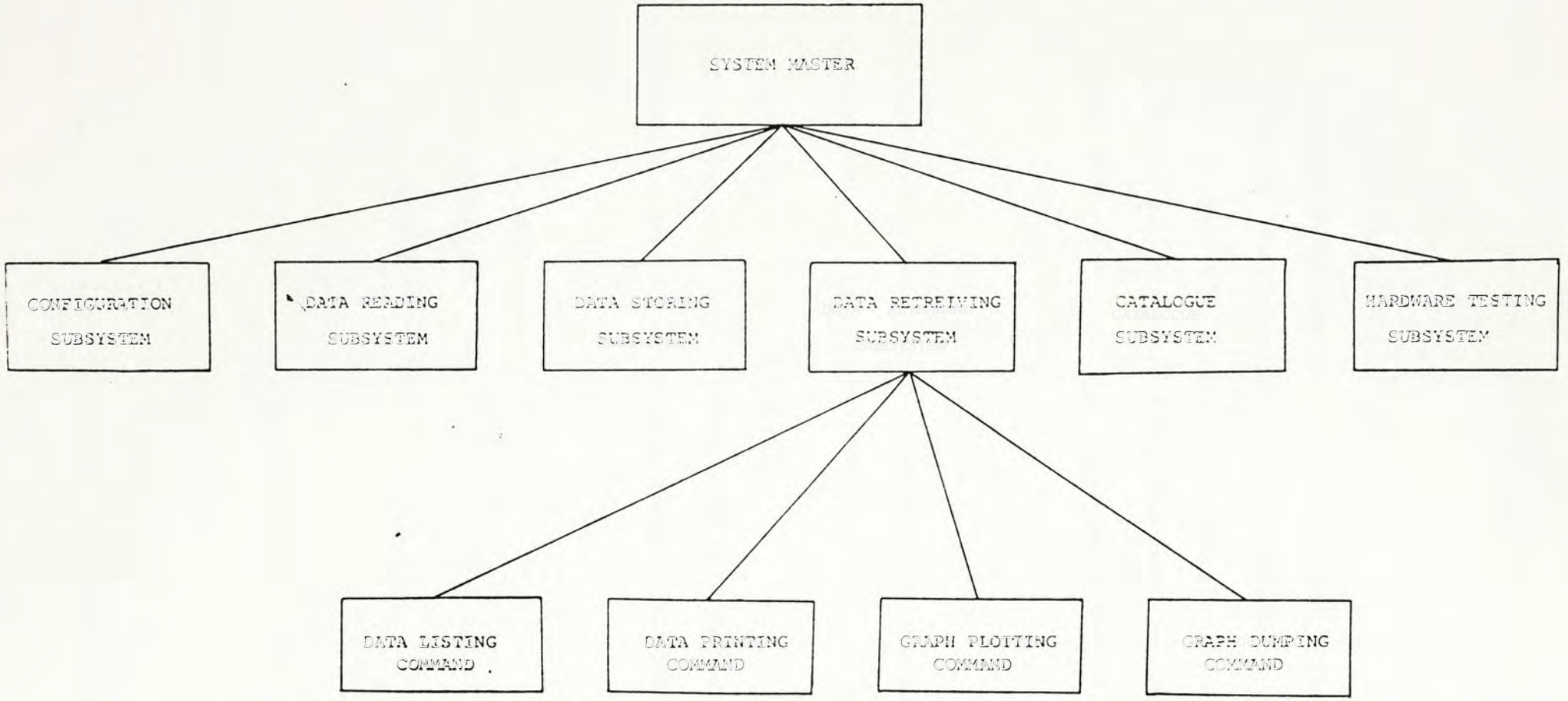

Figure 4.3 The hierarchical structure of the software

graphic interface card, Grappler printer interface card and modified Grappler printer interface card.

4.2.2.2 Data Reading Subsystem

This subsystem transfers the recorded signals from the data logger mentioned previously to the memory of the micro computer. After the completion of byte to byte data transfer, the user will be instructed to input the time, date, year and site of the data being recorded. The data can then be stored with the addition of this information on a diskette by executing the data storing subsystem.

4.2.2.3 Data Storing Subsystem

This subsystem enables users to transfer the recorded data from the memory of the micro computer to a diskette.

4.2.2.4 Data Retrieving Subsystem

This part allows users to retrieve the recorded data from the diskette back into the memory of the micro computer for further analysis and computation.

4.2.2.5 Data Listing Command

Data retrieved either from the diskette or from the data logger can be listed on the screen of a monitor.

4.2.2.6 Data Printing Command

Listing of data in the memory of the micro computer can be executed by this command.

4.2.2.7 Graph Plotting Command

Data retrieved either from a diskette or from the data logger can

be plotted on the screen of a monitor. The horizontal and the vertical axes of the graph are time and the measured quantity (for instance, the amount of solar radiation in this study) respectively. Auto scaling is available and provided. The plotted graph can also be shifted, diminished or enlarged. Printing of hardcopies is also possible by executing the graph dumping command.

4.2.2.8 Graph Dumping Command

If a graphic printer is provided, the graph of the data can be dumped on.

4.2.2.9 Hardware Testing Subsystem

This subsystem enables the users to check the performance of the data logger before going out to the field. When the data logger is being tested, the built-in timer (MC14541) is bypassed. Instead, the clock pulses are controlled and sent under the command of the micro computer through the PIA 8255A (which is built in the interface card) so that the sampled data can be transferred to the memory of the micro computer and displayed on the screen of a monitor instantaneously. By doing so, the performance of the data logger can be checked.

4.2.2.10 Catalogue Subsystem

This part enables users to catalogue the data file diskettes whenever necessary.

4.3 Operation Procedures of the Data Logger

The data logger and the associated software are designed to be

easily operated. The operation procedures are as follows:

(a) Data Collecting Stage

1. Push the Power Switch and the Start-Stop Switch to "off" and "stop" position respectively to reset and clear the memory of the data logger.

2. Select the desired scanning rate by turning the Scanning Rate Selector as indicated on the panel.

3. Select the channel of input by using the Input Type Selector. The data logger can be set to record channel 1, channel 2 or both channels alternately.

4. Connect the sensors to the appropriate channels. Start recording by pushing the Power Switch to "on" position and the Start-Stop Switch to "start" position so that the clock-time is initiated.

5. After the completion of data collection, push the Start-Stop Switch to "stop" position. Be sure that, the Power Switch remains at "on" position, otherwise, the collected data will be lost.

6. The data logger can now be moved to an Apple II+ micro computer for further research.

(b) Data Transferring Stage

1. Boot the master diskette under an Apple II+ micro computer

system.

2. After the main menu of the system appears on the the monitor screen, insert the extension plug of the interface card to the Connection Outlet of the data logger.

3. Push the "arrow" key on the keyboard until the cursor moves to "Data Reading Subsystem", then press the "return" key.

4. Data stored in the 2K RAM of the data logger will be transferred to the memory of the Apple II+ micro computer instantaneously. The user will then be instructed to input the starting time, date, site, scanning rate and the option channel as selected during the recording period. After the information has been input, the user is then asked to check it and press Y if the information is correct and N if any correction needs to be made. This manually input information will be stored for reference at the heading of a diskette data file.

(c) Data Storing Stage

1. Remove the master diskette from the drive and insert an initialized data diskette or a data diskette that has been previously used.

2. Select the data storing subsystem and press "return" key. The user is asked to assign a file name for the data file.

3. Press "return" key, the data is then permanently stored in the data diskette.

The associated software also enables the users to test the performance of the data logger whenever desired. The operation procedures are as follows:

1. Repeat procedures a.2 to a.5.

2. Repeat procedures b.1 to b.3.

3. Select the hardware testing subsystem and press "return" key.

4. Follow the instructions of the subsystem.

5. If the data logger is working properly, signals taken from any transducers, as specified in section 4.2.1.1 and 4.2.1.4, can be instantaneously displayed on the screen. Otherwise, the data logger or the transducers (sensors) should be carefully re-examined.

4.4 Calibration and Testing of the Sensors

There are two sensors designed for the field study of urban Hong Kong solar radiation, conducted by the Department of Geography of the Chinese University of Hong Kong, i.e. the solar sensor and the temperature sensor.

4.4.1 Calibration of the Solar Sensor

The solar panels are individually calibrated against the Solarex Standard Cell, which is standardized using an Eppley Pyranometer (Model 8-48) by Solarex Electric Limited. The maximum intensity of the light

source spectrum for the calibration is 0.88 um. Results of calibration under different level of "full sun" intensity are provided by the manufacturer and shown in Table 4.1.

4.4.2 Testing of the Temperature Sensor

Testing of the linearity of the temperature sensor was carried out at the Environmental Laboratory of the Geography Department of the Chinese University of Hong Kong. The temperature sensor together with a mercury thermometer were placed in a Sanyo incubator (MIR - 251), which is used to generate a temperature ranging from 0 - 50^{o}C. The output voltages of the temperature sensor are directly calibrated against the readings of the mercury thermometer.

Table 4.1 Calibration results of the solar panels against Standard Reference Cell (*)

	(in volts)					(mV)
	Panel 1	Panel 2	Panel 3	Panel 4	Panel 5	SRC
Full sun	4.43	4.45	4.44	4.35	4.45	136
90%	4.00	3.96	3.93	3.92	3.92	122
80%	3.55	3.42	3.48	3.48	3.49	109
70%	3.04	2.99	3.12	3.11	3.14	95
60%	2.92	2.90	2.88	2.84	2.85	82
50%	2.47	2.46	2.41	2.42	2.41	68
40%	1.99	2.01	2.01	2.01	2.01	55
30%	1.57	1.57	1.56	1.58	1.58	41
20%	1.11	1.10	1.11	1.10	1.10	28
10%	0.73	0.73	0.73	0.76	0.73	14
0%	0.00	0.00	0.00	0.00	0.00	0

(*) provided by the Solarex Electric Limited

Remark : SRC stands for Standard Reference Cell.

CHAPTER V

THE EFFECT OF BUILDING MORPHOLOGICAL STRUCTURES

5.1 Introduction

There are many different types of surfaces used on buildings in Hong Kong. The downtown section is characterized by high-rise buildings which are commonly clad with highly reflective materials (curtain-wall). Buildings in the residential and industrial areas are usually smoothly configured and also become higher and higher in order to maximize space utilization. Medium size apartment buildings are typical in suburban areas and Mid-levels. In contrast to the commercial, residential and industrial buildings in the urban area, they are relatively low and ruggedly configured since most of them are balconied.

However, due to limitations on manpower and available resources, only a few types are selected for study. Three buildings are located in the suburban area while the other is located in Tsim Sha Tsui East, which is a newly developed commercial and hotel district. The orientation, colour, height and configuration of the selected buildings are summarised in Table 5.1. Detailed descriptions can be found in section 3.3.1.

When evaluating the effect of building morphological structures on the reception of solar radiation, two basic aspects must be investigated. These include the study of (a) their reflectance indices at various solar geometric conditions; and (b) the amount of increase in solar radiation due to the reflection from the building. In addition, the relationship between

Table 5.1 The physical properties of the four selected wall surfaces

site	orientation	location	height	construction material	configuration	colour
(*) PHCE	90 (east)	suburban	30m	concrete	rugged and balconied	light brown
(**) BMSBE	90 (east)	suburban	20m	concrete	smooth	grey
(#) MHHS	180 (south)	suburban	20m	concrete and with 30% glass coverage	smooth	grey
(##) TSTCE	180 (south)	downtown	45m	aluminium coated reflective glass	smooth	silver

(*) : the east wall of the Postgraduate Hall Complex

(**) : the east wall of the Basic Medical Science Building

(#) : the south wall of the Madam Ho Hall

(##) : the south wall of the Tsim Sha Tsui Centre

the solar altitude, which is defined as the complement to the solar zenith angle, and the reflectance index of the building is also studied through bivariate regression analysis.

5.2 The Reflectance Index

Due to variations in the orientation, cladding material, height, colour and configuration of the selected buildings, their reflectance indices naturally vary. The reflectance index is defined as the ratio of the solar radiation intensity received in front of a wall surface to that at a control site where the reflecting effect is minimized.

5.2.1 Site A : The Postgraduate Hall Complex (east wall)

The wall being investigated is balconied and ruggedly configured (see Plate 3.1). Field measurements were conducted on 03/10/84, 10/10/84 and 24/10/84. Daily variations in the reflectance index with respect to solar altitude and wall-solar azimuth angle are shown in Tables 5.2 to 5.4. The wall-solar azimuth angle (see Figure 5.1) is defined as the angle measured from the sun to the normal of the wall.

The result shows that reflectance index is inversely related to solar altitude and wall-solar azimuth angle; that is, the higher the solar altitude and the wall-solar azimuth angle, the smaller the reflectance index.

The mean intensity of solar radiation received five meters in front of the wall surface is 2.4 mW/cm^2 (5.5%), 0.4 mW/cm^2 (0.73%) and

Table 5.2 The reflectance index of the Postgraduate Hall Complex (east wall) on the 3rd October, 1984.

Hong Kong Local Time	Solar Altitude	Wall-solar Azimuth	Control	Reflected	Reflectance Index
7:40	18	14	23.5	27.3	1.16
7:48	20	15	26.5	29.8	1.12
8:00	22	22	29.3	32.3	1.10
8:08	24	24	33.6	37.3	1.10
8:12	26	25	36.1	38.1	1.05
8:24	28	26	38.9	41.1	1.05
8:32	30	28	42.3	45.3	1.06
8:44	32	30	44.9	47.7	1.06
8:52	34	32	50.7	52.5	1.03
9:04	36	34	53.1	54.4	1.02
9:12	38	35	54.3	56.8	1.04
9:24	40	37	56.9	59.4	1.04
9:36	42	41	58.0	61.0	1.05
9:52	44	43	63.5	65.3	1.03

Remark : the solar altitude and wall-solar azimuth are in degrees and the measured solar radiation intensity is in mW/cm^2.

Table 5.3 The reflectance index of the Postgraduate Hall Complex (east wall) on the 10th October, 1984.

Hong Kong Local Time	Solar Altitude	Wall-solar Azimuth	Control	Reflected	Reflectance Index
8:24	30	21	33.4	37.2	1.12
8:36	32	23	33.8	39.0	1.15
8:44	34	25	41.3	44.5	1.07
8:52	36	26	43.6	46.6	1.07
9:04	38	28	47.6	49.6	1.04
9:12	40	30	49.3	52.2	1.05
9:28	42	32	50.7	52.9	1.04
9:36	44	34	clouds	clouds	clouds
9:48	46	36	clouds	clouds	clouds
9:56	48	38	59.3	59.1	0.99
10:08	50	41	60.5	60.7	1.00
10:20	52	45	61.8	62.9	1.01
10:32	54	49	64.9	63.9	0.98
10:48	56	55	66.2	66.7	1.00
11:00	58	59	67.1	68.7	1.01
11:20	60	68	80.7	79.3	0.98
11:36	61	76	83.4	78.9	0.94

Remark : the solar altitude and wall-solar azimuth are in degrees and the measured solar radiation intensity is in mW/cm^2.

Table 5.4 The reflectance index of the Postgraduate Hall Complex (east wall) on the 24th October, 1984.

Hong Kong Local Time	Solar Altitude	Wall-solar Azimuth	Control	Reflected	Reflectance Index
8:20	26	25	30.2	31.9	1.05
8:28	28	27	34.8	35.9	1.03
8:36	30	28	37.4	38.9	1.04
8:48	32	30	41.3	42.4	1.02
9:00	34	31	43.3	44.9	1.03
9:12	36	33	46.7	47.9	1.03
9:24	38	36	49.7	50.3	1.02
9:32	40	38	52.1	53.1	1.02
9:44	42	40	55.1	55.6	1.01
9:56	44	43	56.3	56.7	1.00
10:04	46	46	57.8	58.6	1.01
10:16	48	50	61.2	60.9	0.99
10:32	50	55	62.7	62.9	1.00
10:48	52	60	65.4	64.6	0.98
11:00	54	64	66.7	66.5	0.99
11:32	56	77	68.8	67.3	0.99
12:00	57	90	69.2	67.3	0.97

Remark : the solar altitude and wall-solar azimuth are in degrees and the measured solar radiation intensity is in mW/cm^2.

Figure 5.1 The geometric illustration of solar altitude and wall-solar azimuth angle .

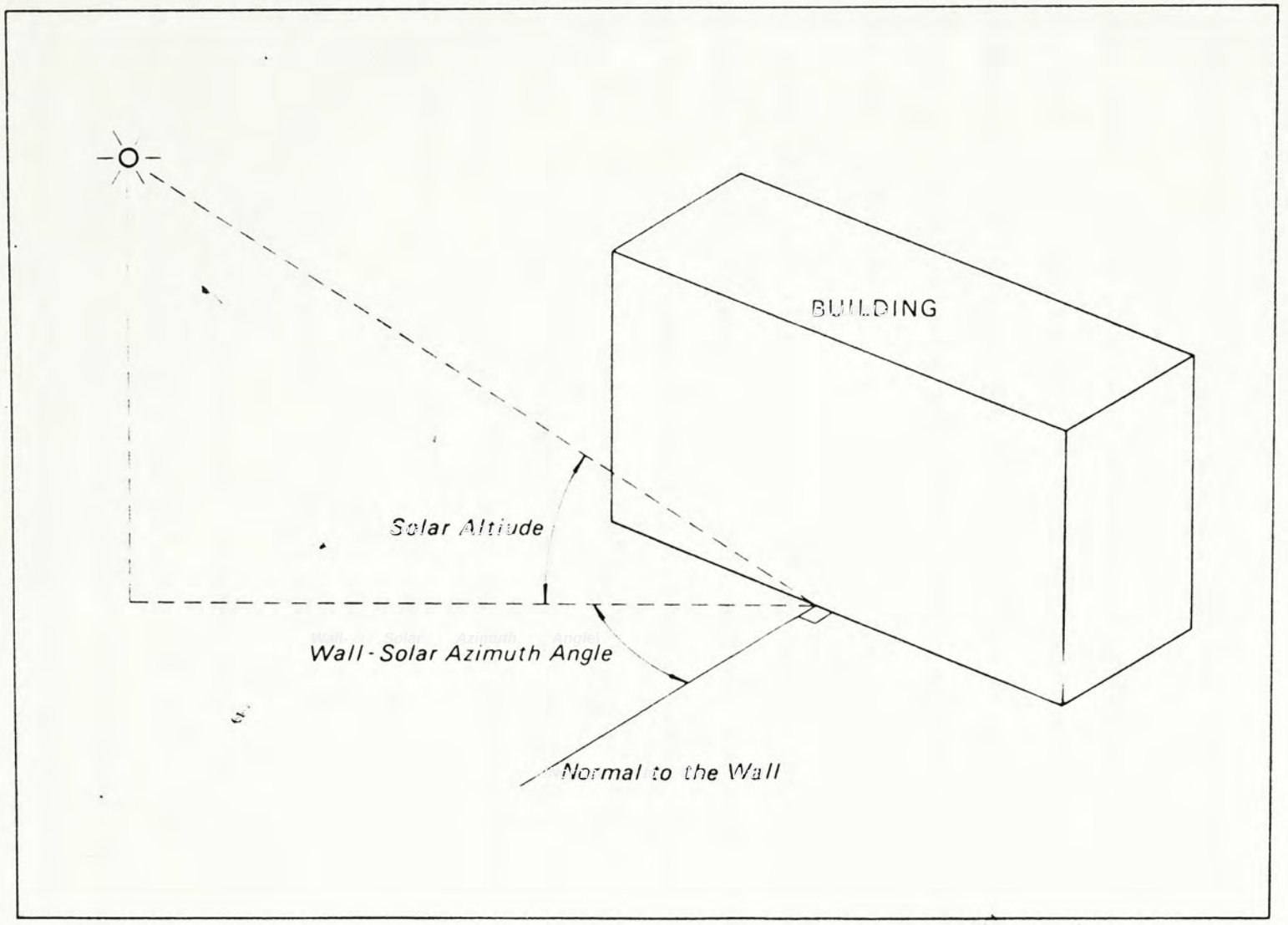

0.5 mW/cm^2 (0.94%) higher than that at the control site on the three field measuring days. However, the results from a paired t-test show that these differences, except for day 1 (03/10/84), are statistically insignificant at the 0.05 level of significance (see Table 5.5).

5.2.2 Site B : The Basic Medical Science Building (east wall)

The wall being studied is rather smoothly configured and is less than 10% covered by glass (see Plate 3.2). Field measurements were conducted on 04/10/84, 12/10/84 and 08/11/84. Tables 5.6 to 5.8 show the daily variations in the reflectance index with respect to solar altitude and wall-solar azimuth angle.

It is shown that the reflectance index of the wall surface is inversely related to solar altitude and wall-solar azimuth angle. The mean solar radiation intensity received in front of the wall surface is 4.1 mW/cm^2 (8.05%), 0.7 mW/cm^2 (1.08%) and 2.4 mW/cm^2 (4.55%) higher than that at the control site on the three field measuring days. In accordance with the results from a paired t-test, these differences are all statistically significant at the 0.05 level (Table 5.9).

5.2.3 Site C : The Madam Ho Hall (south Wall)

The wall of the building facing south is selected for study. More than 30% of the wall is covered with glass and it is smoothly configured (see Plate 3.3). Field measurements were conducted on 12/10/84, 20/10/84 and 29/10/84. Daily variations in the reflectance index in relation to solar altitude and wall-solar azimuth angle are illustrated in Tables 5.10

Table 5.5 The paired t-test for comparison of the mean intensity of solar radiation being received in front of the east wall of the PHC[1] and that at the control site

experimental date		(*) mean	mean (**) difference	simple correlation	t value	# df	2-tail prob.
03/10/84	wall	46.3	2.4 (5.5%)	0.999	19.06	34	0.00
	control	43.8					
10/10/84	wall	60.7	0.4 (0.73%)	0.996	1.05	29	0.35
	control	60.3					
24/10/84	wall	56.4	0.5 (0.94%)	0.999	0.69	54	0.49
	control	55.9					

PHC[1] : the Postgraduate Hall Complex

* : mean solar radiation intensity in mW/cm^2

** : the mean of difference between the paired observations

\# : degrees of freedom

Table 5.6 The reflectance index of the Basic Medical Science Building (east wall) on the 4th October, 1984.

Hong Kong Local Time	Solar Altitude	Wall-solar Azimuth	Control	Reflected	Reflectance Index
8:04	26	17	31.1	39.2	1.26
8:12	28	18	32.3	39.7	1.23
8:24	30	20	35.3	42.4	1.20
8:32	32	21	37.8	45.4	1.19
8:40	34	22	41.0	46.4	1.13
8:56	38	26	44.5	49.4	1.11
9:04	40	27	45.7	50.9	1.11
9:16	42	30	49.3	53.3	1.08
9:24	44	31	51.8	55.4	1.06
9:32	46	33	54.8	58.4	1.06
9:48	48	36	61.7	64.8	1.05
10:00	50	39	62.7	66.1	1.05
10:12	52	42	65.4	66.9	1.02
10:20	54	45	69.0	69.6	1.00
10:28	56	49	71.2	70.4	0.98

Remark : the solar altitude and wall-solar azimuth are in degrees and the measured solar radiation intensity is in mW/cm^2.

Table 5.7 The reflectance index of the Basic Medical Science Building (east wall) on the 12th October, 1984.

Hong Kong Local Time	Solar Altitude	Wall-solar Azimuth	Control	Reflected	Reflectance Index
8:00	24	20	37.0	40.2	1.08
8:08	26	21	39.6	43.2	1.09
8:20	28	22	42.9	45.5	1.05
8:28	30	23	48.8	51.1	1.04
8:36	32	24	47.9	51.0	1.06
8:48	34	27	clouds	clouds	clouds
8:56	36	28	clouds	clouds	clouds
9:08	38	30	clouds	clouds	clouds
9:16	40	32	clouds	clouds	clouds
9:28	42	34	57.8	58.4	1.01
9:36	44	36	58.6	60.3	1.02
9:48	46	39	60.7	61.9	1.02
10:00	48	42	62.0	63.5	1.02
10:12	50	45	64.3	65.2	1.01
10:24	52	49	67.1	67.1	1.00
10:36	54	53	67.7	68.4	1.01
10:52	56	31	68.8	69.5	1.01
11:08	58	65	70.5	71.6	1.01
11:42	60	76	72.8	71.1	0.97

Remark : the solar altitude and wall-solar azimuth are in degrees and the measured solar radiation intensity is in mW/cm^2.

Table 5.8 The reflectance index of the Basic Medical Science Building (east wall) on the 8th November, 1984.

Hong Kong Local Time	Solar Altitude	Wall-solar Azimuth	Control	Reflected	Reflectance Index
8:12	20	28	26.0	31.7	1.21
8:24	22	30	29.2	34.3	1.17
8:32	24	31	32.1	36.8	1.14
8:44	26	33	32.3	35.5	1.10
8:52	28	34	33.6	37.7	1.11
9:04	30	36	42.3	45.8	1.08
9:16	32	38	41.5	44.3	1.07
9:20	34	39	45.5	49.4	1.08
9:32	36	42	47.4	51.1	1.07
9:48	38	45	52.9	55.6	1.05
10:00	40	48	55.0	57.3	1.04
10:08	42	51	55.9	58.6	1.04
10:20	44	54	57.4	59.9	1.04
10:36	46	59	60.1	62.0	1.03
11:52	48	62	62.3	64.2	1.01
11:56	52	90	64.5	63.9	0.99

Remark : the solar altitude and wall-solar azimuth are in degrees and the measured solar radiation intensity is in mW/cm^2.

Table 5.9 The paired t-test for comparison of the mean intensity of solar radiation being received in front of the east wall of the BMSB[1] and that at the control site

experimental date		(*) mean	mean (**) difference	simple correlation	t value	# df	2-tail prob.
04/10/84	wall	55.1	4.1 (8.05%)	0.997	10.82	35	0.00
	control	50.9					
12/10/84	wall	61.9	0.6 (1.08%)	0.995	2.40	37	0.02
	control	61.3					
24/10/84	wall	54.4	2.4 (4.55%)	0.998	9.49	52	0.00
	control	52.4					

BMSB[1] : the Basic Medical Science Building

* : mean solar radiation intensity in mW/cm^2

** : the mean of difference between the paired observations

\# : degrees of freedom

Table 5.10 The reflectance index of the Madam Ho Hall (south wall) on the 12th October, 1984.

Hong Kong Local Time	Solar Altitude	Wall-solar Azimuth	Control	Reflected	Reflectance Index
13:56	52	41	65.7	67.8	1.03
14:16	50	45	63.1	64.2	1.02
14:32	48	48	61.1	62.7	1.02
14:40	46	51	59.5	60.9	1.02
14:48	44	54	56.7	58.4	1.02
15:00	42	56	54.4	55.8	1.02
15:08	40	58	51.6	53.3	1.03
15:20	38	60	49.7	50.9	1.02
15:28	36	62	46.9	48.2	1.02
15:36	34	63	44.9	46.1	1.02
15:52	32	65	42.3	43.4	1.02
15:56	30	67	38.7	39.8	1.02
16:08	28	68	37.0	38.4	1.03
16:24	26	69	34.6	35.5	1.02
16:28	24	70	29.4	29.5	1.00
16:36	22	71	27.7	28.7	1.03
16:48	20	73	22.2	23.5	1.06

Remark : the solar altitude and wall-solar azimuth are in degrees and the measured solar radiation intensity is in mW/cm^2.

Table 5.11 The reflectance of the Madam Ho Hall (south wall) on the 20th October, 1984.

Hong Kong Local Time	Solar Altitude	Wall-solar Azimuth	Control	Reflected	Reflectance Index
14:24	42	51	52.7	53.8	1.02
14:36	40	54	50.8	52.2	1.02
14:44	38	55	47.5	48.5	1.02
15:00	36	57	44.5	46.3	1.03
15:04	34	59	38.8	40.7	1.05
15:20	32	61	37.3	39.5	1.05
15:24	30	62	33.1	35.0	1.05
15:36	28	64	31.2	33.1	1.06
15:48	26	65	27.8	30.2	1.08
15:54	24	66	26.3	28.9	1.09
16:04	22	68	23.7	26.2	1.10
16:12	20	69	20.6	23.4	1.13
16:24	18	70	17.9	20.5	1.14
16:32	16	71	14.9	17.5	1.16
16:40	14	72	13.1	15.4	1.17
16:48	12	73	10.7	12.6	1.17

Remark : the solar altitude and wall-solar azimuth are in degrees and the measured solar radiation intensity is in mW/cm^2.

to 5.12.

The result indicates that the reflectance index is inversely related to solar altitude but positively related to wall-solar azimuth angle; that is, the larger wall-solar azimuth angle, the larger the reflectance index, whereas the higher the solar altitude, the smaller the reflectance index.

The mean solar radiation intensity received five meters in front of the wall surface is 2.1 mW/cm^2 (7.52%), 2.0 mW/cm^2 (6.59%) and 2.9 mW/cm^2 (5.94%) higher when compared with the control site on the three field measuring days. The results from a paired t-test illustrate that these differences are significant at the 0.05 level of significance (Table 5.13).

5.2.4 Site D : The Tsim Sha Tsui Centre (south wall)

The south wall of the Tsim Sha Tsui Centre, which is located in Tsim Sha Tsui East (a newly developed retailing and hotel district), is selected for study. The building is fully clad with highly reflective glass and smoothly configured (see Plate 3.4). Field measurements were conducted on 27/01/85 and 02/02/85. Tables 5.14 and 5.15 show the daily variation in the reflectance index with respect to solar altitude and wall-solar azimuth angle.

The reflectance index of the wall surface also shows an inverse relationship with solar altitude but a positive relationship with wall-solar azimuth angle.

The mean solar radiation intensity is 3.5 mW/cm^2 (11.19%) and 4.1 mW/cm^2 (8.37%) higher than that at the control site on the two field

Table 5.12 The reflectance index of the Madam Ho Hall (south wall) on the 29th October,1984.

Hong Kong Local Time	Solar Altitude	Wall-solar Azimuth	Control	Reflected	Reflectance Index
12:04	54	2	62.8	64.8	1.03
12:56	52	22	60.7	64.6	1.03
13:12	50	29	59.0	62.0	1.05
13:28	48	34	56.5	60.7	1.07
13:48	46	39	54.3	58.6	1.07
14:00	44	42	51.8	55.2	1.06
14:16	42	45	51.2	54.5	1.06
14:28	40	48	46.9	50.3	1.07
14:40	38	51	44.0	47.9	1.09
14:44	36	53	41.5	45.1	1.08
15:00	34	55	40.2	43.4	1.08
15:20	30	58	34.4	37.8	1.09
15:28	28	60	31.7	34.9	1.10
15:36	26	61	29.0	32.3	1.11
15:44	24	62	26.6	29.1	1.09
15:56	22	64	23.0	24.8	1.07

Remark : the solar altitude and wall-solar azimuth are in degrees and the measured solar radiation intensity is in mW/cm^2

Table 5.13 The paired t-test for comparison of the mean intensity of solar radiation being received in front of the south wall of the MHH[1] that and at the control site

experimental date		(*) mean	mean (**) difference	simple correlation	t value	# df	2-tail prob.
12/10/84	wall	29.8	2.1 (7.52%)	0.997	11.47	28	0.00
	control	27.7					
20/10/84	wall	32.3	2.0 (6.59%)	1.000	23.08	35	0.00
	control	30.3					
29/10/84	wall	51.6	2.9 (5.94%)	0.998	24.55	58	0.00
	control	48.7					

MHH[1] : the Madam Ho Hall

* : mean solar radiation intensity in mW/cm^2

** : the mean of difference between the paired observations

\# : degrees of freedom

Table 5.14 The reflectance index of the Tsim Sha Tsui Center (south wall) on the 19th January, 1985.

Hong Kong Local Time	Solar Altitude	Wall-solar Azimuth	Control	Reflected	Reflectance Index
13:12	36	40	51.5	55.3	1.07
13:28	34	43	49.2	52.3	1.06
13:44	32	45	44.3	46.6	1.05
13:56	30	48	40.5	43.8	1.08
14:12	28	50	38.0	41.7	1.09
14:20	26	52	34.2	38.3	1.12
14:28	24	54	31.8	35.9	1.12
14:36	22	55	29.5	33.7	1.14
14:52	20	57	27.2	30.8	1.13
14:56	18	58	25.3	28.8	1.13
15:08	16	60	19.2	23.0	1.20
15:20	14	61	16.3	19.5	1.20
15:28	12	62	14.1	17.5	1.23
15:36	10	63	11.8	14.8	1.25
15:48	8	64	10.0	12.2	1.22

Remark : the solar altitude and wall-solar azimuth are in degrees and the measured solar radiation intensity is in mW/cm^2.

Table 5.15 The reflectance index of the Tsim Sha Tsui Center (south wall) on the 2nd February,1985.

Hong Kong Local Time	Solar Altitude	Wall-solar Azimuth	Control	Reflected	Reflectance Index
12:04	52	2	62.2	68.7	1.10
12:52	50	21	59.1	65.6	1.11
13:12	48	28	56.5	64.4	1.13
13:28	46	33	53.8	62.1	1.15
13:44	44	37	52.1	60.1	1.15
13:48	42	40	51.3	58.5	1.13
13:56	40	43	50.6	57.3	1.13
14:04	38	46	46.5	52.3	1.14
14:16	36	49	43.6	50.5	1.15
14:28	34	51	41.1	47.8	1.16
14:40	32	52	38.9	46.0	1.18
14:48	30	55	36.8	42.4	1.15
15:04	28	57	33.3	40.5	1.21
15:08	26	59	31.1	35.9	1.15
15:20	24	60	29.0	34.6	1.19
15:28	22	61	24.6	26.6	1.19
15:40	20	63	20.3	24.1	1.18

Remark : the solar altitude and wall-solar azimuth are in degrees and the measured solar radiation intensity is in mW/cm^2.

measuring days. The results from a paired t-test shows that these differences are significant at the 0.05 level (Table 5.16). It also seems that the difference is much more marked in contrast to the other experimental sites.

From the results of the above analysis, it can be concluded that the solar radiation intensity received in front of a wall surface during periods of sunlight is generally higher than that at the control site where the reflective effect is minimized.

Moreover, the reflectance index of the wall surface is inversely related to the solar altitude as a larger reflectance index occurs at a lower solar altitude. However, the relationship between the reflectance index and the wall-solar azimuth angle seems to be determined by the orientation of the wall. The relationship will be negative if the wall is east facing, whereas the relationship will be positive if the wall is south facing.

Furthermore, it is also observed that the percentage of radiation difference at the monitoring site of the Tsim Sha Tsui center seems to be more marked in comparison with the other experimental sites.

5.3 The Relationship Between Reflectance Index and Solar Altitude

From the preceding section, it seems that the reflectance index of a building has an inverse relationship with solar altitude. In order to demonstrate the nature of the relationship, bivariate regression analysis is employed. It provides not only the the magnitude of the trend, but also

Table 5.16 The paired t-test for comparison of the mean intensity of solar radiation being received in front of the south wall of the TSTC[1] and that at the control site

experimental date		(*) mean	mean (**) difference	simple correlation	t value	# df	2-tail prob.
27/01/85	wall	34.9	3.6 (11.19%)	0.999	37.21	38	0.00
	control	31.3					
02/02/85	wall	52.5	4.0 (8.37%)	0.996	26.61	58	0.00
	control	48.5					

TSTC[1] : the Tsim Sha Tsui Centre

* : mean solar radiation intensity in mW/cm^2

** : the mean of difference between the paired observations

\# : degrees of freedom

the sign of the change. Solar altitude is taken as the independent variable while reflectance index is taken as the dependent variable.

From the application of bivariate regression analysis, the equations produced are as follows :

$$Y_R = -0.003X + 1.159 \text{ (PGHCE)}$$

$$Y_R = -0.004X + 1.257 \text{ (BMSBE)}$$

$$Y_R = -0.002X + 1.156 \text{ (MHHS)}$$

$$Y_R = -0.003X + 1.259 \text{ (TSTCS)}$$

Where X = the solar altitude in degrees

Y_R = the reflectance index

PHCE = the east wall of the Postgraduate Hall Complex

BMSBE = the east wall of the Basic Medical Science Building

MHHS = the south wall of Madam Ho Hall

TSTCS = the south wall of Tsim Sha Tsui Centre

In order to substantiate whether the variability of the reflectance index is significantly related to the independent variable (solar altitude), the overall F-test for the goodness of the fit of the model and the F-test for the regression coefficient are employed (see Tables 5.17 and 5.18). It is shown that not only the linearity of the models but also the regression coefficients are significant at the 0.05 level. The high significance level for the regression coefficient of the solar altitude implies that it can significantly explain the variation in the reflectance

Table 5.17 The overall F-test for the goodness of fit of regression coefficients (dependent variable: reflectance index)

site	multiple R	R square	df (N-1, M-N-1)	F value	sign. level
PHCE(*)	0.85433	0.72988	1 118	318.83	<0.05
BMSBE(**)	0.88528	0.78372	1 125	241.10	<0.05
MHHS(#)	0.75077	0.56365	1 122	157.59	<0.05
TSTCS(##)	0.91076	0.82949	1 96	467.01	<0.05

Multiple R = the multiple correlation coefficient

R square = the square of the multiple correlation coefficient

df = degrees of freedom

PHCE(*) = the east wall of the Postgraduate Hall Complex

BMSBE(**) = the east wall of the Basic Medical Science Building

MHHS(#) = the south wall of the Madam Ho Hall

TSTCS(##) = the south wall of the Tsim Sha Tsui Centre

Table 5.18 The F-test for the regression coefficients (dependent variable: the reflectance index)

site	Variable	B	Beta	STD error B	df (1, M-N-1)	F value	sign. level
1 PHCE	solar altitude constant	-0.0030 1.1594	-0.854	0.00017	1, 118	318.83	<0.05
2 BMSBE	solar altitude constant	-0.0046 1.2573	-0.885	0.00022	1, 125	452.94	<0.05
3 MHHS	solar altitude constant	-0.0022 1.1565	-0.750	0.00018	1, 122	157.59	<0.05
4 TSTCS	solar altitude constant	-0.0038 1.2591	-0.910	0.00018	1, 96	467.01	<0.05

^{1}PHCE = the east wall of the Postgraduate Hall Complex

^{2}BMSBE = the east of the Basic Medical Science Building

^{3}MHHS = the south wall of the Madam Ho Hall

^{4}TSTCS = the south wall of the Tsim Sha Tsui Centre

index at each experimental site. Since the regression coefficients are all found to be negative, the existence of a negative relationship between the reflectance index of building morphological structure and solar altitude is substantiated.

Although buildings reflect incoming solar radiation, they, on the other hand, block a considerable portion of diffuse radiation. Usually, the intensity of diffuse radiation becomes relatively higher at mid-day, and its proportion of the total horizontal solar radiation is also comparatively larger. This then implies that the absolute intensity of solar radiation blocked by the building will increase when the solar altitude becomes higher. Therefore, it is not surprising that the reflectance index tends to decrease and even becomes smaller than one when the solar altitude becomes higher. This is because the difference between the reflected radiation and the amount of solar radiation blocked by the building is continuously reduced. When the reflected radiation is less than the blocked diffuse radiation, the reflectance index will be smaller than one.

Interestingly, from the results in the above, it is indicated that the reflectance index of the south wall of Tsim Sha Tsui Centre is comparatively higher at any solar altitude which may be due to its highly reflective cladding material (curtain-wall). A comparative low reflectance index is found for the east wall of the Postgraduate Hall Complex which is believed to be due to the ruggedness and non-reflective cladding material of the wall. Also, the reflectance indices of south facing walls (the south walls of Tsim Sha Tsui Center and the Madam Ho Hall) are never found to be smaller than one during the field measurements, perhaps this is

because the relatively high reflectivity of the buildings due to the larger portion of glass coverage or the highly reflective cladding material.

5.4 Conclusion and Discussion

The reflectance index of the building morphological structure is found to be negatively correlated with the solar altitude. Usually, the higher the solar altitude, the smaller the reflectance index is. When the reflectance index is smaller than one, it implies that the solar radiation intensity received in front of the building is lower than that at the control site. This is because the increased reflected solar radiation cannot compensate for the loss of diffuse radiation blocked by the building. The maximum reflectance index of the selected building morphological structures range from 1.06 at the Postgraduate Hall Complex to 1.24 at the Tsim Sha Tsui Center.

The reflectance index of the building morphological structures is mathematically modelled in a simple way as the experimental sites are selected in such a way that the effects of the canyon geometry of other buildings are minimized. It is expected that a model of the reception of total solar radiation in a city canyon composed of many high-rise buildings, as in urban Hong Kong, will be much more difficult and complicated since the shading and multi-reflective effects of other building on the direct and diffuse radiation will have to be taken into consideration.

Although the intensity of solar radiation received in front of the

wall surface is generally higher, the intensity of solar radiation on the other side of the building is believed to be remarkably lower since it is deprived of the reception of direct solar radiation. The difference in the reception of solar radiation at different sides of the building may inevitably create a micro-climate effect on different sides of the building.

CHAPTER VI

SPATIAL VARIATION OF SOLAR RADIATION INTENSITY

6.1 Introduction

The main theme of this section of the study is to measure the spatial variation in solar radiation intensity in Hong Kong. This includes the study of the variation of horizontal and diffuse radiation intensity between urban and suburban areas, and the vertical variation in horizontal solar radiation intensity in the urban area. By employing one-way analysis of variance and the paired t-test, the significance of suburban-urban variation in the intensity for both horizontal and diffuse radiation may be evaluated. The temporal variation of the vertical difference in the horizontal solar radiation will also be determined through the bivariate regression analysis. The horizontal solar radiation will be referred to as solar radiation in the rest of the chapter unless specified.

The suburban sampling site is located at the Meteorological Station of the Geography Department of the Chinese University of Hong Kong, which is about 12 km NNE of the downtown area of Hong Kong. The air quality of this monitoring location was classified as clean by Yau (1982) and the mean concentration of total suspended particulates (TSP) is less than 150 ug/m^3. Major atmospheric aerosols and particulates are believed to come from (1) the reclamation at the south-east fringe of the campus in Tolo Harbour; (2) the daily meet-class shuttle buses; and (3) the flow of traffic along Tai Po Road, which links the Kowloon urban area and the northern part of the New Territories, and winds past the western fringe of

the campus.

Two urban reference sites are located at different heights in Sham Shui Po District. The lower monitoring site is on the roof of a residential building, while the upper monitoring site is at the top of a knoll with elevation of 120 meters. The two monitoring sites are 100 meters apart vertically and 150 meters apart horizontally (see section 3.4.1.2 and 3.4.1.3).

Liang (1972) classified Sham Shui Po as a typical commercial and residential district. In this district, retailing and service businesses dominate at the ground floor, whereas the upper floors are used for residential and industrial purposes. According to the 1981 Hong Kong population census, the population density of this district is the highest in Hong Kong.

Due to the complex land use pattern and the dense population in this district, considerable anthropogenic pollutants and aerosols are believed to be discharged into the atmosphere, especially in the near-ground layer. These pollutants and aerosols mainly come from the heavy flow of traffic; the public and private construction; the numerous restaurants, cooked food shops, bakeries and roasted meat shops; and various industrial activities in this district. Apart from the pollutants and aerosols derived locally, atmospheric aerosols may also come from the nearby industrial and commercial areas such as Mong Kok, Cheung Sha Wan and Lai Chi Kok.

Other major pollution point sources exist to the west, including Lai Chi Kok Incinerator (1 km) and the Peninsula oil-fired power station (6 km). Kwai Chung Incinerator lies roughly 4 km to the north-west.

Undesirable gaseous pollutants and aerosols are discharged into the atmosphere whenever the power station and the incinerators are in operation. Sham Shui Po District will be downwind from these sources when westerly and northwesterly winds prevail.

6.2 Suburban-urban Variation of Solar Radiation Intensity

To assess the suburban-urban variation in solar radiation intensity, a total of thirty-two sampling hours were conducted within the period of field work. Visual examination of the data shows that the intensity of solar radiation received at the suburban reference site seems to be stronger when compared with either the upper or the lower urban site.

In order to determine whether there is a significant difference in the solar radiation intensity among the three monitoring sites, one-way analysis of variance is performed (section 3.4.3.1).

The result shows that the between areas mean squares is 6181.82, while the within areas mean squares is 973.06. The F-value, thus, is 6.353, and an observed significance level of 0.0018 is obtained by a comparison to the F-distribution with 2 and 785 degrees of freedom (see Table 6.1). The null hypothesis that the mean intensity of solar radiation among the three monitoring sites is equivalent is rejected at the 0.05 level.

Although the result of the one-way analysis of variance indicates that there is a significant difference in the mean solar radiation intensity among the monitoring sites, it fails to give any idea on which

Table 6.1 The result of one-way analysis of variance

source	(*) df	sum of square	mean square	F value	level of significance
between areas	2	12363.6	6181.82		
within areas	785	763858.0	973.6	6.353	0.0018
total	787	776221.6			

(*) : degrees of freedom

means are significantly different from each other since the between areas variability may be enlarged due to an extreme value of a mean. To further substantiate which means are significantly different from each other, paired t-test method is performed.

The result shows that the mean intensity of solar radiation received at the suburban reference site on the sampling days is significantly higher than that at the upper urban site at the 0.05 level of significance (see Table 6.2). Based on thirty-two hours of sampling data, the mean intensity of solar radiation at the suburban reference site is 2.9 mW/cm^2(5.16%) higher than that at the upper urban site. The difference in the mean intensity of solar radiation varies from 4.7 mW/cm^2(7.33%) to 1.2 mW/cm^2(1.80%) on different sampling days.

The mean intensity of solar radiation received at the suburban reference site is also significantly higher than that at the lower urban site at the 0.05 level of significance on the sampling days (see Table 6.3). The mean intensity of solar radiation at the suburban reference site is 3.4 mW/cm^2(6.29%) higher in comparison with the lower urban site. The difference in the mean intensity of solar radiation varies from 6.9 mW/cm^2(10.76%) to 1.6 mW/cm^2(3.13%) on different sampling days.

From the results of the analyses above, it may be concluded that the intensity of solar radiation in the suburban area is significantly higher than that in either the upper or lower urban sites. Also, the attenuation of solar radiation at the lower urban site seems to be stronger when compared to the upper urban site. Detailed investigation on the vertical variation of the solar radiation will be presented in section 6.4.

Table 6.2 The paired t-test for the comparison of the mean solar radiation intensity of the suburban reference site (SRS) and that of the upper urban site (UUS)

experimental date		(1) mean	mean (2) difference	simple correlation	t value	(3) df	2-tail prob.
21/10/84	SRS	64.1	4.7 (7.33%)	0.992	11.99	57	0.00
	UUS	59.4					
22/10/84	SRS	66.6	1.2 (1.80%)	0.989	8.27	33	0.00
	UUS	65.4					
26/10/84	SRS	60.9	2.4 (3.94%)	0.973	5.76	44	0.00
	UUS	58.5					
(#) 04/11/84	SRS	52.3	2.9 (5.54%)	0.996	19.28	58	0.00
	UUS	49.4					

Table 6.2 The paired t-test for the comparison of the mean solar radiation intensity of the suburban reference site (SRS) and that of the upper urban site (UUS) (con't)

05/11/84	SRS UUS	50.0 46.5	3.5 (7.00%)	0.997	24.95	63	0.00
23/11/84	SRS UUS	48.9 47.1	1.8 (3.68%)	0.994	9.99	58	0.00
overall	SRS UUS	56.1 53.2	2.9 (5.16%)	0.986	23.78	320	0.00

(1) : mean horizontal solar radiation intensity in mW/cm^2

(2) : the mean of difference between the paired observations

(3) : degrees of freedom

(#) : no lower urban site measurement is conducted

Table 6.3 The paired t-test for the comparison of the mean solar radiation intensity of the suburban reference site (SRS) and that of the lower urban site (LUS)

experimental date		(1) mean	mean (2) difference	simple correlation	t value	(3) df	2-tail prob.
21/10/84	SRS	64.1	6.9 (10.76%)	0.988	17.82	57	0.00
	LUS	57.2					
(*) 22/10/84	SRS	56.8	2.2 (3.87%)	0.997	9.76	61	0.00
	LUS	54.6					
(#) 26/10/84	SRS	60.9	3.3 (5.41%)	0.977	7.40	44	0.00
	LUS	57.6					
05/11/84	SRS	50.0	4.2 (8.40%)	0.996	29.60	63	0.00
	LUS	45.8					
(#) 21/11/84	SRS	51.1	1.6 (3.13%)	0.998	12.81	61	0.00
	LUS	49.5					

Table 6.3 The paired t-test for the comparison of the mean solar radiation intensity of the suburban reference site (SRS) and that of the lower urban site (LUS) (con't)

23/11/84	SRS LUS	48.9 46.0	2.9 (5.93%)	0.996	19.87	58	0.00
(#) 24/11/84	SRS LUS	46.8 43.7	3.1 (6.62%)	0.999	35.49	68	0.00
overall	SRS LUS	54.0 50.6	3.4 (6.29%)	0.986	31.63	420	0.00

(1) : mean horizontal solar radiation intensity in mW/cm^2

(2) : the mean of difference between the paired observations

(3) : degrees of freedom

(*) : the experimental field measurment is started one and half hour later

(#) : no upper urban site measurement is conducted

6.3 Suburban-urban Variation of Diffuse Radiation

Atmospheric pollutants not only attenuate the incoming solar radiation, but also increase the amount of diffuse solar radiation. Usually when more atmospheric aerosols, dust, gaseous pollutants and airborne particulates are found, the intensity of diffuse radiation is stronger. It is therefore expected that the intensity of diffuse radiation will be higher in the urban area due to the contamination of its atmosphere with aerosols and pollutants. To assess the suburban-urban variability of diffuse radiation, a total of fifteen sampling hours were conducted within the period of field work.

Visual examination of the collected data shows that the mean diffuse radiation intensity at the lower monitoring site in the urban area seems to be higher than that of the suburban reference site on the sampling days. These differences range from 0.1 mW/cm^2(1.37%) to 1.2 mW/cm^2(15.58%).

In order to determine whether the mean diffuse radiation intensity at the lower urban site is significantly higher than that at the suburban reference site, the paired t-test method is employed. Its result shows that these differences are not all significant at the 0.05 level of significance. However, the overall mean diffuse radiation intensity of the lower urban site is 0.4 mW/cm^2(5.19%) higher when compared with that of the suburban reference area (see Table 6.4).

6.4 Vertical Variation of Solar Radiation Intensity

In this section of the study, the focus is directed towards a

Table 6.4 The paired t-test for the comparison of the mean diffuse radiation intensity of the suburban reference site (SRS) and that of the lower urban site (LUS)

experimental date		(1) mean	mean (2) difference	simple correlation	t value	(3) df	2-tail prob.
25/11/84	SRS	7.3	-0.1 (-1.37%)	0.876	-1.06	59	0.29
	LUS	7.4					
26/11/84	SRS	7.7	-1.2 (-15.58%)	-0.359	-18.87	50	0.00
	LUS	8.9					
01/12/84	SRS	8.3	-0.1 (-1.20%)	0.473	-0.88	57	0.38
	LUS	8.4					
06/12/84	SRS	7.0	-0.3 (-4.29%)	0.954	-5.32	33	0.00
	LUS	7.3					
overall	SRS	7.7	-0.4 (-5.19%)	0.741	-8.63	202	0.00
	LUS	8.1					

(1) : mean diffuse radiation intensity in mW/cm^2
(2) : the mean of difference between the paired observations
(3) : degrees of freedom

comparison of the reception of solar radiation at the lower site and at the upper site in the urban area. The temporal variation of the vertical difference in the reception of solar radiation is also investigated.

In order to assess the vertical variation in the reception of solar radiation, a total of twenty-three sampling hours have been conducted within the period of field work. The result shows that the reception of solar radiation at the upper urban site is not consistently higher than that of the lower urban site and undergoes daily variation (see Table 6.5). It is found that the mean intensity of solar radiation received at the lower urban site on 22nd October, 1984 is even slightly higher than that of the upper urban site. However, the difference is extremely small (0.2 mW/cm^2) and is less than instrument error, therefore, it may be assumed that there is no difference in the reception of solar radiation intensity between the two sites on that day.

To determine the significance of the radiation difference between the upper site and the lower site in the urban area, the paired t-test method is employed. The result (see Table 6.6) shows that the daily solar radiation received at the upper urban site is not always significantly higher than that of the lower urban site at the 0.05 level of significance. Overall, the reception of solar radiation at the upper urban site is 1.1 mW/cm^2(1.98%) higher in comparison with that at the lower urban site.

6.4.1 Trend Analysis of the Vertical Difference

Visual examination of the collected data from the monitoring sites shows that the vertical difference in the intensity of solar radiation seems to decrease as the solar altitude becomes higher. In order to

Table 6.5 The mean solar radiation intensity received at upper and lower sites of the urban area in mW/cm^2

date	upper urban site	lower urban site	difference
20/10/84	61.9	60.8	1.1
21/10/84	59.5	57.2	2.3
22/10/85	65.4	65.6	-0.2
26/10/84	57.6	56.7	0.9
05/11/84	46.5	45.8	0.7
23/11/84	47.1	46.0	1.1
overall	55.5	54.4	1.1

Table 6.6 The paired t-test for the comparison of the mean solar radiation intensity being received at the UUS (1) and LUS (2) in mW/cm^2

experimental date		(3) mean	mean (4) difference	simple correlation	t value	(5) df	2-tail prob.
20/10/84	UUS	61.9	1.1 (1.77%)	0.999	8.50	59	0.00
	LUS	60.8					
21/10/84	UUS	59.5	2.3 (3.86%)	0.999	33.30	57	0.00
	LUS	57.2					
22/10/84	UUS	65.4	-0.2 (-0.003%)	0.995	-1.52	33	0.14
	LUS	65.6					
26/10/84	UUS	57.6	0.9 (1.56%)	0.998	8.72	52	0.00
	LUS	56.7					

(1) : upper urban site
(2) : lower urban site
(3) : the mean intensity of the horizontal solar radiation in mW/cm^2
(4) : the mean of the difference between the paired observation
(5) : the degrees of freedom

Table 6.6 The paired t-test for the comparison of the mean solar radiation intensity being received at the UUS and LUS in mW/cm^2 (con't)

experimental date	(1)(2)	(3) mean	mean (4) difference	simple correlation	t value	(5) df	2-tail prob.
05/11/84	UUS	46.5	0.7 (1.51%)	0.997	4.51	63	0.00
	LUS	45.8					
23/11/84	UUS	47.1	1.1 (2.33%)	0.998	10.18	58	0.00
	LUS	46.0					
overall	UUS	55.5	1.1 (1.98%)	0.997	17.50	328	0.00
	LUS	54.4					

(1) : the upper urban site
(2) : the lower urban site
(3) : the mean intensity of the horizontal solar radiation in mW/cm^2
(4) : the mean of difference between the paired observations
(5) : the degrees of freedom

illustrate the nature of the temporal change in the vertical difference in solar radiation intensity with respect to the change in solar altitude, bivariate regression analysis is used. It provides not only the magnitude of the trend, but also the sign of the change. For the details of the bivariate regression analysis, please refer to section 3.4.3.3.

The result shows that the vertical difference in the solar radiation intensity is negatively correlated with the solar altitude. The simple correlation coefficients for the different measuring days varies from -0.9068 to -0.3160. The established mathematical models are as follows:

$$Y = -1.0082X + 65.07664 \quad \text{..... (on 20/10/84)}$$

$$Y = -0.2711X + 8.90936 \quad \text{..... (on 21/10/84)}$$

$$Y = -1.3008X + 72.47846 \quad \text{..... (on 22/10/84)}$$

$$Y = -0.3290X + 24.88453 \quad \text{..... (on 26/10/84)}$$

$$Y = -0.2987X + 19.12948 \quad \text{..... (on 05/11/84)}$$

$$Y = -0.2988X + 22.94699 \quad \text{..... (on 23/11/84)}$$

$$Y = -0.2397X + 22.18712 \quad \text{..... (overall)}$$

where Y is the vertical difference in the solar radiation intensity in mW/cm^2.

X is the solar altitude.

In order to substantiate whether the variability of the vertical difference in the reception of solar radiation can be explained by the dependent variable (the solar altitude), the overall F-test for the goodness of fit of the models and the F-test for the significance of the regression coefficient are performed (see Tables 6.7 and 6.8). The result shows that not only the linearity of the models but also the regression

Table 6.7 The overall F-test for the goodness of fit of regression coefficients (dependent variable: vertical difference in mW/cm^2)

date	multiple R	R square	df (N-1, M-N 1)		F value	sign. level
22/10/84	0.9068	0.8224	1	58	268.57	<0.05
21/10/84	0.5240	0.2745	1	56	21.19	<0.05
22/10/84	0.8206	0.6734	1	32	66.04	<0.05
26/10/84	0.3290	0.1083	1	51	6.19	<0.05
05/11/84	0.3160	0.0999	1	62	6.88	<0.05
23/11/84	0.4006	0.1604	1	57	10.90	<0.05
overall	0.2584	0.0668	1	327	23.40	<0.05

Multiple R = the multiple correlation coefficient

R square = the square of the multiple correlation coefficient

df = degrees of freedom

Table 6.8 The F-test for the regression coefficient (dependent variable: vertical difference in mW/cm^2)

exp. date	Variable	B	Beta	STD error B	df (1, M-N-1)	F value	sign. level
20/10/84	solar altitude	-1.0081	-0.907	0.06152	1, 58	268.57	<0.05
	constant	65.0766					
21/10/84	solar altitude	-0.2774	-0.524	0.05889	1, 56	21.19	<0.05
	constant	8.9093					
22/10/84	solar altitude	-1.3008	-0.821	0.16012	1, 32	66.00	<0.05
	constant	72.4784					
26/10/84	solar altitude	-0.2981	-0.329	0.11981	1, 51	6.19	<0.05
	constant	24.8845					

df = the degrees of freedom

Table 6.8 The F-test for the regression coefficient (dependent variable : vertical difference in mW/cm^2) (con't)

05/11/84	solar altitude constant	-0.2987 19.1294	-0.316	0.11388	1, 62	6.88	<0.05
23/11/84	solar altitude constant	-0.2988 22.9469	-0.401	0.09054	1, 57	10.89	<0.05
overall	solar altitude constant	-0.2397 22.1872	-0.258	0.04955	1, 327	23.40	<0.05

df = the degrees of freedom

coefficient are significant at the 0.05 level.

From the result of the analyses above, it can be concluded that the vertical difference in the solar radiation intensity will significantly decrease as the solar altitude becomes higher.

6.5 Summary and Discussion

The result of the above analyses illustrates that the reception of solar radiation at the suburban reference area is 2.9 mW/cm^2(5.16%) higher in comparison with that at the upper urban site and 3.4 mW/cm^2(6.29%) higher when compared with the lower urban site. However, the reception of diffuse radiation at the suburban reference site is 0.4 mW/cm^2(5.19%) lower than that of the lower urban site. In addition, it is also shown that the solar radiation received at the upper urban site is about 1.1 mW/cm^2(1.98%) higher than that of the lower urban site.

The solar radiation intensity in the suburban area is higher when compared either with the lower urban site or the upper urban site. The result is expected as the atmospheric pollutants and aerosols concentration of the urban area is believed to be higher when compared with the suburban area due to the greater concentration of human and economic activities.

The diffuse radiation intensity in the urban area is found to be higher than that in the suburban area. This is because the scattering of solar radiation in the urban atmosphere will be much more intensified because of its contamination by aerosols.

The solar radiation intensity in the upper urban site is found to be higher when compared with the lower urban site. The cause is suggested to be the vertical variation in the concentration of atmospheric pollutants and aerosols in the urban atmosphere. The accumulation of airborne pollutants in the lower layer of the urban atmosphere is more abundant since the majority of man-made pollutants are discharged from or near the ground. Due to the higher concentration of the airborne pollutants in the lower layer, more solar radiation is expected to be attenuated. Besides, the vertical difference in the solar radiation intensity is shown to be negatively correlated with the solar altitude; that is, the higher the solar altitude, the smaller the vertical difference in the solar radiation intensity. This pattern of change is probably because of the reduced vertical variation in airborne pollutant concentrations in the urban atmosphere in the late morning and afternoon hours due to the raising of the mixing height. Generally speaking, the height of the mixing layer is proportional to the solar altitude since the higher the solar altitude, the more intensive the insolation is.

Table 6.9 summarises the meteorological conditions on the field measuring days. On these days, Hong Kong was either under the influence of an anticyclone or a high pressure ridge, and mean sea level atmospheric pressure ranging from 1018 mb to 1024 mb. Temperature inversion conditions were also found on five of the field measuring days. Due to the relatively stable meteorological conditions, atmospheric pollutants derived from the urban area cannot be easily diluted and dispersed . As a result, the suburban-urban difference in the concentration of atmospheric pollutants will be strengthened and more solar radiation will be attenuated and

Table 6.9 The meteorological condition of Hong Kong of the field measuring days

date	atmospheric pressure	wind speed (knot/hr)	wind direction	temp (in ^{o}C)	temperature inversion	remark
23/10/84	1018 mb	7.4	NE	22		anticyclone located at the central China
22/10/84	1018 mb	6.0	ENE	22		anticyclone located at the central China
26/10/84	1012 mb	5.8	E	24		anticyclone located at the north China
04/11/84	1018 mb	5.5	E	22		ridge extended from east China Sea
05/11/84	1018 mb	2.5	E	22	inversion at 800 mb	ridge extended from east China Sea
21/11/84	1022 mb	5.8	NNE	17		anticyclone located at the north China

Table 6.9 The meteorological condition of Hong Kong of the field measuring days (con't)

date	atmospheric pressure	wind speed (knot/hr)	wind direction	temp (in ^{o}C)	temperature inversion	remark
23/11/84	1022 mb	4.8	NE	20	inversion at 870 mb and 670 mb	anticyclone located at the central China
24/11/84	1022 mb	3.5	NE	19	inversion at 600 mb	anticyclone located at the central China
25/11/84	1024 mb	6.5	NE	18	inversion at 700 mb	anticyclone located at the north China
26/11/84	1024 mb	7.3	NE	21		anticyclone located at the north China
01/12/84	1022 mb	5.3	NE	20		anticyclone located at the SW China
06/12/84	1020 mb	6.4	NE	18	inversion at 800 mb	anticyclone located at the north China

Source : Royal Hong Kong Observatory (1984)

scattered in the urban area.

The prevailing wind direction on the field measuring days ranges from east to northeast. As mentioned above, major pollutant point sources are located to the west and northwest of Sham Shui Po District. As a result of that, the attenuation of solar radiation in the district may be much stronger if the wind direction change to be west or northwest.

The atmospheric pollution of Sham Shui Po District is not so serious when compared with other urban districts such as Kwun Tong, Kwai Chung and Hung Hom (H.K. Government, 1969; Kwong, 1981; and Yau, 1982). It is believed that the attenuation of incoming solar radiation in these regions will be much stronger, whereas the increase of diffuse radiation will be much more marked due to their more serious atmospheric pollution situation.

Table 6.10 summarizes the depletion of incoming solar radiation and the increase in the amount of diffuse radiation in some other urban centres. It is indicated that the depletion of incoming solar radiation and the increase in the amount of diffuse radiation in Hong Kong cannot be considered as remarkable. The problems are similar to those of other industrialized and modernized urban centres in the world.

Table 6.10 The depletion of solar radiation and the increse of diffuse radiation in various metropolitan centre

centre	increase of diffuse radiation	decrease of global solar radiation	source
Cincinnati	NA	6%	Bach and Peterson (1969)
Hamilton	NA	12%	Rouse and Noad (1972)
Larwick	5%	3%	Hamilton and Forbes (1970)
Los Angeles	NA	6 to 8%	Peterson and Flowers (1978)
St. Louis	NA	1 to 4.5%	Peterson and Stoffel (1980)
Toulouse	NS	3.5%	Estournel at al. (1983)
Hong Kong	5%	6%	

NA : not analyzed

NS : no significant difference is found

CHAPTER VII

THE POLLUTION EPISODE

7.1 Introduction

Air pollution concentrations in an urban area often fluctuate considerably with time. A long-lasting period with high ambient pollution levels is usually referred to as a pollution "episode".

The increase of atmospheric pollutants and aerosols in the air not only deteriorates the ambient air quality but also decreases the amount of solar radiation at the ground surface. Generally speaking, the higher the level of pollutants and aerosols, the more the solar radiation is being attenuated.

A pollution episode often occurs when the atmospheric conditions are unfavourable for efficient dispersion of pollutants. These conditions are often related to low wind speed, limited mixing depth, or the presence of a temperature inversion. In other words, the pollution concentration is liable to build up under such stable atmospheric condition.

Pollutant concentrations in the air are inversely proportional to wind speed. As wind speed increases, the effluent from the pollutant sources is introduced into a greater volume of air per unit time interval. For this reason, many formulae, such as the Gaussian Model for pollution concentration, contain a factor for wind speed. In addition to this dilution due to wind speed, the spreading of pollutants by turbulence and eddies is also important in the dispersion process. Eddies and turbulence

are formed by the flow of air over buildings, trees and other rough terrain and their intensity is proportional to the wind speed (Turner, 1970 and Scorer, 1974)

Mixing depth is defined as the top of a ground surface-based layer in which turbulence and vertical mixing is relatively vigorous and in which the lapse rate is the same as dry adiabatic. During a ground-based inversion or in a relatively stable air, the mixing depth does not exist and vertical turbulence is either low or nil, therefore, emitted pollutants remain concentrated or can only disperse into a thin layer. An extremely high concentration of pollutants may be detected in such situations. If the air becomes unstable and the mixing depth is high, the pollutants may be dispersed into a large space and the concentration may be reduced. Therefore, the mixing depth is an important parameter in atmospheric dispersion (Holzworth, 1974).

Temperature inversions usually occur during relatively stable atmospheric conditions, and may severely trap air pollutants or restrict free vertical dispersion.

When assessing the implication of the concentration of atmospheric pollutants and aerosols on the attenuation of solar radiation, other meteorological conditions should, therefore, be also considered since they may greatly influence the concentration of pollutants and aerosols.

In this study, the data for pollution levels and meteorological conditions are provided by the Environmental Protection Agency of Hong Kong and the Royal Hong Kong Observatory, respectively. Only the impact of aerosols and pollutants on the daily variation in the solar radiation

intensity in the urban area (the radiation data used were collected at the lower level monitoring site in Sham Shui Po) will be evaluated due to the inavailability of data for pollutant concentrations and aerosol levels in the suburban area. Days selected for investigation were those when aerosol levels were highest and lowest within the period of field measurement.

7.2 The Impact of a Pollution Episode

Total suspended particulates (TSP) and sulphur dioxide concentrations measured at Sham Shui Po during the period of field measurement for solar radiation are listed in Table 7.1. It should be noted that the daily average level of total suspended particulates is not available for some of the field measuring days because a one-day-in-three sampling schedule is operated by the Environmental Protection Agency of Hong Kong. It is found that the level of total suspended particulates is greatest (130 ug/m^3) on the 23rd of November, and smallest (48 ug/m^3) on the 21st of October. The sulphur dioxide concentration shows the same pattern; greatest (53 ug/m^3) on the 23rd of November and smallest (13 ug/m^3) on the 21st of October.

Table 7.2 summarizes the hourly average solar radiation intensity on these two days. It is shown that the average solar radiation intensity on the 23rd of November is lower than on the 21st of October by 10%. The hourly difference in the radiation intensity between two days varies from 6% to 29%.

Table 7.1 Air pollution levels in Sham Shui Po (in ug/m^3)

date	sulphur dioxide	total suspended particulates
21/10/84	13	48
22/10/84	23	--
/10/84	19	--
04/11/84	16	--
05/11/84	27	105
21/11/84	29	--
23/11/84	53	130
24/11/84	32	--

source : The Environmental Protection Agency of Hong Kong

Table 7.2 The hourly averaged solar radiation intensity on 21/10/84 and 23/11/84 (in mW/cm^2)

H.K. local time	21/10/84	(1) 23/11/84	(2) 23/11/84	(3) ratio
0800 to 0900	35.42	26.22	27.39	1.29
0900 to 1000	48.47	43.19	45.13	1.07
1000 to 1100	60.37	54.29	56.73	1.06
1100 to 1200	65.86	57.92	60.52	1.08
average	52.53	45.41	47.44	1.10

(1) : measured solar radiation intensity

(2) : normalized to the identical incidence angle as on 21/10/84 by multiplying a factor, which is a ratio of the cosine function of the mean solar altitude in ith hour on 21/10/84 to that on the cosine function of mean solar altitude in ith hour on 23/11/84

(3) : the hourly averaged intensity of 21/10/84 to that of the normalized intensity on 23/11/84

7.3 The Meteorological Implications

Good dispersion conditions on the 21st of October result in a low concentration of sulphur dioxide and total suspended particulates, and poor dispersion conditions on the 23rd of November result in high concentration of both. The meteorological implications of the air pollution levels can help us understand the daily variation in the intensity of solar radiation. The hourly solar radiation intensity on the 21st of October is consistently higher than that on the 23rd of November.

7.3.1 The Atmospheric Pressure

Starting from the 21st of November and onward, the mean sea level atmospheric pressure of Hong Kong maintained a level of 1022 mb (about 5 mb higher than the monthly normal) due to the influence of an intensive anticyclone located in mainland China. This is the most undesirable condition in terms of air pollution since there is usually a subsidence inversion in addition to little horizontal air movement. Pollutants and aerosols are therefore easily built up. On the 21st of October, the mean sea level atmospheric pressure was only about 1016 mb. A comparatively low atmospheric pressure might result in a more efficient dispersion of pollutants and aerosols.

7.3.2 The Wind Speed and Direction

Tables 7.3 and 7.4 summarize the observed surface and upper air wind speed and wind direction on the 21st of October and the 23rd of November. It is shown that there seems to be a marked difference in the vertical wind

Table 7.3 The wind speed (knot/hr) and direction (in whole circle bearing) at 0800 sounding on 21/10/84 and 23/11/84

	21/10/84	23/11/84
surface	5.0 (050)	1.0 (040)
1000 mb	5.5 (043)	1.7 (070)
900 mb	5.6 (064)	7.3 (054)
800 mb	4.8 (066)	8.0 (018)
700 mb	5.6 (360)	10.1 (343)
600 mb	7.3 (328)	7.8 (294)
500 mb	6.2 (315)	13.6 (304)

source : Royal Hong Kong Observatory (1984)

Table 7.4 The wind speed (knot/hr) and direction (in whole circle bearing) at 2000 sounding on 21/10/84 and 23/11/84

	21/10/84	23/11/84
surface	2.0 (090)	1.0 (020)
1000 mb	2.0 (101)	0.8 (027)
900 mb	4.3 (037)	6.3 (026)
800 mb	6.6 (065)	7.3 (003)
700 mb	2.6 (318)	5.7 (323)
600 mb	5.1 (278)	11.0 (278)
500 mb	4.9 (287)	17.3 (299)

source : Royal Hong Kong Observatory (1984)

profile, particularly in wind speed. Lower wind speeds on the surface level (up to 900 mb) seem to be partially responsible for the higher pollutant concentration as measured on the 23rd of November. Higher upper air wind speed on the 23rd of November does not seem to have reduced the high pollutant concentration at the surface level, since most of the emission sources are within 900 mb.

Although an increase in wind speed may generate better dispersion of atmospheric pollutants and aerosols, street debris and surface dirt may also be kicked off the ground into the atmosphere. The minimum surface wind speed that can initiate the blowing off of street debris and surface dirt is termed "critical wind speed". Hsu (1981) showed that the critical wind speed in Hong Kong is about 5.6 knot/hr. However, the surface wind speed at 0800 and 2000 sounding are only 5.0 knot/hr and 2.0 knot/hr, respectively. It can then be concluded that the higher surface wind speed on the 21st of October only results in better dispersion conditions for atmospheric pollutants and aerosols, but not the blowing off of surface dust and street debris into the air as the surface wind speed does not exceed the critical wind speed.

7.3.3 The Mixing Depth

Another factor to be considered is mixing depth, which is most likely to be responsible for the vertical transport of pollutants and aerosols. Figure 7.1 and 7.2 illustrate the upper air temperature profile at 0800 and 2000 (Hong Kong Local Time) sounding on these two days. It is found that a double temperature inversion occur at 0800 sounding above 880 mb and 670 mb and a temperature inversion above 670 mb is still maintained

Figure 7.1 The temperature profile (0800 H.K. Local Time) on 21/10/84 and 23/11/84

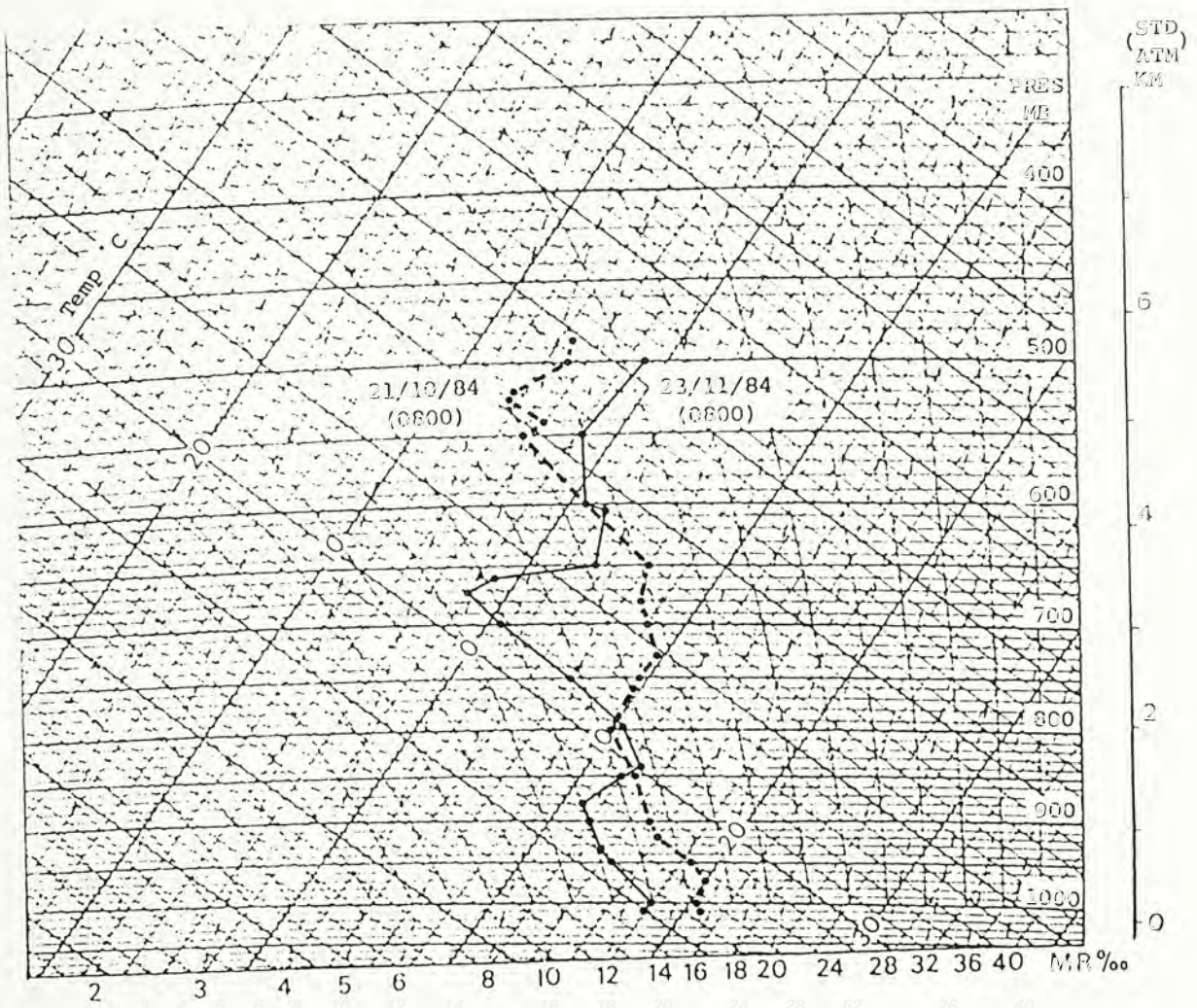

Figure 7.2 The temperature profile (2000 H.K. Local Time) on 21/10/84 and 23/11/84

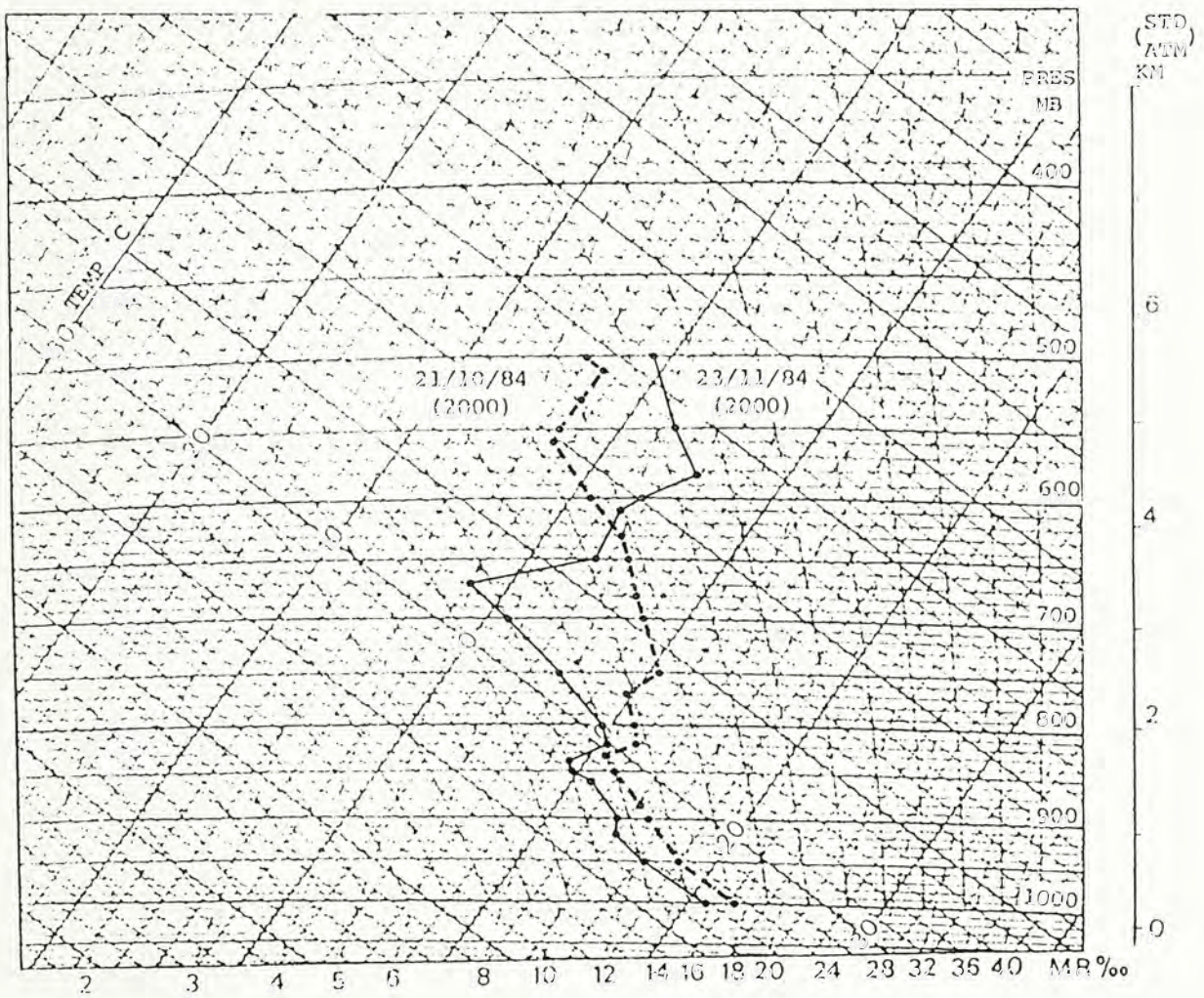

at 2000 sounding on the 23rd of November. This implies that the free vertical dispersion of air pollutants and aerosols is restricted as the mixing depth has been reduced.

Besides, it is also observed that from the 16th of November onward, there was no record of rainfall in the Colony. Dry dirt and fine debris from the ground are vulnerable to aeolian erosion and are easily blown into the air. On the other hand, 3.6 mm rainfall was recorded on the 18th of October. During a wet rainy d , the amount of soil particles and other fine debris discharged into the air from the ground is greatly reduced. Also, rainfall can efficiently cleanse particulate matter and aerosols in the air by washout. This mechanism applies to nearly all particles with size ranges below 2 um. Rainfall therefore not only serves to minimize surface emissions, but also effectively scavenges many of the pollutants and aerosols present in the atmosphere. The continuous absence of rainfall for a long period of time, may therefore contribute to the pollution episode on the 23rd of November.

Meteorological evidence for the pollution episode is clear. An anticyclonic system accompanied by low surface winds, a subsidence temperature inversion aloft, and a dry spell is expected to provide rather poor atmospheric dispersion during the episode.

7.4 Summary and Conclusion

Based on the analyses described above, it is reasonable to conclude that more incoming solar radiation will be attenuated when there is a

higher concentration of pollutants and aerosols. It is also confirmed that a high pollution episode may result in unfavourable atmospheric dispersion condition for the efficient dispersion, for example, limited atmospheric mixing depth or the presence of a temperature inversion. The pollution episode on the 23rd of November has produced a decrease of 10% in incoming solar radiation as compared to that on the 21st of October.

CHAPTER VIII

CONCLUSION AND POLICY IMPLICATION

8.1 Conclusion

This study has shown that the morphological structure of buildings has a significant effect on the reflection of solar radiation. Among all the selected buildings, the Tsim Sha Tsui Centre, clad with highly reflective material and smoothly configured, is found to have the highest reflectance index. The maximum reflectance index of the buildings ranges from 1.22 at the Tsim Sha Tsui centre to 1.06 at the Postgraduate Hall Complex. Bivariate regression analysis shows that reflectance index and the solar altitude are negatively correlated. This result is similar to that suggested by Louie and Terjung (1974). Besides, it is also found that the reflectance indices of the building may be smaller than one, which implies that the solar radiation intensity received in front of the building is lower than that at the control site. This is because the increased reflected solar radiation cannot compensate for the loss of diffuse radiation blocked by the building.

The amount of solar radiation received in the study area varies with time and with atmospheric contamination. Spatial variation of total horizontal radiation as well as diffuse radiation does exist in Hong Kong. On the average, the reception of horizontal solar radiation in the urban area is about 6% less than in the suburban location while the reception of diffuse radiation is about 5% higher in the urban area.

The vertical variation of solar reception is comparatively small (about 2%). The percentage of difference, in general, is larger in the morning and smaller in the afternoon. This could be explained in terms of mixing height, which is lower in the morning and higher in the afternoon. Consequently, depletion of solar radiation at a finite elevation above the ground surface is smaller in the morning than in the afternoon.

A pollution episode may exist during atmospheric conditions such as low wind speed, high atmospheric pressure, limited mixing depth and continuous rain-free period. The amount of solar radiation received at ground level may be attenuated due to the intensity of air pollution. This attenuation is obvious on 23rd November 1984 when compared with other monitoring days.

8.2 Policy Implication

Terjung (1974) and Nunez (1980) suggested and outlined a solar radiation reception model in an urban area. They noted that the solar radiation received at the urban ground level comprises of direct radiation, diffuse radiation and reflected radiation. Chapter V has shown the significant effect of building structures on the reflection of solar radiation, which further substantiates the need for adopting this model in studying the reception of solar radiation in an urban area.

The research reveals only the single reflection of solar radiation from urban blocks. Study of the multiple reflections in a city canyon is also a worthwhile project, since it will provide more valuable details of

the city's micro climate.

In Hong Kong, urban and economic development was concentrated within the city in the past decades. As there is little land for further urban development, new towns are being developed rapidly in the New Territories. The establishment of a new town not only alters the ground characteristics but also changes the atmospheric environment. Consequently, modification of incoming solar radiation in rural areas will be inevitable due to the suburbanization process. Details of the urban micro-climate induced by buildings should therefore become significant in research of urban energy budgets.

In comparison with some other large cities in the world, the present status of solar radiation depletion in urban Hong Kong is not yet serious. However, if there is not an efficient monitoring network and valid control measures for air quality in Hong Kong, deterioration may get worse in the future. Though the Clean Air Ordinance issued in 1959 has been replaced by the newly enacted Air Quality Control Ordinance issued in 1983, continuous and extensive monitoring seems to be definitely required.

In this study of the effect of air pollution on the solar radiation, only Sham Shui Po district was selected for evaluation due to a lack of manpower and instruments. The addition of other sites for extensive monitoring is essential to the understanding of solar radiation depletion and other aspects of Hong Kong's micro climate.

BIBLIOGRAPHY

Ackerman, T.P. (1977), "A Model of the Effect of Aerosols on Urban Climates with Particular Application to the Los Angeles Basin", Journal of Atmospheric Sciences, Vol. 34, pp. 531-547.

Bach, W. and Peterson, W. (1969), "Heat Budget Study In Greater Cincinnati", Proceedings of the Association of the American Geographers, Vol. 1, pp. 7-11.

Barry, R.G. and Chorley, R.J. (1968), Atmosphere, Weather and Climate, Chapter 1, pp. 23-76. The English Language Book Society and Methuen & Co. Ltd, 1968-1978.

Bergstrom, R.W. and Peterson, J.T. (1977), "Comparison of Predicted and Observed Solar radiation in an Urban Area", Journal of Applied Meteorology, Vol. 16, pp. 1107-1116.

Bruce, A. (1977), Solar Energy: Fundamentals in Building Design Part II - A, pp 34-54. Fotal Environmental Action Inc., The United States of America.

Budgen, P. and Price, N.M. (1981), "Routine Calibration of Solar Radiation Instruments", Meteorological Magazine, Vol. 110, pp. 253-259.

Coulson, K.L. (1975), Solar and Terrestrial Radiation - Method and Measurement, Chapters 3-4, pp 40-137. Academic Press.

Estournel, et al. (1983), "Observation and Modelling of Downward Radiation Flux (Solar and Infrared) in Urban/Rural Areas", Journal of Climate and Applied Meteorology, Vol. 22, No.1, pp. 134-142.

Fedorova, M.P. "Scattered and Reflected Radiation" in Kondrat'er K. Ya. ed, Radiation Characteristics of the Atmosphere and the Earth's Surface, Amerind Publishing Co. Pvt. Ltd. New Delhi, 1973.

Forbes, A.J. and Hamilton, R.A. (1971), "Clear Sky Radiation Measurements at Lerwick", Quart. Journal Royal Meteorological Society, Vol. 97, pp. 99-102.

Glazier, J., Monteith, J.L. and Unsworth, M.H. (1976), "Effect of Aerosol on the Local Heat Budget of the Lower Atmosphere", Quart. Journal Royal Meteorological Society, Vol. 102, pp 95-102.

Holzworth, C.C. (1974), "Climatological Aspects of the Composition and Pollution of the Atmosphere", WMO-No. 139, pp. 4-27.

Hong Kong Government (1969), A Report on Air Pollution in Hong Kong. The Committee on Air Pollution, Hong Kong Government.

Hsu, S.I. (1981), The Effects of Wind Speeds on the Deterioration of Atmospheric Visibilities, Occasional Paper No. 19, Dept. of Geography, The Chinese University of Hong Kong, Hong Kong.

John, F.G. (1976), Applied Climatology - An Introduction, Oxford University Press, London.

Kwong, L.S. (1978), A Study of Air Pollution in Hong Kong: Non-Destrictive Multi-element Determination of Air Particulates by Means of Reacter Neutrons and Ge (Li) Gamma-ray Spectrometer. M. Phil. Thesis, unpublished, Department of Physics, the Chinese University of Hong Kong, Hong Kong.

Liang, C.S. (1972), "The Mixing Features and Vertical Variations in Urban Land Use", in Urban Land Use Analysis, Chapter 4, pp. 79-11, Ernest Publication, Hong Kong.

Lyons, T.J. and Forgan, B.W. (1975), " Atmospheric Attenuation of Solar Radiation at Adelaide", Quart. Journal Royal Meteological Society Vol. 101, pp. 1013-1017.

Mateer, C.L. (1961), "Note on the Effect of the Weekly Cycle of Air Pollution on Solar radiation on Toronto", International Journal of Air and Water Pollution, Vol. 14, pp 52-54.

Nunez, M. and Oke, T.R. (1980), "Modelling the Daytime Urban Surface Energy Balance", Geographical Analysis, Vol. 12, No. 4, pp. 373-386.

Paltridge, G.W. and Platt, C.M.R. (1973), "Absorption and Scatter of Radiation by an Aerosol Layer in the Free Atmosphere", Journal of the Atmopheric Science, Vol. 30, pp. 734-737.

Peter, S. (1976), Developments in Atmospheric Science 6 - Physical Principles of Micro-Meteorological Measurements, Chapter 2, pp 19-27. Elsevier Scientific Publishing Company, Amsterdam.

Peterson, J.T. and Stoffel, T.L. (1979), "Analysis of Urban-Rural Data From St. Louis, Missouri", Journal of Applied Meteorology, Vol. 19, pp. 275-283.

Peterson, J.T. and Flowers, E.C. (1978), "Urban-rural Solar Radiation and Atmospheric Turbidity Measurements in the Los Angeles Basin", Journal of Applied Meteorology, Vol. 17, pp. 1595-1609.

Reed, R.K. (1982), "Comparison of Measured and Estimated Insolation over the Eastern Pacific Ocean", Journal of Applied Meteorology, Vol. 21, pp. 339-341.

Roberton, E.D., ed. (1981) Guide to Solar Electricity, the Solarex Coporation. The United States of America, 1981.

Rouse, W.R., Noad, D. and McCutcheon, J. (1973), "Radiation, Temperature and Atmospheric Emissivities in a Polluted Urban Atmosphere at Hamilton, Ontario", Journal of Applied Meteorology, Vol. 12, No.1, pp. 798-807.

Scorer, R.S. (1974), "Technical Aspects of Air Pollution" in Environmental Pollution Control, A.D. McKnight et al. edited, Chapter 3, pp. 43-62.

Simonson, J.R. (1984), Computing Methods in Solar Heating Design, Chapter 2, pp. 10-21. The Macmillian Press, London.

Terjung, W.H. and Louie, S. S-F (1973), "Solar Radiation and Urban Heat Islands", Annals, Association of American Geographers, 63, pp. 181-207.

Terjung, W.H. and Louie, S. S-F (1974), "A Climatic Model of Urban Energy Budgets", Geographical Analysis, Vol. 6, pp. 181-207.

Twomey, S. (1977), "Optics of Atmospheric Aerosol", in Atmospheric Aerosols, Chapter 9, pp 200-204. Elsevier Scientific Publishing Company.

Twomey, S. (1977), "Removal Process", in Atmospheric Aerosols, Chapter 6, pp. 143-146. Elsevier Scientific Publishing Company.

Trerskoi, P.N. (1962), Physics of the Atmosphere, trans. A. Sen and R. N. Sen, E. S. Salazneva edited. Chapter 8, pp 143 - 163. Israel Program for Scientific Translations, Jerusalem, 1965.

Vesilind, P.A. (1980), Environmental Pollution and Control, Ann Arbor Science Publishers Inc., North Carolina.

Weber, M.R. and Baker, C.B. (1982), "Comments on the Ratio of Diffuse to Direct Solar Irradiance (Perpendicular to the Sun's Rays with Clear Skies - A Conserved Quantity Through the Day", Journal of Applied Meteorology, Vol 21, No. 6, pp. 883-886.

Wesley, M. (1982), "Simplified Technique to Study Components of Solar Radiation Under Haze and Clouds", Journal of Applied Meteorology, Vol. 21, pp. 373-383.

White, J.M., Eaton, F.D. and Auer, A.H. (1978), "The Net Radiation Budget of the St. Louis Metropolitan Area", Journal of Applied Meteorology, Vol. 17, pp. 593-599.

William, D.S. (1965), Physical Climatology, Chapter 3 & 6, pp 11-40 and 89-82, The University of Chicago Press.

Yau, Y.M. (1983), Airborne Suspended Particulates Pollution in Hong Kong. M. Phil. Thesis, unpublished, Department of Geography, the Chinese University of Hong Kong, Hong Kong.

李懷瑾，于靜明(1978)，"蘭州大氣污染對太陽可能輻射的影响"。全國氣候變化學術討論會文集，中央氣象局氣候科學研究院天氣氣候研究所編。北京科學出版社。

邵德民(1982)，"上海地區太陽輻射和空氣污染變化情況的初步分析"。大氣湍流擴散及污染氣象論文集，中央氣象局氣象科學研究院編。北京氣象出版社。

黃偉峰，沈雪萍(1985)，廣州地區的大氣透明度與空氣污染，廣州中山大學地理系。

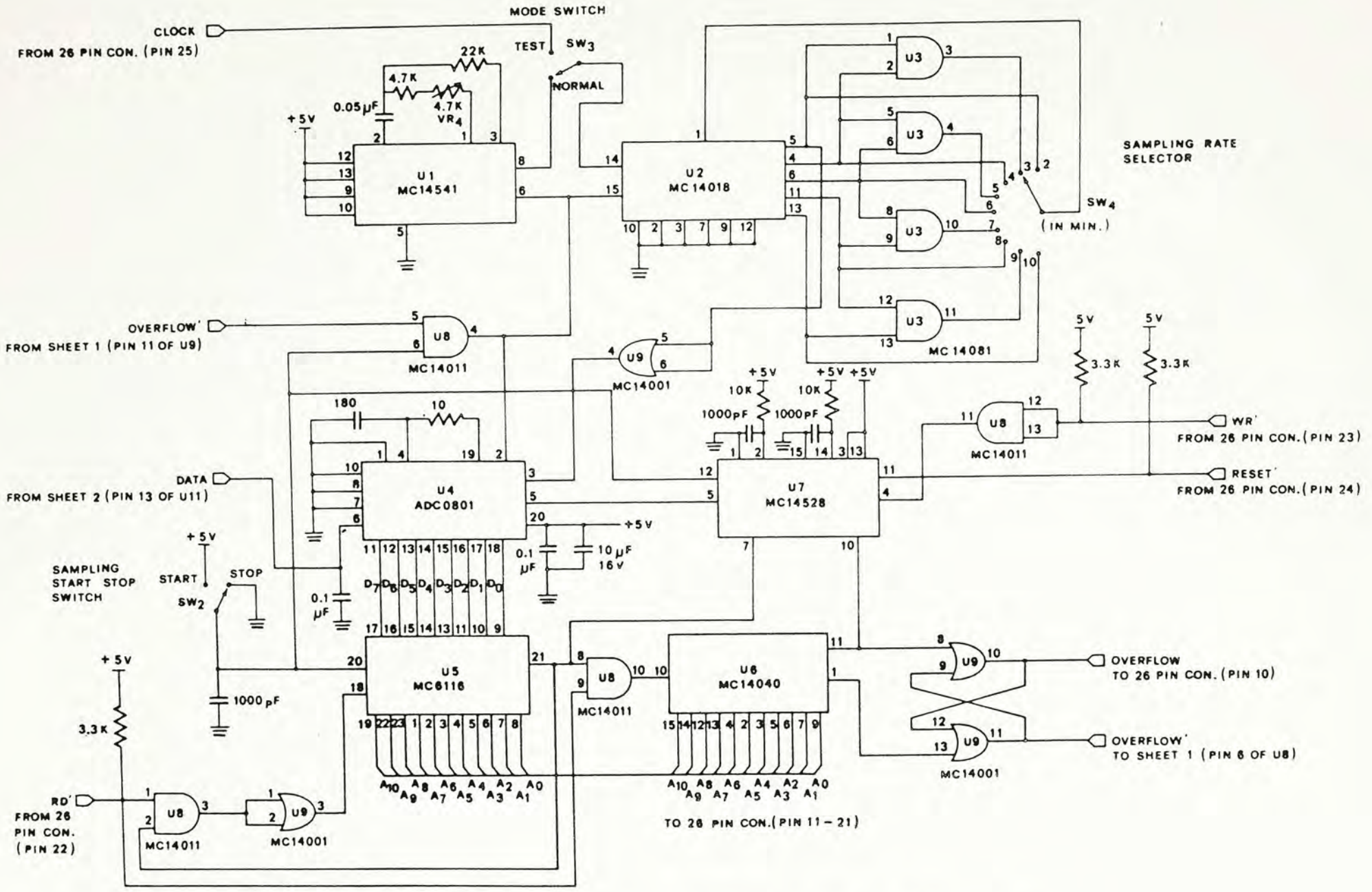

Appendix 4.1 The circuit diagram of the data logger

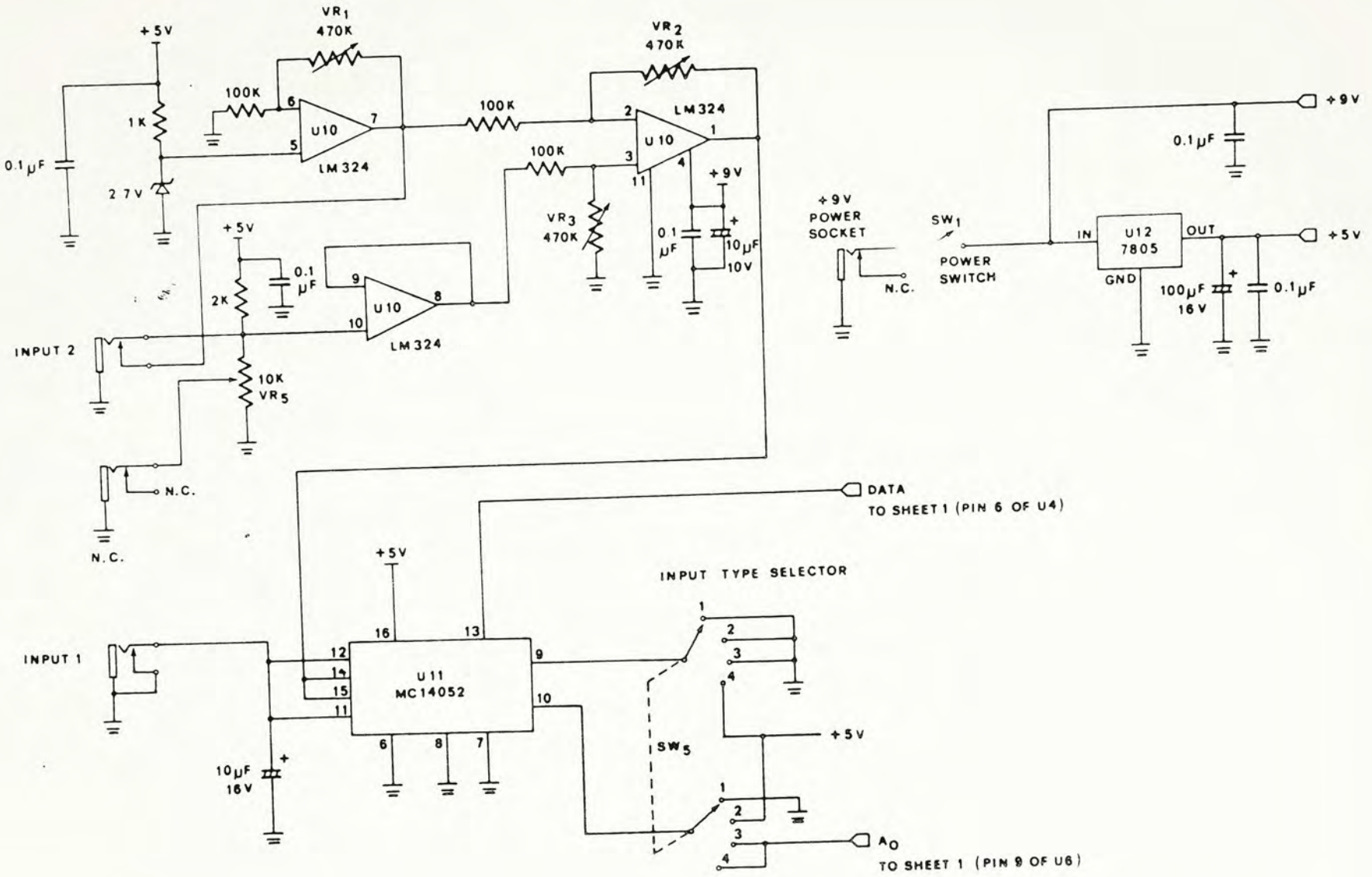

Appendix 4.1 The circuit diagram of the data logger (con't)

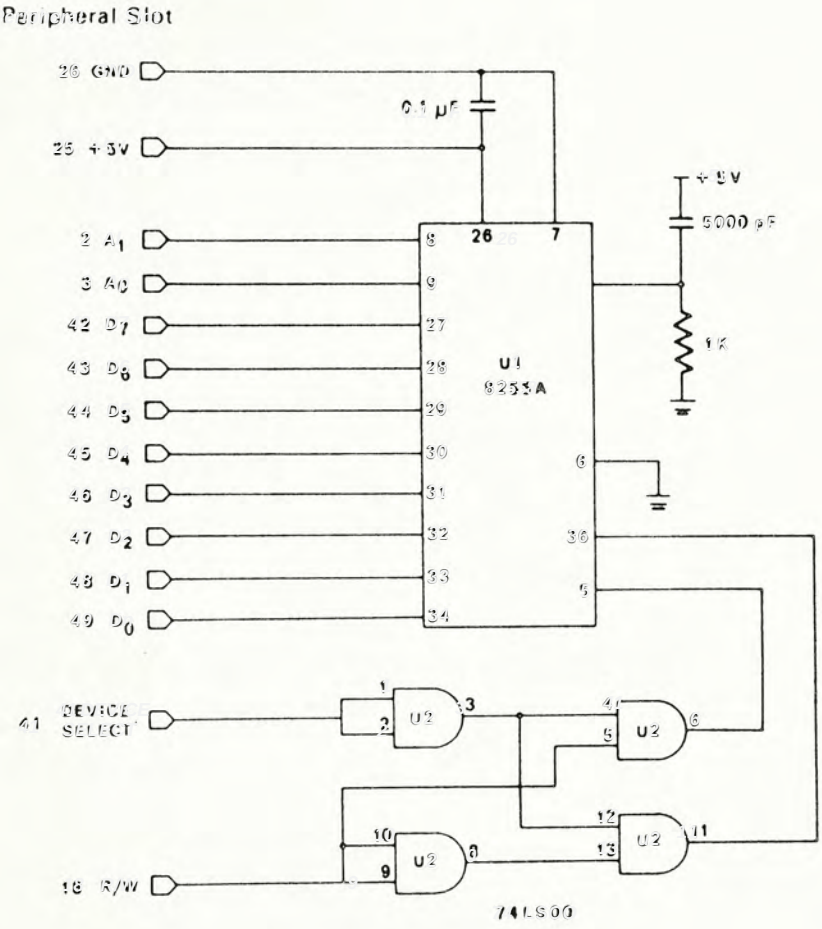

NOTE : Other signals of U1 are connected as stated in sheet 4 of the circuit diagram of the Automatic Data Recorder.

Appendix 4.1 The circuit diagram of the data logger (con't)

Appendix 4.1 The circuit diagram of the data logger - detailed pin pin connection of the 26 pin connector (con't)

on recoder	pin no.	on interface
GND	1	GND
D0	2	PA0 (pin 4 of 8255)
D1	3	PA1 3
D2	4	PA2 2
D3	5	PA3 1
D4	6	PA4 40
D5	7	PA5 39
D6	8	PA6 38
D7	9	PA7 37
overflow	10	PC3 17
A0	11	PB0 18
A1	12	PB1 19
A2	13	PB2 20
A3	14	PB3 21
A4	15	PB4 22
A5	16	PB5 23
A6	17	PB6 24
A7	18	PB7 25
A8	19	PC0 14
A9	20	PC1 15
A10	21	PC2 16
RD'	22	PC4 13
WR'	23	PC5 12

Appendix 4.1 The circuit diagram of the data logger - detailed pin connection of the 26 pin connector (con't)

on recoder	pin no.	on interface	
RESET'	24	PC6	11
CLOCK	25	PC7	10
GND	26	GND	

Appendix 4.2 The program listing (Applesoft part)

```
100  HIMEM: 38792
110  DIM M$(12),WT$(4),T(1)
120  PRINT  CHR$ (4);"BLOAD SYS.A$95F0"
130 SYS = 9 * 16 * 3 + 5 * 256 + 15 * 16
140 SLOT =  PEEK (SYS)
150 PR =  PEEK (SYS + 1)
160 PT =  PEEK (SYS + 2)
170  PRINT  CHR$ (4);"BLOAD RD DATA.OBJ0"
180 AD = 9 * 16 * 3 + 4 * 256
190  POKE AD,0: POKE AD + 1,0: POKE AD + 2,0
200  POKE AD + 3,SLOT
210  CALL AD + 4
220 D = 8 * 16 * 3 + 12 * 256
230  FOR I = D - 8 TO D - 1: POKE I,2: NEXT I:YR% = 514:MO% = 2:DA% =
    2:HR% = 2:MI% = 2:IN% = 2:IT% = 2
240  FOR I = 1 TO 12: READ M$(I): NEXT I
250  DATA  JAN,FEB,MAR,APR,MAY,JUN,JUL,AUG,SEP,OCT,NOV,DEC
260  FOR I = 1 TO 4: READ WT$(I): NEXT I
270  DATA  "INPUT 1","INPUT 2","INPUT 1,2 (ALTERNATE)","INPUT 2,1 (A
    LTERNATE)"
280 N = 8 * 16 * 3 + 11 * 256 + 13 * 16
290 SI$ = "": FOR I = N TO N + 24: POKE I,32:SI$ = SI$ + " ": NEXT I

300 EQ$ = "======="
310 T(0) = 0:T(1) = 20
320  GOTO 340
330  CALL AD + 22: GOTO 350
340  ONERR  GOTO 330
350  PR# 0: CALL 1002
360  TEXT : HOME : POKE 34,5: VTAB 2
370  PRINT EQ$;" SOLAR RADIATION ANALYSIS ";EQ$
380  PRINT  TAB( 34);"VER 2.0"
390  VTAB 6
400  PRINT " 1. CHANGE SYSTEM CONFIGURATION"
410  PRINT " 2. READ DATA FROM DETECTOR"
420  PRINT " 3. CATALOG"
430  PRINT " 4. LOAD DATA FROM FILE"
440  PRINT " 5. SAVE DATA TO FILE"
450  PRINT " 6. LIST DATA ON SCREEN"
460  PRINT " 7. LIST DATA ON PRINTER"
470  PRINT " 8. PLOT GRAPH ON SCREEN"
480  PRINT " 9. DUMP GRAPH TO PRINTER"
490  PRINT "10. TEST DETECTOR HARDWARE"
500  PRINT "11. END"
510  VTAB 20: PRINT "USE <- AND -> TO SELECT": PRINT "AND THEN PRESS
    RETURN KEY"
520 VP = 1
530 VI = 5
540  VTAB VP + VI
550  FLASH
560  PRINT  SPC( 2 -  LEN ( STR$ (VP)));VP
570  NORMAL
580  GOSUB 680
```

```
590  IF KB <  > 13 AND KB <  > 8 AND KB <  > 21 THEN 580
600  IF KB = 13 THEN 730
610  VTAB VI + VP
620  PRINT  SPC( 2 -  LEN ( STR$ (VP)));VP
630  IF KB = 8 THEN 660
640 VP = VP + 1: IF VP >  = 12 THEN VP = 1
650  GOTO 540
660 VP = VP - 1: IF VP <  = 0 THEN VP = 11
670  GOTO 540
680  REM
690 KB =  PEEK ( - 16384)
700  IF KB < 128 THEN 690
710 KB = KB - 128: POKE  - 16368,0
720  RETURN
730  ON VP GOTO 760,1240,1690,1760,2080,2240,2630,3310,3850,4340,456
    0
740  CALL AD + 22: IF  PEEK (222) <  > 4 THEN 760
750  VTAB 22: PRINT "ERROR! WRITE-PROTECTED!": CALL  - 198: GOSUB 68
    0
760  ONERR  GOTO 740
770  HOME : NORMAL
780  VTAB 4: PRINT "1. CHANGE SYSTEM CONFIGURATION"
790  VTAB 6
800  PRINT "DETECTOR I/F CARD -> SLOT ";SLOT
810  PRINT "PRINTER I/F CARD  -> SLOT ";PR
820  PRINT "PRINTER I/F TYPE  -> TYPE ";PT
830  PRINT "RETURN TO MAIN MENU  ....."
840  VTAB 13: PRINT "NOTE: PRINTER I/F TYPE"
850  PRINT  TAB( 6);"1. APPLE II PARALLEL INTERFACE"
860  PRINT  TAB( 6);"2. PARALLEL GRAPHIC PRINTER I/F"
870  PRINT  TAB( 6);"3. GRAPPLER+ PRINTER INTERFACE": PRINT  TAB( 6)
    ;"4. MODIFIED GRAPPLER+ PRINTER I/F"
880 VP = 1
890 VI = 5
900  VTAB VP + VI: HTAB 27: FLASH
910  GOSUB 1180
920  GOSUB 680
930  IF KB <  > 13 AND KB <  > 8 AND KB <  > 21 THEN 920
940  IF KB = 13 THEN  GOTO 1010
950  VTAB VP + VI: HTAB 27: NORMAL : GOSUB 1180
960  IF KB = 8 THEN 990
970 VP = VP + 1: IF VP >  = 5 THEN VP = 1
980  GOTO 900
990 VP = VP - 1: IF VP <  = 0 THEN VP = 4
1000  GOTO 900
1010  NORMAL
1020  IF VP >  = 4 THEN 1060
1030  GOTO 1050
1040  CALL  - 198: VTAB 20: PRINT  SPC( 39): VTAB 20: HTAB 1
1050  VTAB 20: INPUT "NEW VALUE -> ";NV%
1060  ON VP GOTO 1110,1130,1150,1070
1070  POKE SYS,SLOT: POKE SYS + 1,PR: POKE SYS + 2,PT
1080  POKE AD + 3,SLOT: CALL AD + 4
1090  PRINT  CHR$ (4);"UNLOCK SYS": PRINT  CHR$ (4);"BSAVE SYS,A$95F
    0,L$8": PRINT  CHR$ (4);"LOCK SYS"
1100  GOTO 340
1110  IF NV% <  = 0 OR NV% > 7 THEN 1040
```

```
1120 SLOT = NV%: VTAB 20: PRINT  SPC( 38): GOTO 950
1130  IF NV% <  = 0 OR NV% > 7 THEN 1040
1140 PR = NV%: VTAB 20: PRINT  SPC( 38): GOTO 950
1150  IF NV% <  = 0 OR NV% > 4 THEN 1040
1160 PT = NV%
1170  VTAB 20: PRINT  SPC( 38): GOTO 950
1180  ON VP GOTO 1200,1210,1220
1190  PRINT " ": RETURN
1200  PRINT  STR$ (SLOT): RETURN
1210  PRINT  STR$ (PR): RETURN
1220  PRINT  STR$ (PT): RETURN
1230  CALL AD + 22: GOTO 1260
1240  ONERR  GOTO 1230
1250  CALL AD + 7
1260  VTAB 4: PRINT "2. READ DATA FROM DETECTOR"
1270  HOME
1280  IF  PEEK (AD + 2) <  > 0 THEN  VTAB 6: PRINT "OVERFLOW": PRINT
    "DATA ARE LOST": GOTO 1650
1290 NO =  PEEK (AD) +  PEEK (AD + 1) * 256
1300  IF NO = 0 THEN  VTAB 6: PRINT "NO DATA": GOTO 1650
1310  VTAB 6: PRINT "NUMBER OF DATA -> ";NO
1320  POKE 34,7: HOME
1330  VTAB 8: INPUT "YEAR     -> ";YR%
1340  IF YR% < 0 OR YR% >  = 10000 THEN  CALL  - 198: GOTO 1330
1350  VTAB 9: INPUT "MONTH    -> ";MO%
1360  IF MO% < 1 OR MO% > 12 THEN  CALL  - 198: GOTO 1350
1370  VTAB 10: INPUT "DAY      -> ";DA%
1380  IF DA% < 1 OR DA% > 31 THEN  CALL  - 198: GOTO 1370
1390  VTAB 12: INPUT "HOUR     -> ";HR%
1400  IF HR% < 0 OR HR% > 23 THEN  CALL  - 198: GOTO 1390
1410  VTAB 13: INPUT "MINUTE   -> ";MI%
1420  IF MI% < 0 OR MI% > 59 THEN  CALL  - 198: GOTO 1410
1430  VTAB 15: INPUT "INTERVAL (IN MIN.) -> ";IN%
1440  IF IN% < 2 OR IN% > 10 THEN  CALL  - 198: GOTO 1430
1450  VTAB 16: INPUT "SITE     -> ";SI$
1460  IF  LEN (SI$) >  = 25 THEN SI$ =  LEFT$ (SI$,25): GOTO 1480
1470  FOR I =  LEN (SI$) + 1 TO 25:SI$ = SI$ + " ": NEXT I
1480  VTAB 18: INPUT "I/P TYPE-> ";IT%
1490  IF IT% <  = 0 OR IT% > 4 THEN  CALL  - 198: GOTO 1480
1500  HOME
1510  VTAB 8: PRINT "DATE     -> ";DA%;"-";M$(MO%);"-";YR%
1520  PRINT "TIME     -> ";HR%;":";MI%
1530  PRINT "INTERVAL-> ";IN%;" MIN."
1540  PRINT "SITE     -> ";SI$
1550  PRINT
1560  PRINT "I/P TYPE-> ";IT$(IT%)
1570  NORMAL
1580  VTAB 15: HTAB 1: PRINT "OK! (";: INVERSE : PRINT "Y";: NORMAL
    : PRINT "ES OR ";: INVERSE : PRINT "N";: NORMAL : PRINT "O) -> "
    ;: GET A$
1590  IF A$ <  > "Y" AND A$ <  > "N" THEN 1580
1600  IF A$ = "N" THEN 1320
1610  POKE D - 8, INT (YR% / 256): POKE D - 7,YR% -  INT (YR% / 256)
    * 256
1620  POKE D - 6,MO%: POKE D - 5,DA%
1630  POKE D - 4,HR%: POKE D - 3,MI%: POKE D - 2,IN%: POKE D - 1,IT%

1640  FOR I = 1 TO  LEN (SI$): POKE N - 1 + I, ASC ( MID$ (SI$,I,1))
    : NEXT I
```

```
1650  PRINT : VTAB 20: PRINT "PRESS ANY KEY TO RETURN TO MAIN MENU"
1660  GOSUB 680
1670  GOTO 340
1680  CALL AD + 22: GOTO 340
1690  ONERR  GOTO 1680
1700  HOME : NORMAL
1710  VTAB 4: PRINT "3. CATALOG"
1720  PRINT  CHR$ (4);"CATALOG"
1730  GOSUB 680
1740  GOTO 340
1750  CALL AD + 22: GOTO 2030
1760  ONERR  GOTO 1750
1770  HOME
1780  VTAB 4: PRINT "4. LOAD DATA FROM FILE"
1790  VTAB 6: INPUT "FILE NAME -> ";F$
1800  IF  LEN (F$) = 0 THEN 340
1810  PRINT  CHR$ (4);"BLOAD ";F$
1820  HOME
1830  IF  PEEK (AD + 2) <  > 0 THEN  VTAB 6: PRINT "OVERFLOW": PRINT
    "DATA ARE LOST": GOTO 1870
1840 NO =  PEEK (AD) +  PEEK (AD + 1) * 256
1850  IF NO = 0 THEN  VTAB 6: PRINT "NO DATA": GOTO 1870
1860  VTAB 6: PRINT "NUMBER OF DATA -> ";NO
1870  VTAB 20: PRINT "PRESS ANY KEY TO RETURN TO MAIN MENU"
1880 YR% =  PEEK (D - 8) * 256 +  PEEK (D - 7)
1890 MO% =  PEEK (D - 6)
1900 DA% =  PEEK (D - 5)
1910 HR% =  PEEK (D - 4)
1920 MI% =  PEEK (D - 3)
1930 IN% =  PEEK (D - 2)
1940 IT% =  PEEK (D - 1): IF IT% > 4 THEN IT% = 1
1950 SI$ = "": FOR I = N TO N + 24:SI$ = SI$ +  CHR$ ( PEEK (I)): NEXT
    I
1960  VTAB 8: PRINT "DATE     -> ";DA%;"-";M$(MO%);"-";YR%
1970  PRINT "TIME     -> ";HR%;":";MI%
1980  PRINT "INTERVAL-> ";IN%;" MIN."
1990  PRINT "SITE     -> ";SI$
2000  PRINT : PRINT "I/P TYPE-> ";IT$(IT%)
2010  GOSUB 680
2020  GOTO 340
2030  CALL  - 198
2040  GOTO 1770
2050  CALL AD + 22: IF  PEEK (222) = 10 THEN 2160
2060  IF  PEEK (222) = 4 THEN  VTAB 22: PRINT "ERROR! WRITE-PROTECTE
    D!": CALL  - 198: GOSUB 680: GOTO 2080
2070  IF  PEEK (222) = 9 THEN  VTAB 22: PRINT "ERROR! DISK FULL!": CALL
     - 198: GOSUB 680: GOTO 2080
2080  ONERR  GOTO 2050
2090  HOME
2100  VTAB 4: PRINT "5. SAVE DATA TO FILE"
2110  VTAB 6: HTAB 1: INPUT "FILE NAME -> ";F$
2120  IF  LEN (F$) = 0 THEN 340
2130  PRINT  CHR$ (4);"BSAVE ";F$;",A$8BD0,L$833"
2140  PRINT  CHR$ (4);"LOCK ";F$
2150  GOTO 340
2160  CALL  - 198
2170  VTAB 8: NORMAL : PRINT "ALREADY EXISTED! (";: INVERSE : PRINT
    "R";: NORMAL : PRINT "EPLACE/";: INVERSE : PRINT "C";: NORMAL : PRINT
    "ANCEL) -> ";: GET A$
```

```
2180  PRINT
2190  IF A$ <  > "R" AND A$ <  > "C" THEN 2170
2200  IF A$ = "C" THEN  HOME : GOTO 2110
2210  PRINT  CHR$ (4);"UNLOCK ";F$
2220  GOTO 2130
2230  CALL AD + 22: GOTO 2250
2240  ONERR  GOTO 2230
2250  HOME : NORMAL
2260  VTAB 4: PRINT "6. LIST DATA ON SCREEN"
2270  IF  PEEK (AD + 2) <  > 0 THEN  VTAB 6: PRINT "OVERFLOW": PRINT
    "DATA ARE LOST": VTAB 20: PRINT "PRESS ANY KEY TO RETURN TO MA
    IN MENU": GOSUB 680: GOTO 340
2280 NO =  PEEK (AD) +  PEEK (AD + 1) * 256
2290  IF NO = 0 THEN  VTAB 6: PRINT "NO DATA": VTAB 20: PRINT "PRE
    SS ANY KEY TO RETURN TO MAIN MENU": GOSUB 680: GOTO 340
2300  VTAB 6: PRINT "NO. OF DATA -> ";NO
2310  VTAB 7: INVERSE : PRINT "L";: NORMAL : PRINT "IST DATA OR ";
    : INVERSE : PRINT "R";: NORMAL : PRINT "ETURN TO MAIN MENU ->
    ";: GET A$: PRINT
2320  POKE 34,8
2330  IF A$ <  > "L" AND A$ <  > "R" THEN 2310
2340  IF A$ = "R" THEN 340
2350  VTAB 7: PRINT  SPC( 39): VTAB 7: HTAB 1: INPUT "FROM ";DF%
2360  IF DF% <  = 0 OR NO < DF% THEN  CALL  - 198: GOTO 2350
2370  VTAB 7: PRINT  SPC( 39): VTAB 7: HTAB 1: INPUT "TO ";DE%
2380  IF DE% <  = 0 OR NO < DE% OR DE% < DF% THEN  CALL  - 198: GOTO
    2370
2390  VTAB 7: PRINT  SPC( 39): HOME
2400  VTAB 8: HTAB 1: PRINT  TAB( 7);"INPUT 1"; TAB( 27);"INPUT 2"
    :I = DF%
2410 J =  PEEK (D - 4) * 60 +  PEEK (D - 3) + 1
2420 J = J +  PEEK (D - 2) * (I - 1)
2430 J = J -  INT (J / 24 / 60) * 24 * 60
2440  ON IT% GOTO 2450,2460,2470,2480
2450 T = 0: GOTO 2490
2460 T = 21: GOTO 2490
2470 T = T(1 - (I -  INT (I / 2) * 2)): GOTO 2490
2480 T = T(I -  INT (I / 2) * 2): GOTO 2490
2490  PRINT  TAB( T + 1);I; TAB( T + 6); INT (J / 60);":";J -  INT
    (J / 60) * 60; TAB( T + 12);" -> "; PEEK (D - 1 + I)
2500 KB =  PEEK ( - 16384)
2510  IF KB < 128 THEN 2550
2520 KB = KB - 128: POKE  - 16368,0
2530  IF KB = 32 THEN 2310
2540  IF KB = 19 THEN 2590
2550 I = I + 1: IF DE% < I THEN 2310
2560  GOTO 2410
2570  GOSUB 680
2580  GOTO 340
2590  GOSUB 680
2600  IF KB <  > 19 THEN 2590
2610  GOTO 2550
2620  CALL AD + 22: GOTO 2640
2630  ONERR  GOTO 2620
2640  PR# 0: VTAB 4: PRINT "7. LIST DATA ON PRINTER"
2650  HOME
```

```
2660  IF  PEEK (AD + 2) <  > 0 THEN  VTAB 6: PRINT "OVERFLOW": PRINT
    "DATA ARE LOST": VTAB 20: PRINT "PRESS ANY KEY TO RETURN TO MA
    IN MENU": GOSUB 680: GOTO 340
2670 NO =  PEEK (AD) +  PEEK (AD + 1) * 256
2680  IF NO = 0 THEN  VTAB 6: PRINT "NO DATA": VTAB 20: PRINT "PRE
    SS ANY KEY TO RETURN TO MAIN MENU": GOSUB 680: GOTO 340
2690  VTAB 6: HTAB 1: INVERSE : PRINT "L";: NORMAL : PRINT "ONG FO
    RM OR ";: INVERSE : PRINT "S";: NORMAL : PRINT "HORT FORM -> "
    ;: GET A$
2700  IF A$ =  CHR$ (13) THEN 340
2710  IF A$ <  > "L" AND A$ <  > "S" THEN 2690
2720  HOME : VTAB 20: PRINT "PRESS SPACE BAR TO STOP PRINTING": PRINT
    "PRESS CTRL-S TO PAUSE"
2730  PR# PR
2740  VTAB 6: PRINT "SOLAR RADIATION ANALYSIS"
2750  POKE 35,18: HOME
2760  PRINT
2770  VTAB 6: PRINT "NUMBER OF DATA -> ";NO
2780  PRINT "DATE     -> ";DA%;"-";M$(MO%);"-";YR%
2790  PRINT "TIME     -> ";HR%;":";MI%
2800  PRINT "INTERVAL-> ";IN%;" MIN."
2810  PRINT "SITE     -> ";SI$
2820  PRINT "I/P TYPE-> ";IT$(IT%)
2830  ON PT GOTO 2840,2850,2850,2860
2840  POKE 1656 + PR,80: GOTO 2870
2850  PRINT  CHR$ (9);"80N": GOTO 2870
2860  PRINT  CHR$ (22);"80N"
2870  IF A$ = "S" THEN 3120
2880 I = 1: T = 0
2890 J =  PEEK (D - 4) * 60 +  PEEK (D - 3) + 1
2900 J = J +  PEEK (D - 2) * (I - 1)
2910 J = J -  INT (J / 24 / 60) * 24 * 60
2920  PRINT  SPC( 4 -  LEN ( STR$ (I)));I;" ";
2930 TEMP =  INT (J / 60): PRINT  SPC( 2 -  LEN ( STR$ (TEMP)));TE
    MP;":";
2940 TEMP = J - TEMP * 60: PRINT  SPC( 2 -  LEN ( STR$ (TEMP)));TE
    MP;" -> ";
2950 TEMP =  PEEK (D - 1 + I): PRINT  SPC( 3 -  LEN ( STR$ (TEMP))
    );TEMP;" ";
2960 KB =  PEEK ( - 16384)
2970  IF KB < 128 THEN 3010
2980 KB = KB - 128: POKE  - 16368,0
2990  IF KB = 32 THEN 3060
3000  IF KB = 19 THEN 3100
3010 I = I + 1
3020 T = T + 1: IF T > 3 THEN T = 0
3030  IF I -  INT (I / 4) * 4 = 1 THEN  PRINT
3040  IF I -  INT (I / 200) * 200 = 1 THEN  PRINT  CHR$ (12)
3050  IF NO >  = I THEN 2890
3060  PRINT  CHR$ (12)
3070  PR# 0
3080  CALL 1002
3090  GOTO 340
3100  GOSUB 680: IF KB <  > 19 THEN 3100
3110  GOTO 3010
3120 I = 1
3130  PRINT  SPC( 3 -  LEN ( STR$ ( PEEK (D + I - 1)))); PEEK (D +
    I - 1);
```

```
3140 I = I + 1
3150 KB =  PEEK ( - 16384): IF KB < 128 THEN 3190
3160 KB = KB - 128: POKE  - 16368,0
3170  IF KB = 19 THEN 3270
3180  IF KB = 32 THEN 3230
3190  IF I -  INT (I / 20) * 20 = 1 THEN  PRINT : GOTO 3210
3200  PRINT " ";
3210  IF I -  INT (I / 1000) * 1000 = 1 THEN  PRINT  CHR$ (12)
3220  IF NO >  = I THEN 3130
3230  PRINT  CHR$ (12)
3240  PR# 0
3250  CALL 1002
3260  GOTO 340
3270  GOSUB 680
3280  IF KB <  > 19 THEN 3270
3290  GOTO 3190
3300  CALL AD + 22: GOTO 3320
3310  ONERR  GOTO 3300
3320  HOME : VTAB 4: PRINT "8. PLOT GRAPH ON SCREEN"
3330  IF  PEEK (AD + 2) <  > 0 THEN  VTAB 6: PRINT "OVERFLOW": PRINT
    "DATA ARE LOST": VTAB 20: PRINT "PRESS ANY KEY TO RETURN TO MA
    IN MENU": GOSUB 680: GOTO 340
3340 NO =  PEEK (AD) +  PEEK (AD + 1) * 256
3350  IF NO = 0 THEN  VTAB 6: PRINT "NO DATA": VTAB 20: PRINT "PRE
    SS ANY KEY TO RETURN TO MAIN MENU": GOSUB 680: GOTO 340
3360  VTAB 6: PRINT "NUMBER OF DATA -> ";NO
3370  VTAB 20: PRINT "PRESS ANY KEY TO PLOT GRAPH"
3380  VTAB 8: PRINT "DATE     -> ";DA%;"-";M$(MO%);"-";YR%
3390  PRINT "TIME     -> ";HR%;":";MI%
3400  PRINT "INTERVAL-> ";IN%;" MIN.": PRINT "SITE     -> ";SI$: PRINT
    : PRINT "I/P TYPE-> ";IT$(IT%)
3410  VTAB 18: PRINT "PRESS <-,-> TO SHIFT THE GRAPH"
3420  PRINT "PRESS J,K TO DIMINISH OR ENLARGE"
3430  GOSUB 680
3440 IL = 1
3450 IH = 0
3460 II =  INT ((NO - 1) / 261) + 1
3470 PL = 10
3480 PH = 0
3490  IF NO > 261 THEN PI = 1: GOTO 3520
3500  IF NO = 1 THEN PI = 1: GOTO 3520
3510 PI =  INT (260 / (NO - 1))
3520 DC = 20
3530  IF II > 255 THEN II = 255
3540  IF PI > 255 THEN PI = 255
3550  POKE AD + 10,IL
3560  POKE AD + 11,IH
3570  POKE AD + 12,II
3580  POKE AD + 13,PL
3590  POKE AD + 14,PH
3600  POKE AD + 15,PI
3610  POKE AD + 16,DC
3620  CALL AD + 17
3630  HPLOT 4,20 TO 7,20
3640  HPLOT 4,147 TO 7,147
3650  FOR I = 22 TO 122 STEP 25
```

```
3660  HPLOT 6,I TO 7,I
3670  NEXT I
3680  GOSUB 680
3690  IF KB = 8 AND IL =  PEEK (AD) AND IH =  PEEK (AD + 1) THEN 3
    680
3700  IF KB = 8 THEN IL = IL + II: IF IL >  = 256 THEN IL = IL - 2
    56:IH = IH + 1: IF IH >  PEEK (AD + 1) THEN IL =  PEEK (AD):IH
     =  PEEK (AD + 1)
3710  IF KB = 8 THEN 3530
3720  IF KB = 21 AND IL = 1 AND IH = 0 THEN 3680
3730  IF KB = 21 THEN IL = IL - II: IF IL < 0 THEN IL = IL + 256:I
    H = IH - 1: IF IH < 0 THEN IL = 1:IH = 0
3740  IF KB = 21 THEN 3530
3750  IF KB <  > 75 THEN 3790
3760  IF II = 1 THEN PI = PI + 1: GOTO 3530
3770 II = II - 1: IF II <  = 0 THEN II = 1
3780  GOTO 3530
3790  IF KB <  > 74 THEN 340
3800  IF PI = 1 THEN II = II + 1: IF II > 255 THEN II = 255
3810  IF PI <  > 1 THEN PI = PI - 1: IF PI <  = 0 THEN PI = 1
3820  GOTO 3530
3830  GOTO 340
3840  CALL AD + 22: GOTO 3860
3850  ONERR  GOTO 3840
3860  HOME
3870  VTAB 4: PRINT "9. DUMP GRAPH TO PRINTER"
3880  IF  PEEK (AD + 2) <  > 0 THEN  VTAB 6: PRINT "OVERFLOW": PRINT
    "DATA ARE LOST": VTAB 20: PRINT "PRESS ANY KEY TO RETURN TO MA
    IN MENU": GOSUB 680: GOTO 340
3890 NO =  PEEK (AD) +  PEEK (AD + 1) * 256
3900  IF NO = 0 THEN  VTAB 6: PRINT "NO DATA": VTAB 20: PRINT "PRE
    SS ANY KEY TO RETURN TO MAIN MENU": GOSUB 680: GOTO 340
3910  VTAB 6: HTAB 1: INVERSE : PRINT "N";: NORMAL : PRINT "ORMAL
    SIZE OR ";: INVERSE : PRINT "D";: NORMAL : PRINT "OUBLE SIZE -
    > ";: GET A$
3920  IF A$ =  CHR$ (13) THEN 340
3930  IF A$ <  > "N" AND A$ <  > "D" THEN 3910
3940  VTAB 7: HTAB 1: INVERSE : PRINT "N";: NORMAL : PRINT "ORMAL
    FORM OR ";: INVERSE : PRINT "I";: NORMAL : PRINT "NVERSE FORM-
    > ";: GET B$
3950  IF B$ =  CHR$ (13) THEN  HOME : GOTO 3910
3960  IF B$ <  > "N" AND B$ <  > "I" THEN 3940
3970  PR# PR
3980  VTAB 6: PRINT "SOLAR RADIATION ANALYSIS"
3990  POKE 35,18: HOME
4000  PRINT
4010  VTAB 6: PRINT "NUMBER OF DATA -> ";NO
4020  PRINT "DATE     -> ";DA%;"-";M$(MO%);"-";YR%
4030  PRINT "TIME     -> ";HR%;":";MI%
4040  PRINT "INTERVAL-> ";IN%;" MIN."
4050  PRINT "SITE     -> ";SI$
4060  PRINT "I/P TYPE-> ";IT$(IT%)
4070  ON PT GOTO 4080,4140,4190,4240
4080 TEMP = 2
4090  IF A$ = "D" THEN TEMP = TEMP + 64
```

```
4100  IF B$ = "I" THEN TEMP = TEMP + 32
4110  POKE 1912 + PR,TEMP
4120  PRINT  CHR$ (17)
4130  GOTO 4290
4140  PRINT  CHR$ (20);
4150  IF A$ = "D" THEN  PRINT "L";
4160  IF B$ = "I" THEN  PRINT "I";
4170  PRINT "2"
4180  GOTO 4290
4190  PRINT  CHR$ (9);"G";
4200  IF A$ = "D" THEN  PRINT "D";
4210  IF B$ = "I" THEN  PRINT "I";
4220  PRINT "2"
4230  GOTO 4290
4240  PRINT  CHR$  12);"G";
4250  IF A$ = "D"  HEN  PRINT "D";
4260  IF B$ = "I" THEN  PRINT "I";
4270  PRINT "2"; CHR$ (12)
4280  GOTO 4290
4290  PRINT  CHR$ (12)
4300  PR# 0
4310  CALL 1002
4320  GOTO 340
4330  CALL AD + 22: GOTO 4350
4340  ONERR  GOTO 4330
4350  HOME
4360  VTAB 4: PRINT "10. TEST DETECTOR HARDWARE"
4370  PRINT : PRINT "INSTRUCTIONS:": PRINT
4380  PRINT "1. PUSH MODE SWITCH TO TEST POSITION"
4390  PRINT "2. PUSH POWER SWITCH TO ON POSITION"
4400  PRINT "3. PUSH SAMPLING SWITCH TO START"
4410  PRINT "    POSITION"
4420  PRINT "4. PRESS SPACE BAR TO SIMULATE A CLOCK"
4430  PRINT "    PULSE"
4440  PRINT "5. PRESS RETURN KEY TO RETURN TO MAIN"
4450  PRINT "    MENU"
4460  PRINT : PRINT
4470 IO = 12 * 16 * 3 + (8 + SLOT) * 16
4480 AO =  PEEK (IO + 1)
4490 AN =  PEEK (IO + 1)
4500  IF AN <  > AO THEN AO = AN:I =  PEEK (IO): PRINT  SPC( 4 -  LEN
    ( STR$ (I))); STR$ (I)
4510  GOSUB 680
4520  IF KB = 13 THEN 340
4530  IF KB <  > 32 THEN 4510
4540  POKE IO + 2,7 * 16: POKE IO + 2,15 * 16
4550  GOTO 4490
4560  TEXT
4570  NORMAL : HOME
```

Appendix 4.3 The program listing (6502 assembly language part)

```
0000:              1 *
0000:              2 * PROJECT NAME : SOLAR RADIATION ANALYSIS
0000:              3 * DEVELOPMENT SYSTEM : APPLE II+
0000:              4 * TARGET SYSTEM : SOLAR RADIATION DETECTOR
0000:              5 * TARGET CPU: 6502
0000:              6 *
0000:              7 * ASSEMBLER USED : EDASM
0000:              8 *
0000:              9 * PROGRAM NAME : RD DATA
0000:             10 * PROGRAM DESCRIPTION : READ DATA FROM DETECTOR
0000:             11 *
0000:             12 * VERSION : 2
0000:             13 * DATE : APRIL-1984
0000:             14 *
0000:             15 *
0000:             16 *
0000:             17 *
0000:             18 *
----- NEXT OBJECT FILE NAME IS RD DATA1.OBJ0
8C00:             19          ORG  $8C00
8C00:             20 DATABUF  DS   $800       ;2K BYTES DATA
8FFF:             21 DBUF     EQU  DATABUF-1
9400:             22 BUFEND   EQU  *
9400:             23 *
9400:             24 *
C080:             25 DATA     EQU  $C080      ;DATA OF RAM
C081:             26 ADDRL    EQU  $C081      ;LOW BYTE ADDRESS OF RAM
C082:             27 ADDRH    EQU  $C082      ;HIGH BYTE ADDRESS OF RAM
C082:             28 CTRLREG  EQU  $C082      ;CONTROL READ OR WRITE OF RAM
C083:             29 PIACTRL  EQU  $C083      ;CONTROL REGISTER OF PIA
00FE:             30 BUFPTR   EQU  $FE
9400:             31 *
9400:             32 *
00E0:             33 RDCODE   EQU  $E0
00D0:             34 WRCODE   EQU  $D0
00B0:             35 RSTCODE  EQU  $B0
00F0:             36 RELCODE  EQU  $F0
9400:             37 *
9400:             38 *
9400:             39 * RAM USED BY READ DATA ROUTINES
9400:             40 RAMADDRL DS   $01        ;ADDRESS OF RAM
9401:             41 RAMADDRH DS   $01
9402:             42 OVERFLOW DS   $01        ;$80-OVERFLOW ; $00-NORMAL
9403:             43 SLOTNO   DS   $01        ;SLOT NO. OF I/F CARD
9404:             44 *
9404:             45 *
9404:             46 * READ DATA ROUTINE VECTORS
9404:4C 19 94     47 INIT     JMP  INIT1      ;INIT PIA - ALL PORTS FOR
9407:             48 *    ;INPUT, EXCEPT UPPER C
9407:4C 2C 94     49 READ     JMP  READ1
940A:             50 *
940A:             51 *
940A:             52 *
                     *
```

```
940A:             53
940A:             54 * RAM USED BY PLOT GRAPH ROUTINES
940A:             55 ITEMBEGL DS  $01       ;ITEM NO.
940B:             56 ITEMBEGH DS  $01
9400:             57 ITEMENDL EQU RAMADDRL
9401:             58 ITEMENDH EQU RAMADDRH
940C:             59 ITEMINC DS   $01
940D:             60 POSBEGL DS   $01       ;PLOT POSITION
940E:             61 POSBEGH DS   $01
940F:             62 POSINC  DS   $01
9410:             63 DCVAL   DS   $01
00FE:             64 ITEMPTR EQU  BUFPTR
9411:             65 *
9411:             66 *
9411:             67 * PLOT ROUTINE VECTORS
9411:4C 85 94     68 PLOT    JMP  PLOT1
9414:0E           69 POSENDL DFB  $0E
9415:01           70 POSENDH DFB  $01
F3D8:             71 HGR2    EQU  $F3D8
F6F0:             72 HCOLOR  EQU  $F6F0
F457:             73 HPLOT   EQU  $F457
F53A:             74 HLINE   EQU  $F53A
F411:             75 HPOSN   EQU  $F411
9416:             76 *
9416:             77 *
9416:             78 * ERROR HANDLE ROUTINE VECTOR
9416:4C 72 95     79 ERR     JMP  ERR1
9419:             80 *
9419:             81 *
9419:             82 * SUBROUTINE INIT1
9419:             83 * INIT ALL PORTS OF THE PIA FOR INPUT
9419:             84 * INPUT:SLOTNO -> SLOT NO. OF I/F CARD
9419:             85 * OUTPUT:X -> SLOT NO. * 16
9419:             86 * VOLATILE:EXCEPT Y
9419:AD 03 94     87 INIT1   LDA  SLOTNO
941C:0A           88         ASL  A         ;SLOT * 16
941D:0A           89         ASL  A
941E:0A           90         ASL  A
941F:0A           91         ASL  A
9420:AA           92         TAX
9421:A9 93        93         LDA  #$93
9423:9D 83 C0     94         STA  PIACTRL,X
9426:A9 F0        95         LDA  #REGCODE
9428:9D 82 C0     96         STA  CTRLREG,X ;INIT CONTROL PORT
942B:60           97         RTS
942C:             98 *
942C:             99 *
942C:            100 * SUBROUTINE READ1
942C:            101 * READ 2K BYTES DATA TO DATA BUFFER
942C:            102 * INPUT:SLOTNO -> SLOT NO.
942C:            103 * OUTPUT:RAMADDRL,RAMADDRH,OVERFLOW
942C:            104 * VOLATILE:ALL REGS.
942C:AD 03 94    105 READ1  LDA  SLOTNO
942F:0A          106        ASL  A
9430:0A          107        ASL  A
9431:0A          108        ASL  A
9432:0A          109        ASL  A
9433:AA          110        TAX
```

```
9434:BD 81 C0   111          LDA  ADDRL,X
9437:8D 00 94   112          STA  RAMADDRL  ;GET NO. OF DATA
943A:BD 82 C0   113          LDA  ADDRH,X
943D:48         114          PHA
943E:29 07      115          AND  #$07      TAKE ;TAKE ONLY BITS 0-2
9440:8D 01 94   116          STA  RAMADDRH
9443:68         117          PLA
9444:A0 00      118          LDY  #$00
9446:29 08      119          AND  #$08      TAKE ;TAKE ONLY BIT 3
9448:F0 02      120          BEQ  READ2
944A:A0 80      121          LDY  #$80
944C:8C 02 94   122 READ2.   STY  OVERFLOW
944F:A9 F0      123          LDA  #RELCODE
9451:9D 82 C0   124          STA  CTRLREG,X
9454:A9 B0      125          LDA  #RSTCODE
9456:9D 82 C0   126          STA  CTRLREG,X
9459:A9 F0      127          LDA  #RELCODE
945B:9D 82 C0   128          STA  CTRLREG,X ;RESET THE ADDRESS COUNTER
945E:           129 *
945E:A9 00      130          LDA  #>DATABUF
9460:85 FE      131          STA  BUFPTR
9462:A9 8C      132          LDA  #<DATABUF
9464:85 FF      133          STA  BUFPTR+1  ;SET BUFFER POINTER
9466:A0 00      134 READ4    LDY  #$00
9468:A9 E0      135 READ3    LDA  #RDCODE
946A:9D 82 C0   136          STA  CTRLREG,X ;SEND A READ PULSE
946D:BD 80 C0   137          LDA  DATA,X    ;GET DATA
9470:91 FE      138          STA  (BUFPTR),Y ;STORE IN BUFFER
9472:A9 F0      139          LDA  #RELCODE
9474:9D 82 C0   140          STA  CTRLREG,X
9477:C8         141          INY
9478:D0 EE      142          BNE  READ3
947A:E6 FF      143          INC  BUFPTR+1
947C:A5 FF      144          LDA  BUFPTR+1
947E:C9 94      145          CMP  #<BUFEND
9480:D0 E4      146          BNE  READ4
9482:60         147          RTS
9483:           148 *
9483:           149 *
9483:           150 * SUBROUTINE PLOT1
9483:           151 * PLOT GRAPH
9483:           152 *
03FF:           153 IPTYPE   EQU  $03FF
9483:           154 TEMPBEGL DS   $02
9484:           155 TEMPBEGH EQU  TEMPBEGL+1
9485:20 D8 F3   156 PLOT1    JSR  HGR2      ;CLEAR SCREEN
9488:A2 03      157          LDX  #$03
948A:20 F0 F6   158          JSR  HCOLOR    ;COLOR=WHITE
948D:           159 *
948D:           160 * DRAW AXES
948D:A2 08      161          LDX  #$08
948F:A0 00      162          LDY  #$00
9491:A9 0F      163          LDA  #$0F
9493:20 11 F4   164          JSR  HPOSN
9496:A9 08      165          LDA  #$08
9498:A2 00      166          LDX  #$00
949A:A0 96      167          LDY  #$96
949C:20 3A F5   168          JSR  HLINE     ;DRAW Y AXIS
```

```
949F:A9 0E      169          LDA  #$0E
94A1:A2 01      170          LDX  #$01
94A3:A0 96      171          LDY  #$96
94A5:20 3A F5   172          JSR  HLINE      ;DRAW X AXIS
94A8:           173 *
94A8:AD 0B 94   174 PLOT8    LDA  ITEMBEGH
94AB:CD 01 94   175          CMP  ITEMENDH
94AE:90 0C      176          BCC  PLOT2
94B0:F0 02      177          BEQ  PLOT3
94B2:D0 2B      178          BNE  PLOT4
94B4:AD 00 94   179 PLOT3    LDA  ITEMENDL
94B7:CD 0A 94   180          CMP  ITEMBEGL
94BA:90 23      181          BCC  PLOT4      ;END
94BC:18         182 PLOT2    CLC
94BD:AD 0A 94   183          LDA  ITEMBEGL
94C0:69 FF      184          ADC  #>DBUF
94C2:85 FE      185          STA  ITEMPTR
94C4:AD 0B 94   186          LDA  ITEMBEGH
94C7:69 8B      187          ADC  #<DBUF
94C9:85 FF      188          STA  ITEMPTR+1
94CB:AD 0E 94   189          LDA  POSBEGH
94CE:CD 15 94   190          CMP  POSENDH
94D1:90 0D      191          BCC  PLOT5
94D3:F0 02      192          BEQ  PLOT6
94D5:D0 08      193          BNE  PLOT4      ;END
94D7:AD 14 94   194 PLOT6    LDA  POSENDL
94DA:CD 0D 94   195          CMP  POSBEGL
94DD:B0 01      196          BCS  PLOT5
94DF:60         197 PLOT4    RTS             ;END
94E0:A0 00      198 PLOT5    LDY  #$00
94E2:38         199          SEC
94E3:A9 FF      200          LDA  #$FF
94E5:F1 FE      201          SBC  (ITEMPTR),Y
94E7:4A         202          LSR  A          ;DIVIDE BY 2
94E8:18         203          CLC
94E9:6D 10 94   204          ADC  DCVAL
94EC:AE 0D 94   205          LDX  POSBEGL
94EF:AC 0E 94   206          LDY  POSBEGH
94F2:20 57 F4   207          JSR  HPLOT      ;PLOT A POINT
94F5:AD FF 8B   208          LDA  INPTYPE
94F8:C9 03      209          CMP  #$03
94FA:90 4F      210          BCC  PLOT9      ;INPUT TYPE 1 OR 2
94FC:AD 0C 94   211          LDA  ITEMINC
94FF:C9 01      212          CMP  #$01
9501:F0 48      213          BEQ  PLOT9
9503:18         214          CLC
9504:AD 0A 94   215          LDA  ITEMBEGL
9507:69 01      216          ADC  #$01
9509:8D 83 94   217          STA  TEMPBEGL
950C:AD 0B 94   218          LDA  ITEMBEGH
950F:69 00      219          ADC  #$00
9511:8D 84 94   220          STA  TEMPBEGH
9514:AD 84 94   221          LDA  TEMPBEGH
9517:CD 01 94   222          CMP  ITEMENDH
951A:90 0B      223          BCC  PLOT10
951C:F0 01      224          BEQ  PLOT11
951E:60         225          RTS             ;END
951F:AD 00 94   226 PLOT11   LDA  ITEMENDL
```

```
9522:CD 83 94   227           CMP  TEMPBEGL
9525:90 B8      228           BCC  PLOT4      ;END
9527:18         229 PLOT10    CLC
9528:AD 83 94   230           LDA  TEMPBEGL
952B:69 FF      231           ADC  #>DBUF
952D:85 FE      232           STA  ITEMPTR
952F:AD 84 94   233           LDA  TEMPBEGH
9532:69 8B      234           ADC  #<DBUF
9534:85 FF      235           STA  ITEMPTR+1
9536:A0 00      236           LDY  #$00
9538:38         237           SEC
9539:A9 FF      238           LDA  #$FF
953B:F1 FE      239           SBC  (ITEMPTR),Y
953D:4A         240           LSR  A
953E:18         241           CLC
953F:6D 10 94   242           ADC  DCVAL
9542:AE 0D 94   243           LDX  POSBEGL
9545:AC 0E 94   244           LDY  POSBEGH
9548:20 57 F4   245           JSR  HPLOT      ;PLOT A POINT
954B:18         246 PLOT9     CLC
954C:AD 0D 94   247           LDA  POSBEGL
954F:6D 0F 94   248           ADC  POSINC
9552:8D 0D 94   249           STA  POSBEGL
9555:AD 0E 94   250           LDA  POSBEGH
9558:69 00      251           ADC  #$00
955A:8D 0E 94   252           STA  POSBEGH
955D:18         253           CLC
955E:AD 0A 94   254           LDA  ITEMBEGL
9561:6D 0C 94   255           ADC  ITEMINC
9564:8D 0A 94   256           STA  ITEMBEGL
9567:AD 0B 94   257           LDA  ITEMBEGH
956A:69 00      258           ADC  #$00
956C:8D 0B 94   259           STA  ITEMBEGH
956F:4C A8 94   260           JMP  PLOT8
9572:           261 *
9572:           262 *
9572:           263 * SUBROUTINE ERR1
9572:68         264 ERR1      PLA
9573:A8         265           TAY
9574:68         266           PLA
9575:A6 DF      267           LDX  $DF
9577:9A         268           TXS
9578:48         269           PHA
9579:98         270           TYA
957A:48         271           PHA
957B:60         272           RTS

*** SUCCESSFUL ASSEMBLY: NO ERRORS
```

```
   E0 RSTCODE      ?  D0 WRCODE       E0 RDCODE       F0 RELCODE
   FE ITEMPTR        FE BUFPTR      8BFF IPTYPE     8BFF DBUF
 8C00 DATABUF      9400 RAMADDRL    9400 BUFEND     9400 ITEMENDL
 9401 RAMADDRH     9401 ITEMENDH    9402 OVERFLOW   9403 SLOTNO
?9404 INIT        ?9407 READ        940A ITEMBEGL   940B ITEMBEGH
 940C ITEMINC      940D POSBEGL     940E POSBEGH    940F POSINC
 9410 DCVAL       ?9411 PLOT        9414 POSENDL    9415 POSENDH
?9416 ERR          9419 INIT1      942C READ1      944C READ2
 9466 READ4        9468 READ3      9483 TEMPBEGL   9484 TEMPBEGH
 9485 PLOT1        94A8 PLOT8      9454 PLOT3      945C PLOT2
 94D7 PLOT6        94DF PLOT4      94E0 PLOT5      951F PLOT11
 9527 PLOT10       954B PLOT9      9572 ERR1       C000 DATA
 C081 ADDRL        C082 CTRLREG    C082 ADDRH      C083 PIACTRL
 F3D8 HGR2         F411 HPOSN      F457 HPLOT      F53A HLINE
 F6F0 HCOLOR
```